



**23rd International Symposium
on Plasma Chemistry**

Compte-rendu de congrès AAE - Vincent Rat
ISPC 23 Montréal 30 Juillet – 4 Aout 2017



ISPC 24

24TH INTERNATIONAL SYMPOSIUM ON PLASMA CHEMISTRY
NAPLES (ITALY) JUNE 9-14, 2019

LOCAL ORGANIZING COMMITTEE



Vittorio Colombo, *Chair*

Research Group for Industrial Applications of Plasmas
Alma Mater Studiorum – Università di Bologna
Department of Industrial Engineering



Pietro Favia, *Co-Chair*

Università degli Studi di Bari “Aldo Moro”
Department of Biosciences, Biotechnologies and Biopharmaceutics



Matteo Gherardi, *Co-Chair*

Research Group for Industrial Applications of Plasmas
Alma Mater Studiorum – Università di Bologna
Department of Industrial Engineering

TOPICS

1. Diagnostics and modelling in plasma chemistry
2. Fundamentals of plasma-surface interactions
3. Non-equilibrium effects and atmospheric pressure plasma processes
4. Plasma processing of nanomaterials and nanostructures
5. Plasma deposition of functional coatings
6. Plasmas and nanoparticles; dusty plasmas
7. Thermal plasma fundamentals and applications
8. Plasma-assisted conversion, combustion and aerodynamics
9. Plasma medicine
10. Plasma in and in contact with liquids
11. Plasmas for environmental applications and resource recovery

IMPORTANT DEADLINES

Abstract submission

Oral & Poster

December 14, 2018

Late abstract (only Poster)

April 1, 2019

Registrations

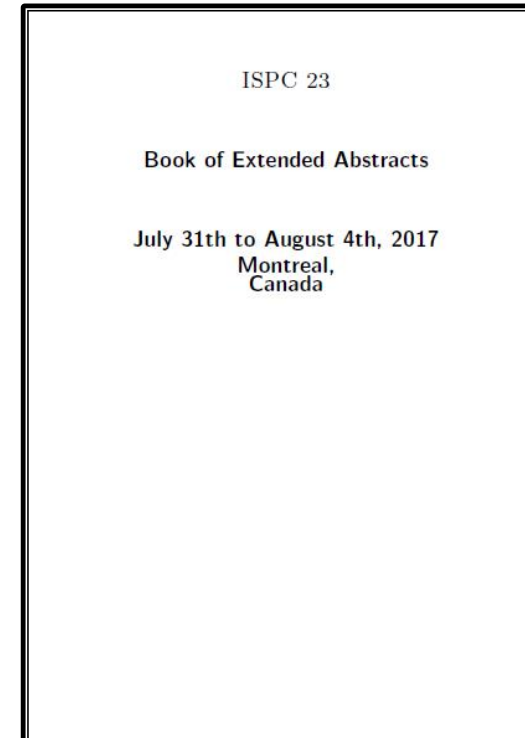
Very early registration

December 14, 2018

<http://www.ispc-conference.org/index.php/proceedings/ispc-23/show-by-track>

Topics:

- Diagnostics and modelling in reactive plasma
- Fundamental of plasma-surface interactions
- Non-equilibrium effects and atmospheric pressure plasma processes
- Plasma processing of nanomaterials and nanostructures
- Plasma deposition of functional coatings
- Plasma and nanomaterials; dusty plasmas
- Thermal plasma fundamentals and applications
- Plasma-assisted conversion, combustion and aerodynamics
- Plasma medicine
- Plasma in and in contact with liquids
- Plasma for environmental applications and resource recovery



Programme



Recueil de résumés

Plenary conferences



Yasunori Tanaka (Kanazawa University, Japan)

Modulated Induction Thermal Plasmas and their Application to High-Throughput Nanopowder Synthesis



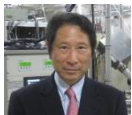
Svetlana Starikovskaia (*Laboratory of Plasma Physics, Palaiseau, France*)

Kinetics of nanosecond discharges at high specific energy release



M. C. M. van de Sanden (DIFFER, Eindhoven, NL)

The Electrified Future: A key Role for Plasma Chemistry?



Masaru Hori (Nagoya University, Japan)

Carrying knowledge into a new vision of plasma chemistry



Uwe Czarnetzki (*Ruhr-University Bochum, Germany*)

Helium ns-pulsed atmospheric pressure discharges and the key role of Rydberg molecules

22 Invited conferences

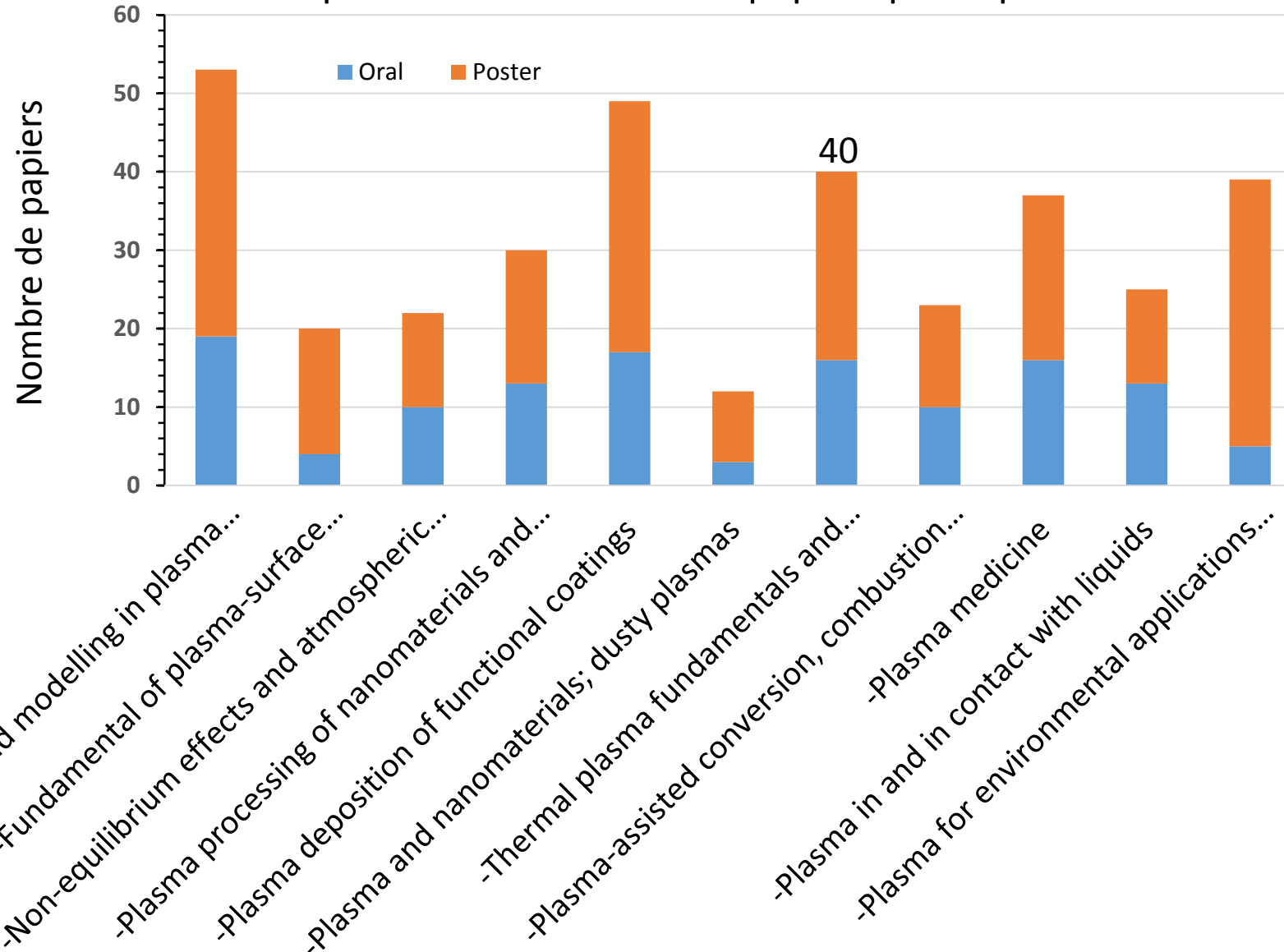
Thierry Belmonte , Université de Nancy, France	<i>Plasma synthesis of nanostructures in liquid environments</i>
Jan Benedikt , Ruhr-Universität Bochum, Germany	<i>Plasma diagnostics and modeling in reactive plasmas</i>
Gheorge Dinescu , National Institute for Laser, Romania	<i>Plasma processing of nanomaterials and nanostructures</i>
Timo Gans , The University of York, UK	<i>Plasma diagnostics and modeling in reactive plasmas</i>
Xavier Glad , Université de Montréal, Canada	<i>Plasma-interactions in material processing</i>
Michael Keidar , George Washington University, USA	<i>Plasma medicine</i>
Gaétan Laroche , Université Laval, Canada	<i>Plasma deposition of functional coatings</i>
Xingwen Li , Xi'an Jiaotong University, China	<i>Plasma diagnostics and modeling in reactive plasmas</i>
Bruce Locke , Florida State University, USA	<i>Plasma in and in contact with liquids</i>
Lorenzo Mangolini , University of California-Riverside, USA	<i>Plasma deposition of functional coatings</i>
Selma Mededovic Thagard , Clarkson University, USA	<i>Plasma in and in contact with liquids</i>
Nicolas Naudé , Université Paul Sabatier, France	<i>Characteristics of dielectric barrier discharges and plasma jets</i>
Maria Guadalupe Neira Velazquez , Centro de Investigación en Química Aplicada, Mexico	<i>Plasma processing of nanomaterials and nanostructures</i>
Zoran Petrovic , Institute of Physics, Serbia	<i>Plasma diagnostics and modeling in reactive plasmas</i>
Vincent Rat , Université de Limoges, France	<i>Thermal plasma fundamentals and applications</i>
François Reniers , Université Libre de Bruxelles, Belgium	<i>Plasma deposition of functional coatings</i>
Antoine Rousseau , École Polytechnique, France	<i>Plasma liquid interactions: applications to biology and agriculture</i>
Lio César Sagás , Universidade do Estado de Santa Catarina, Brazil	<i>Plasma-assisted conversion and combustion</i>
Paolo Tosi , University of Trento, Italy	<i>Plasma-assisted conversion and combustion</i>
Xin Tu , University of Liverpool, UK	<i>Plasma-assisted conversion and combustion</i>
Keiichiro Urabe , K.K. Air Liquide Laboratories, Japan	<i>Plasma diagnostics and modeling in reactive plasmas</i>
Douyan Wang , Kumamoto University, Japan	<i>Characteristics of nanosecond discharges in reactive plasmas</i>

Total : 350 papiers

126 conférences

224 posters

Répartition du nombre de papiers par Topics



ISPC2011 Philadelphia
400 communications
Thermal plasma: 20 comm.

ISPC2013 Cairns
327 communications
Thermal plasma: 26 comm.
7 confs + 19 posters

Modélisation & données

Modelling of fume formation in arc welding: the influence of oxygen

H. Park¹, M. Mudra^{1,2}, M. Trautmann^{1,3} and A. B. Murphy¹

¹CSIRO Manufacturing, PO Box 218, Lindfield NSW 2070, Australia

²University of the Federal Armed Forces Munich, Werner Heisenberg Weg 39, D-85577 Neubiberg, Germany

³Institute of Manufacturing Technology, Dresden University of Technology, George-Bahr-Str. 3c, D-01069 Dresden, Germany

Contexte et objectifs

- Fume is metal oxide nanoparticles, usually agglomerated into chains (Fe, Cr, Ni, Mn)
- 1 to 7 μm chains penetrate deep into lungs and particulates can cause lung cancer

what is the fume formation process?

- Does Fe or FeO or FeO₂ nucleate?
- Do the nanoparticles grow by condensation of Fe or FeO or FeO₂
- What is the effect of oxygen on the fume properties?

Méthodes:

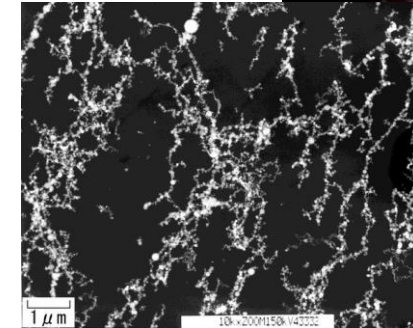
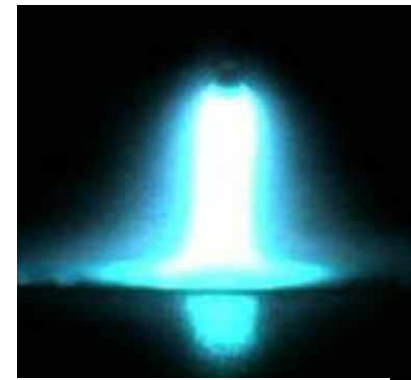
- coupling a model of particle nucleation and growth to a model of the gas-phase chemistry

1- Chemistry : Species Fe, FeO, FeO₂, O₂, O and Ar

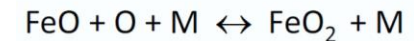
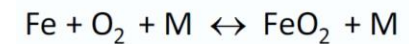
2- Particle growth : calculation of supersaturation pressure and nucleation

Nucleation rates as function of oxygen to argon ration (%mol) and temperature

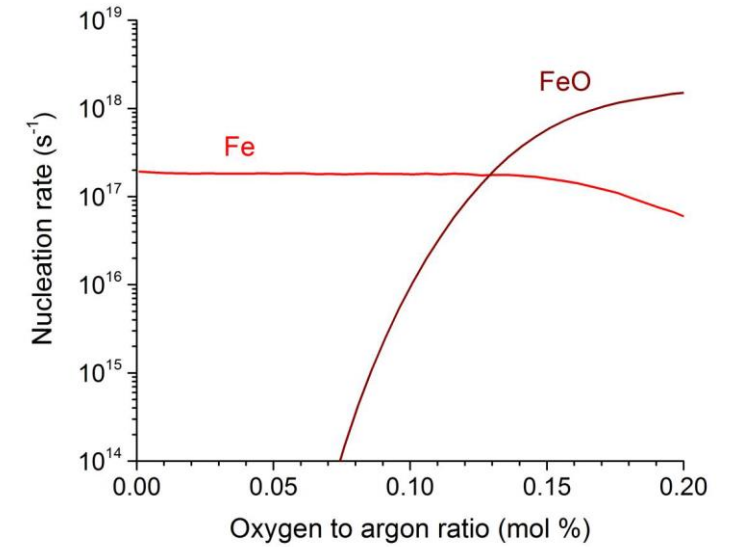
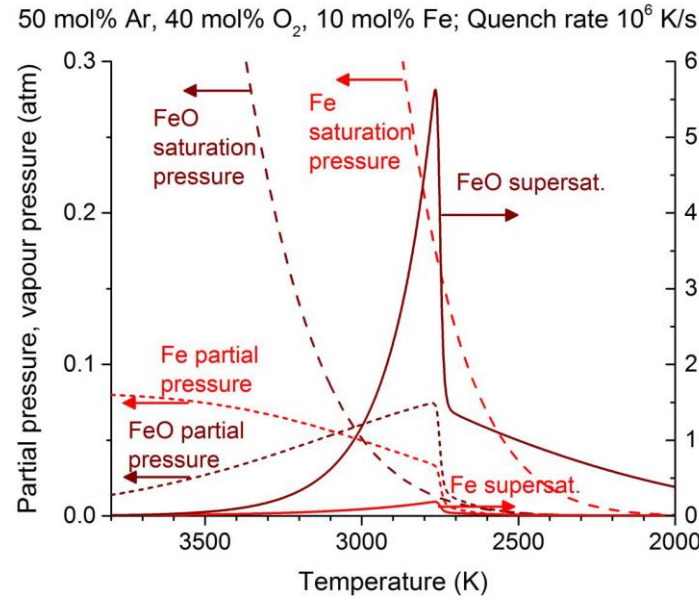
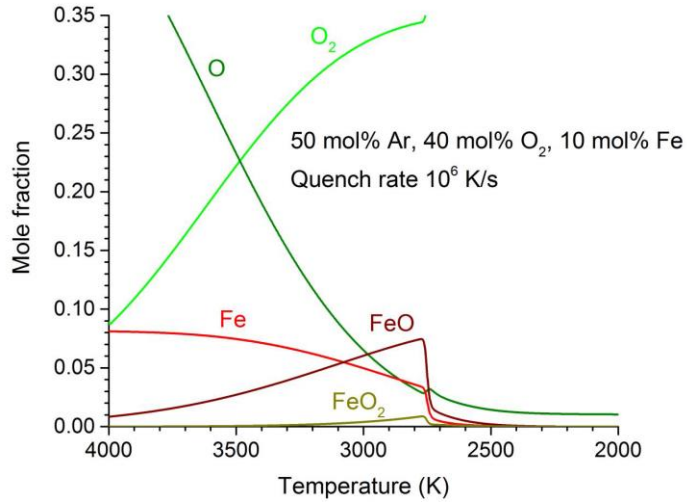
- coupling this chemical kinetic / particle growth model to a 3D arc model that predicts temperature and iron vapour concentration in Ar and Ar-O₂ arcs (one-way coupling from the arc model to the chemical/particle growth model)



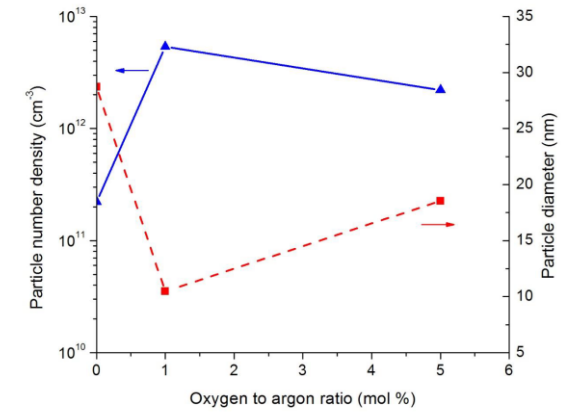
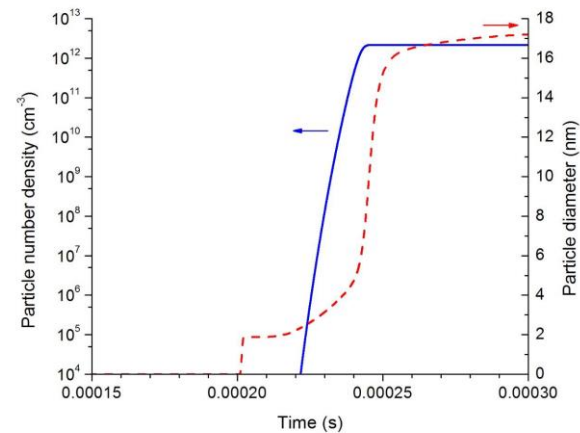
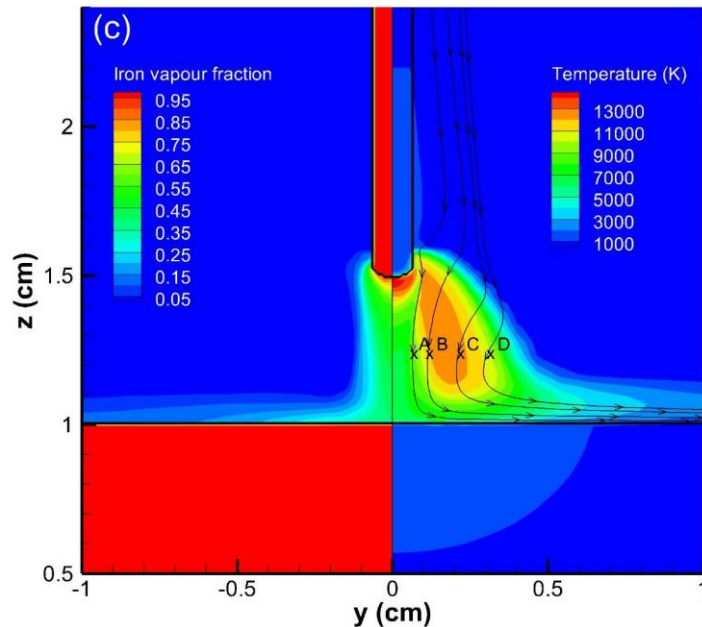
Programme C-3-7 page 14
Recueil résumé page 684
Oral



Résultats



Predictions of particles properties for different streamlines (quenching rates, Fe, O₂/Ar)
Preferential formation of FeO nanoparticles



The effects of temperature and pressure gradients on the species diffusion in a low power nitrogen/hydrogen arcjet thruster

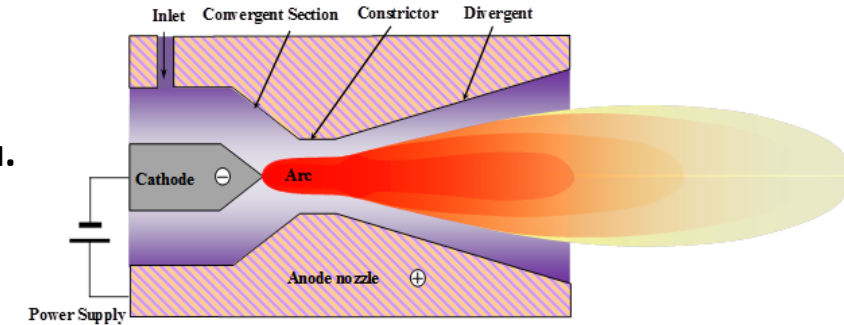
Qing-Song He , Hai-Xing Wang

School of Astronautics, Beihang University, Beijing, China

Programme C-2-7 page 14
Recueil résumé page 646
Oral

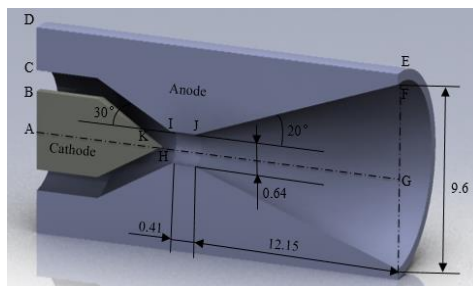
Contexte et objectifs

- Study of N₂/H₂ arcjet thruster considering species diffusion: Non-chemical and thermal equ.
- Pressures varies from **10⁵ Pa** at the inlet to **10² Pa** at the outlet
- Temperature varies from **10⁴ K** at the core to **10³ K** at the wall
- Velocity varies from **10³~10⁴ m/s** at the center to **10⁰ m/s** at the wall

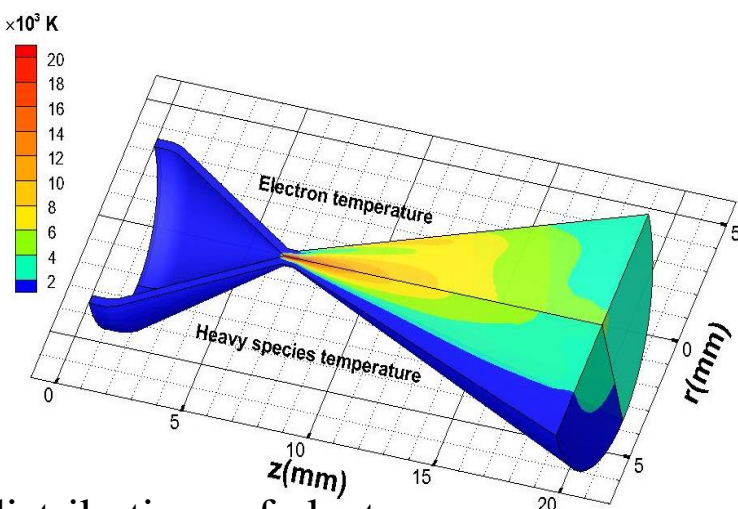


Méthodes:

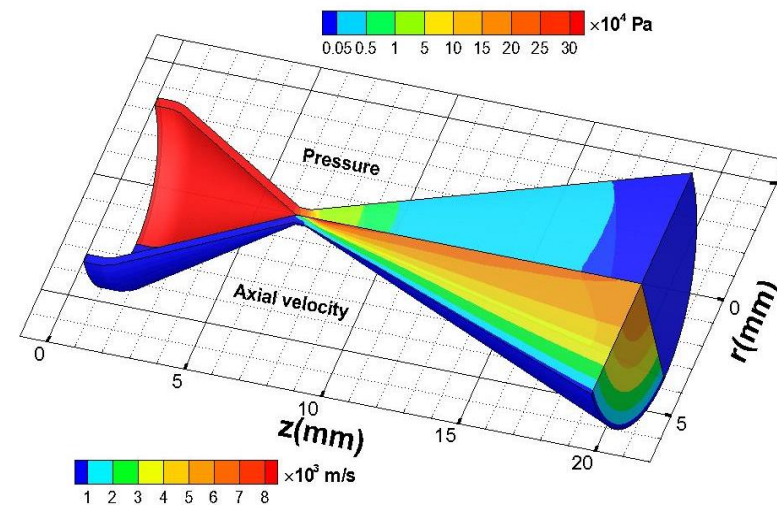
- Working gas: N₂:H₂=1:3 (simulated ammonia), N₂:H₂=1:2 (simulated hydrazine), N₂:H₂=1:1
- Seven species: H₂, N₂, H, N, e, H⁺, N⁺
- Chemical kinetic model: 17 chemical reactions
- Steady, axisymmetric, laminar and compressible, a two-temperature model , optically thin
- Solving conservation equations: Species, mass, momentum, total energy, electron energy, magnetic field



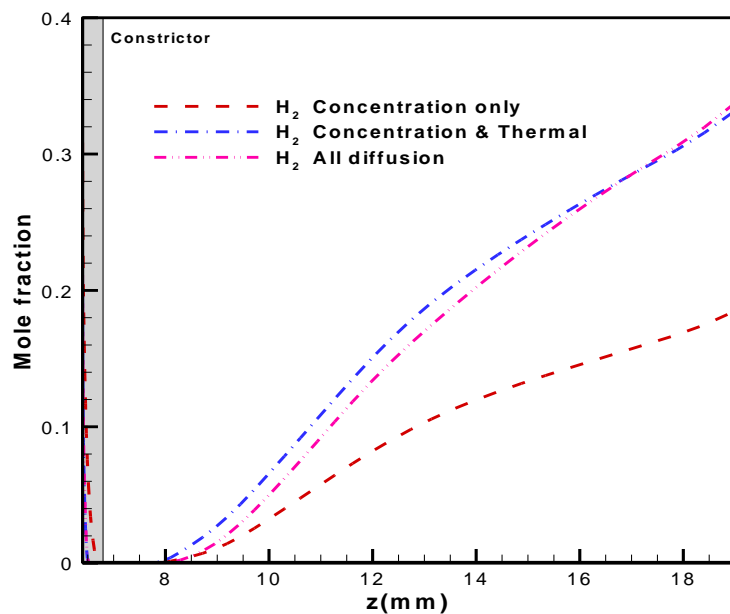
By courtesy of Hai-Xing Wang



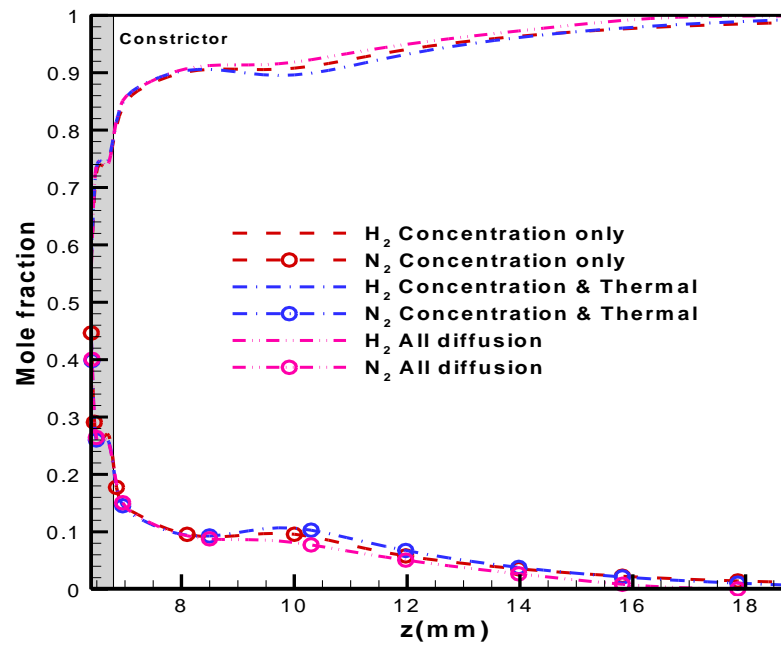
Temperature distributions of electron and heavy species ($N_2:H_2=1:2$)



Distributions of pressure and axial velocity ($N_2:H_2=1:2$)



Species mole fraction of hydrogen molecules along the arcjet axis ($N_2:H_2=1:2$)



Species mole fraction of nitrogen and hydrogen near the nozzle wall ($N_2:H_2=1:2$)

MHD modeling of rotating arc under restrike mode: dynamics and stability

P. Gueye¹, Y. Cressault², V. Rohani¹, L. Fulcheri¹

¹PERSEE, MINES ParisTech, PSL-Research University, France

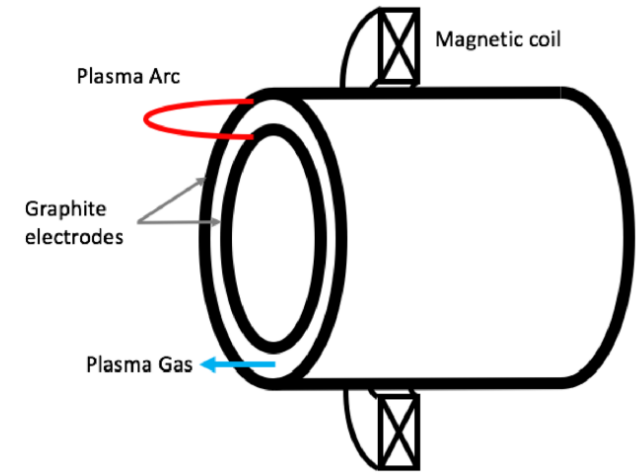
²LAPLACE, University of Toulouse UPS, France

Contexte et objectifs

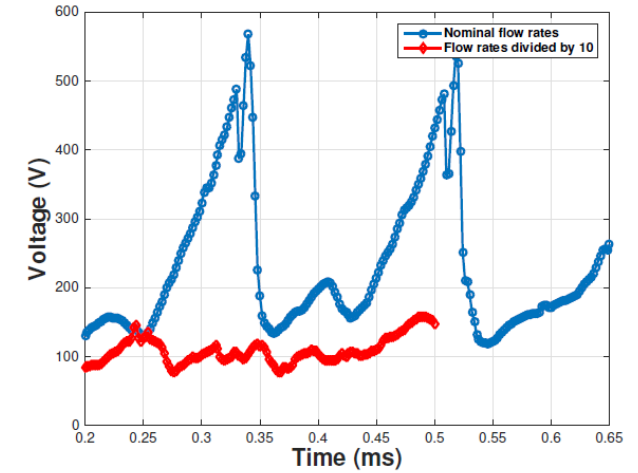
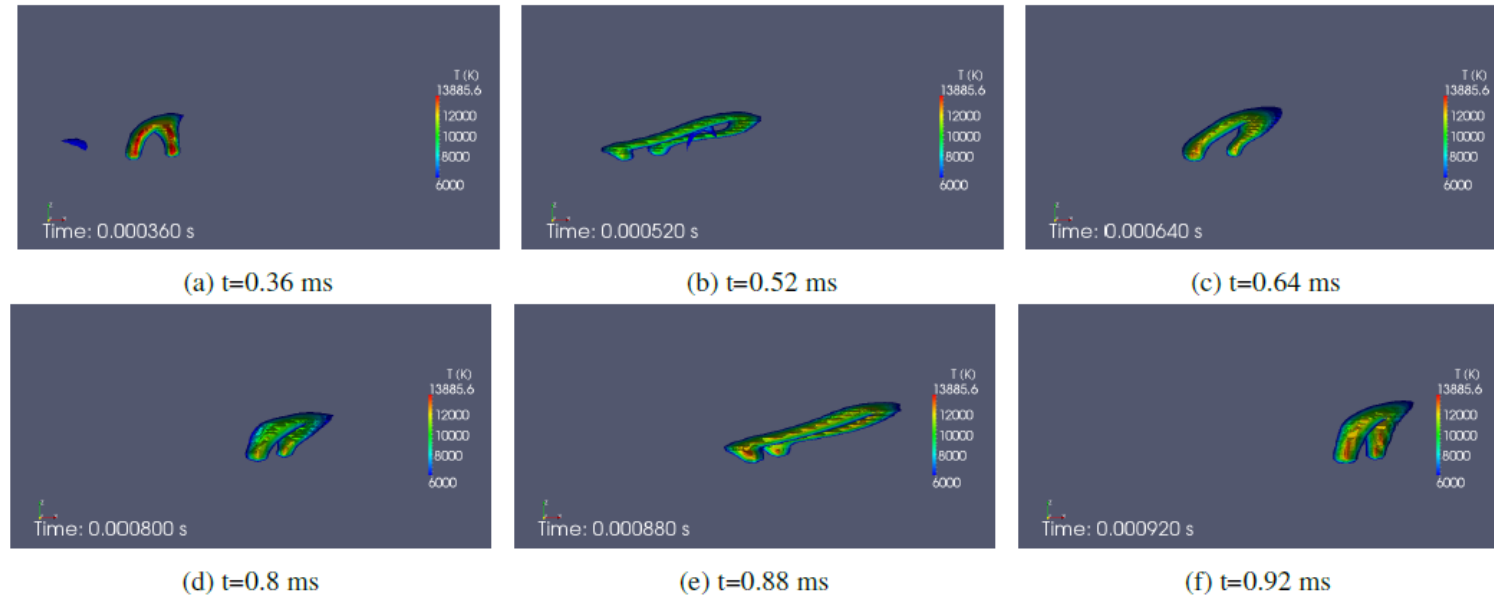
- Developing plasma reactor for syngas production
- Study of Kvaerner torch
- Understand and control arc instabilities under external magnetic field and drag flow

Méthodes:

- MHD model at LTE for hydrogen arc plasma (1 bar, 1000 A)
- Optically thin, laminar, incompressible
- Graphite electrodes incorporated within the computational domain
- Hot gas column reattachment model (arc restrike): local electric field threshold E_b
- Net emission coefficient calculated for H₂ plasma

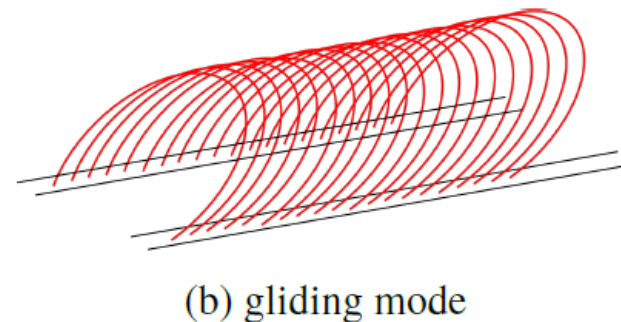
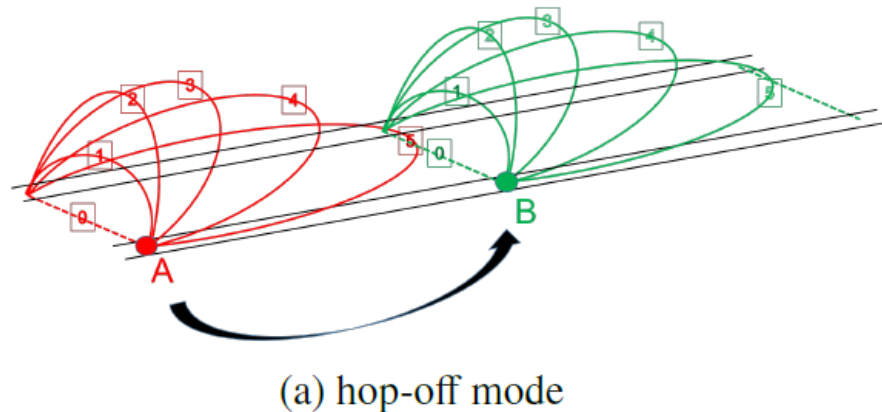


The external magnet causes the tilting of the stretched arc towards the electrodes surfaces



Voltage 1 bar, 1000 A, $E_b = 1e5$ V/m

Figure 5: Time sequence of the PBR arc (side view): Hydrogen, 1 bar, 1000 A, $B_r = -4$ mT, $B_z = 40$ mT and $E_b = 1e5$ V/m



- Hop-off mode
- 0,1,2: stretching
- 3,4,5: tilting
- 0: restriking
- Restriking where preheated regions
- Gliding mode: lower voltage, hotter

X. Baumann¹, Y. Cressault¹, and Ph. Teulet¹, F. Reichert², A. Petchanka²

¹Université de Toulouse, UPS, INPT, LAPLACE (Laboratoire Plasma et Conversion d'Energie), 118 route de Narbonne, F-31062 Toulouse Cedex 9, France

²SIEMENS AG, Berlin, Germany

Contexte et objectifs

- Extinction of an electric arc in the numerical modelling of high-voltage circuit breakers
- Calculation of two-temperature radiative properties in SF6 plasmas

Méthodes:

- Calculation of plasma composition of 2T-SF6 plasma at 1 bar for different $\theta = T_e/T_h$
- The population of internal energy modes are distributed following two assumptions:

case 1: $T_{ex}=T_e$ $T_{vib}=T_e$ $T_{rot}=T_h$

case 2: $T_{ex}=T_h$ $T_{vib}=T_h$ $T_{rot}=T_h$

- Calculation of Net Emission Coefficient separating the contributions of continuum and the lines

- NEC of continuum: → For electron eq.

$$\varepsilon_N^{cont} = \int_0^{\infty} B_{\lambda}(\lambda, T_e) \cdot \kappa_{cont}'(\lambda, T_e, \theta) e^{-\kappa'_{tot}(\lambda, T_e, T_g, T_{ex}) \cdot R_p} d\lambda$$

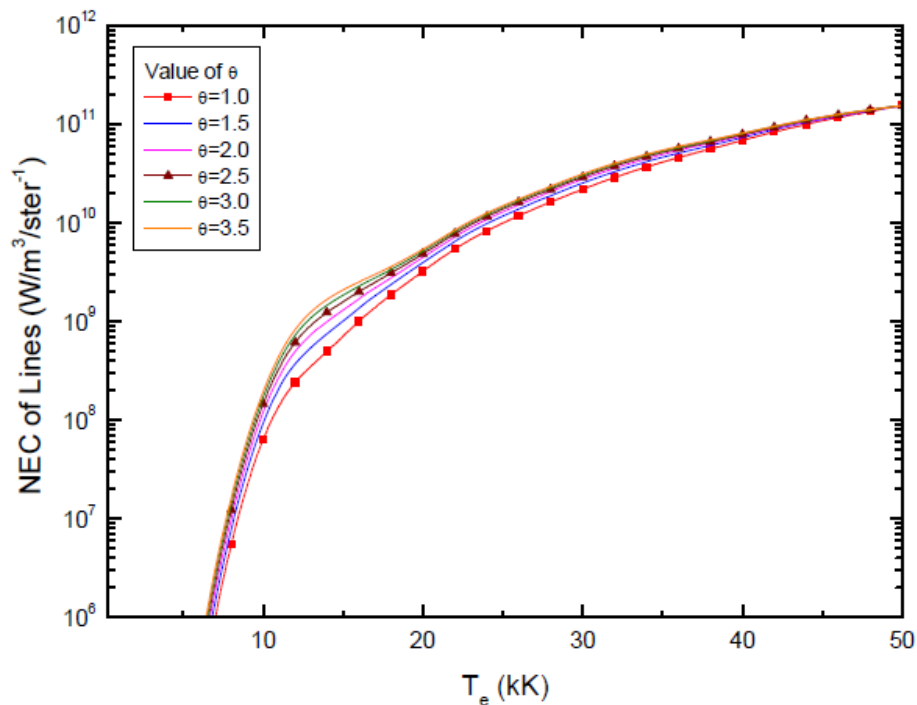
- NEC of atomic lines: → For heavy part. eq.

$$\varepsilon_N^{al} = \int_0^{\infty} B_{\lambda}(\lambda, T_{ex}) \cdot \kappa'_{lines}(\lambda, T_{ex}, \theta) e^{-\kappa'_{tot}(\lambda, T_e, T_g, T_{ex}) \cdot R_p} d\lambda$$

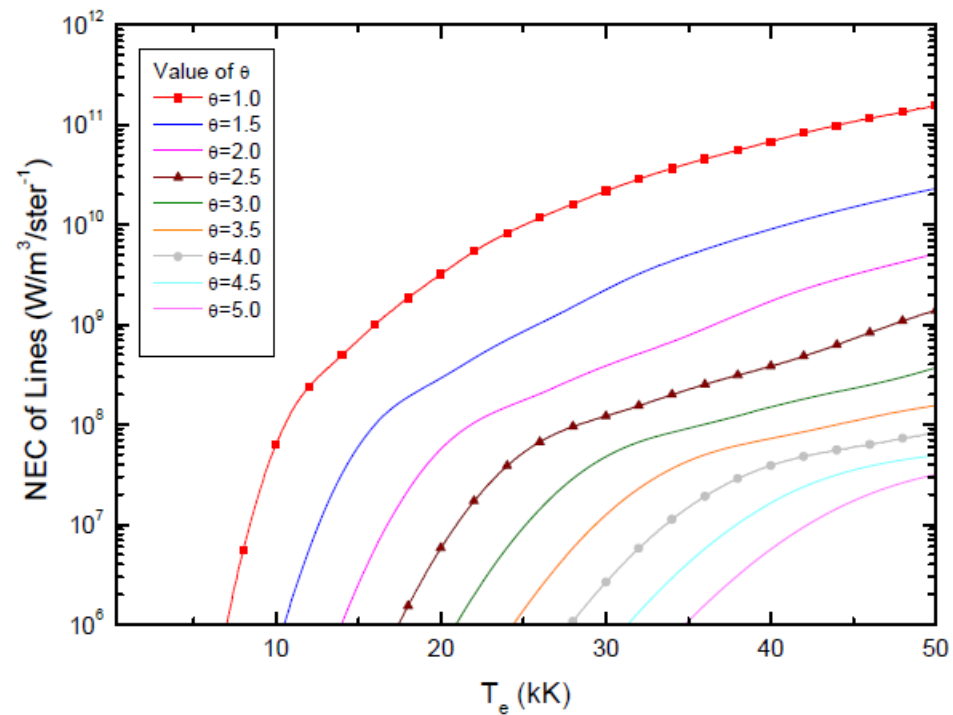
- Absorption coefficient of the atomic lines depend on broadening processes (Doppler effect, pressure effects, Stark) and either T_e or T_h .
- Absorption coefficient of the atomic continuum depends on T_e (radiative attachment and recombination, Bremsstrahlung)
- Absorption coefficient of the molecular continuum supposed only dependent on wavelength

Résultats

Rp = 1mm



Case 1



Case 2

Transport properties of multi-temperature SF6 plasmas: influence of assumptions done in the plasma composition calculation

G. Vanhulle¹, Y. Cressault¹, Ph. Teulet¹, F.Reichert², and A. Petchanka²

¹Université de Toulouse, UPS, INPT, LAPLACE (Laboratoire Plasma et Conversion d'Énergie), 118 route de Narbonne, F-31062 Toulouse Cedex 9, France

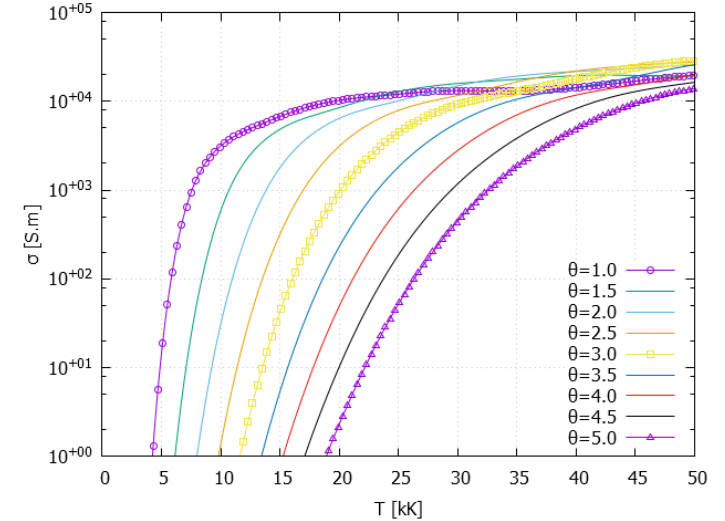
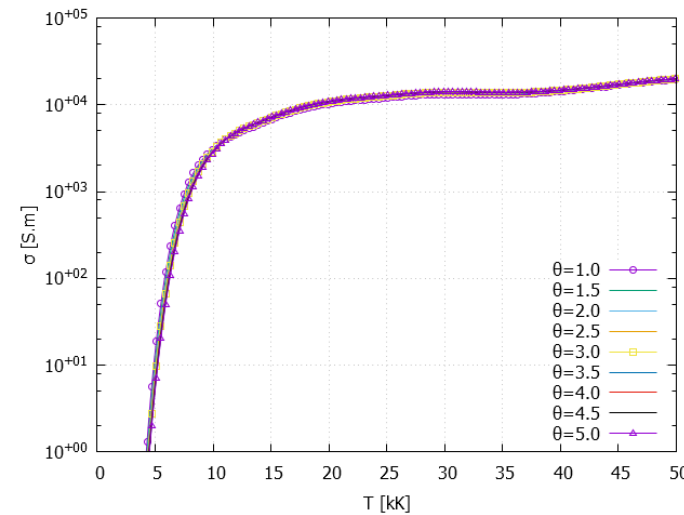
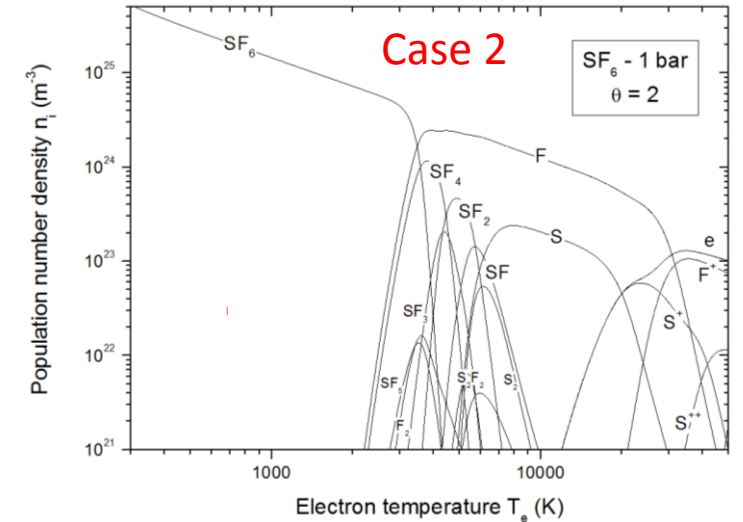
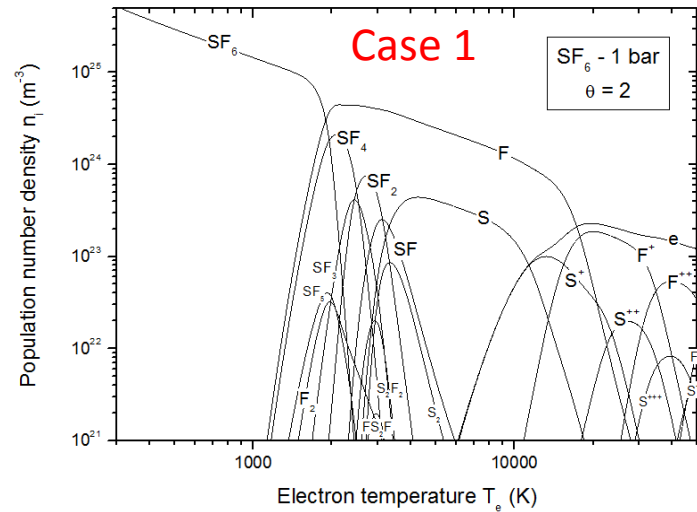
²SIEMENS AG, Berlin, Germany

Contexte et objectifs

- Extinction of an electric arc in the numerical modelling of high-voltage circuit breakers
- Calculation of plasma composition, thermo, transport properties

case 1: $T_{ex}=T_e$ $T_{vib}=T_e$ $T_{rot}=T_h$

case 2: $T_{ex}=T_h$ $T_{vib}=T_h$ $T_{rot}=T_h$



3D modelling of a DC transferred arc twin torch plasma system for the synthesis of copper nanoparticles

D. Basili, M. Boselli, V. Colombo and M. Gherardi

Alma Mater Studiorum-Università di Bologna

Department of Industrial Engineering (DIN), Bologna, Italy

Contexte et objectifs

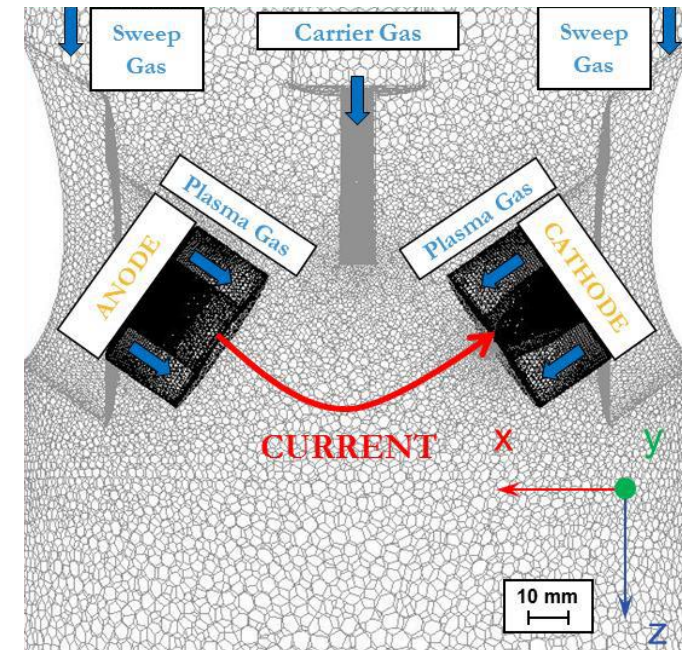
- 3D LTE twin torch model
- Synthesis of copper nanoparticles in argon by evaporation of micrometric solid copper precursors
- Radiative power loss contribution due to the vapour produced in the plasma by the solid precursors : main mechanism limiting the evaporation efficiency

Méthodes:

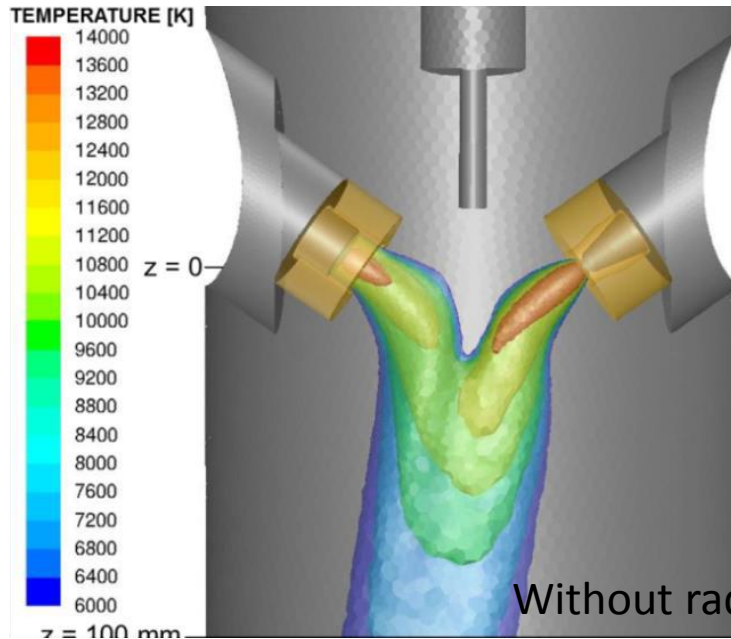
- 3D, steady, LTE plasma, turbulence (k- ϵ model), optically thin
- Neglect of Cu vapour on the transport and thermodynamic properties of the gas mixture
- Radiative losses due to copper evaporation
- Equation motion of particles and evaporation of particles
- Vapour conservation equation (diffusion, evaporation, nucleation/condensation)
- Aerosol general gas dynamic equation solved for a particle size distribution

Pure Ar, 10^5 Pa, 1200 A, Copper mean diameter $7.3 \mu\text{m}$, 70mg/s

ANSYS FLUENT, 3.8 million cells, current density distribution on the cathode surface and a zero voltage potential on the anode



Résultats



Without radiation

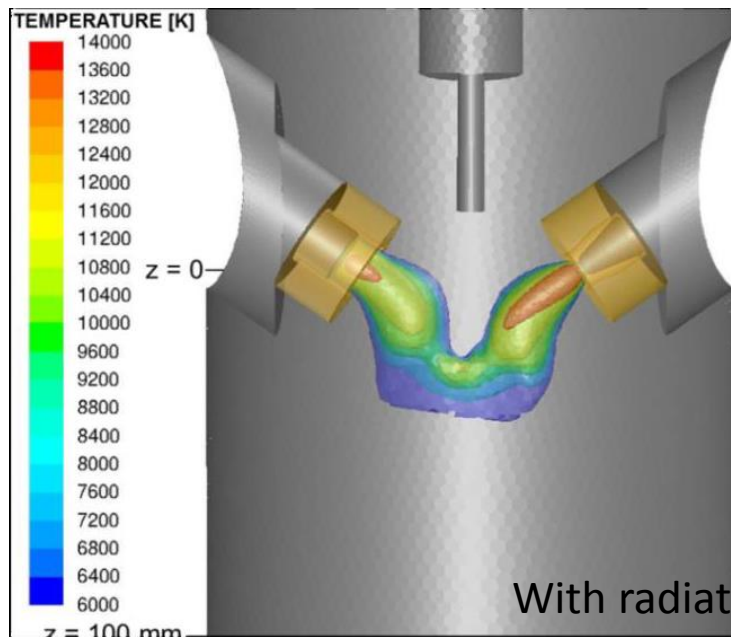
T > 6000 K

100% evaporation

With radiation

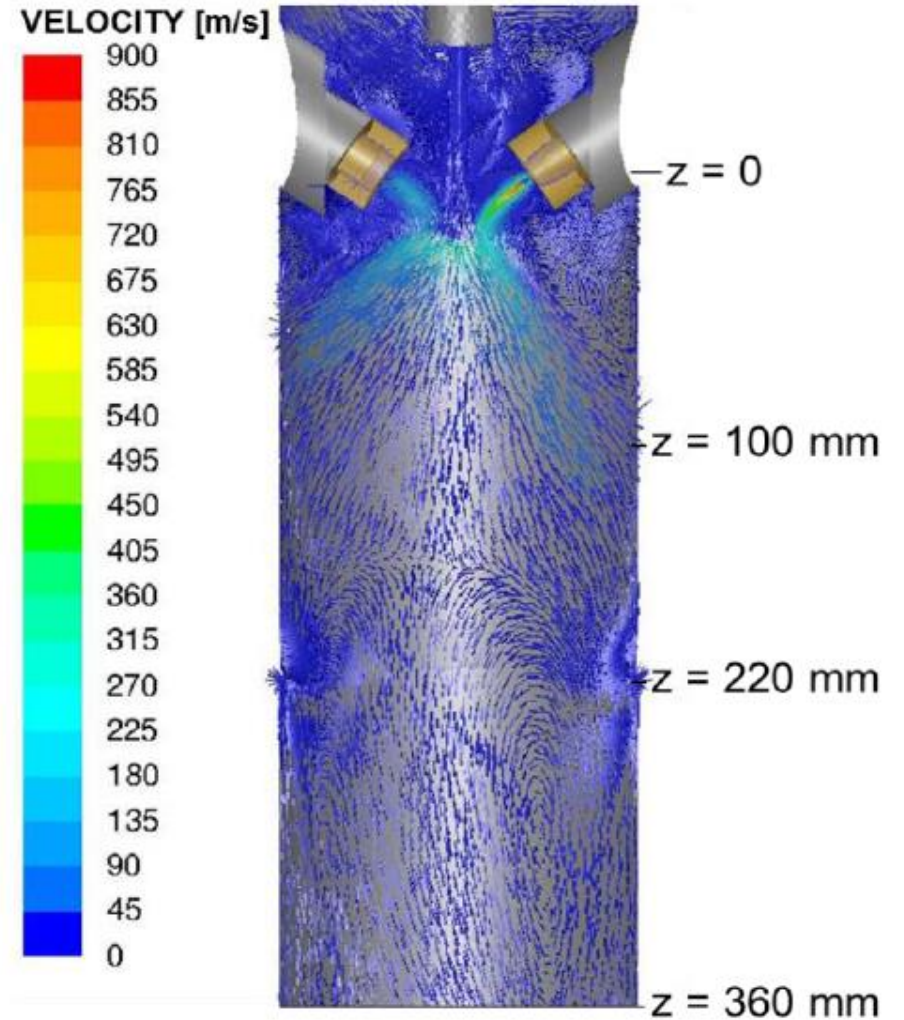
Lower temperature

97% evaporation



With radiation

Complex fluid dynamics
Difficult to efficiently quench
the vapor, even at 1000 slm.
Small amount of nanoparticles
with 14 nm in diameter



The Motion of AC and DC Plasma Arcs under Transverse Cross-Fields: An Analytical Approach

Y.Abdo¹, V. Rohani¹, F. Cauneau¹ and L. Fulcheri¹

¹MINES ParisTech, PSL- Research University, PERSEE- Centre procédés, énergies renouvelables et systèmes énergétiques- 1 Rue Claude Daunesse, 06904 Sophia Antipolis, France

Contexte et objectifs

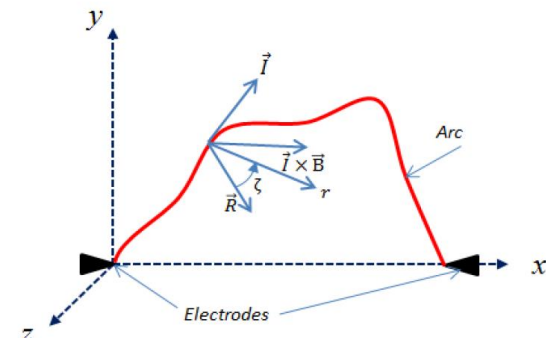
- analytical model of arc in cross-fields (blown arc, under magnetic field- self-induced or external)
- provide basic information about the arc motion
- Comparison of analytical model and MDH simulation (Saturne code)

Méthodes

- Analytical model: negligible radiation and electrode influence, constant arc radius, thermal diffusivity, viscosity, $\sigma=B(S-S_0)$
- Solving the Elenbass-Heller equation in the curvilinear coordinate system using a mathematical formulation of the heat potential for a fully developed arc channel (AC or DC)

$$\frac{1}{\lambda} \left(\frac{\partial S}{\partial t} + \vec{W} \cdot \vec{\nabla} S \right) = \Delta S + \sigma E^2 \quad W = V_{\text{gas}} - V_{\text{arc}}$$

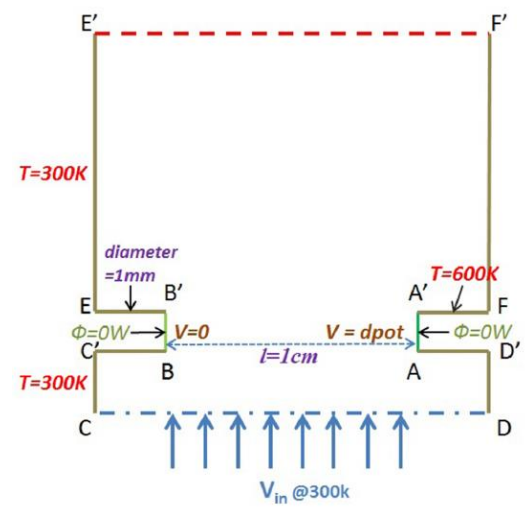
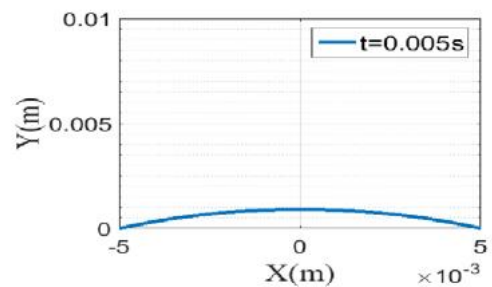
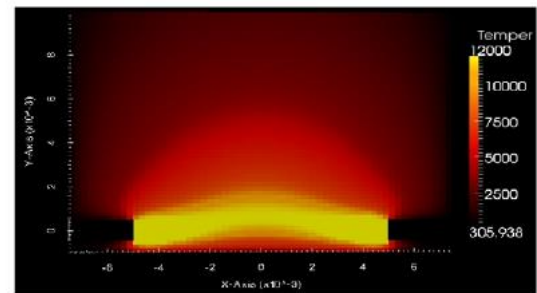
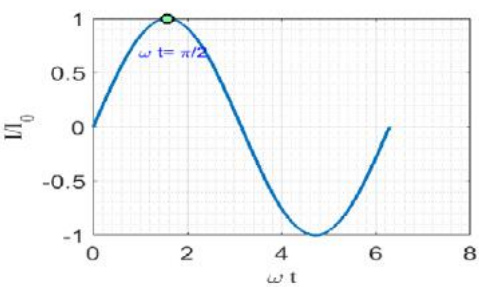
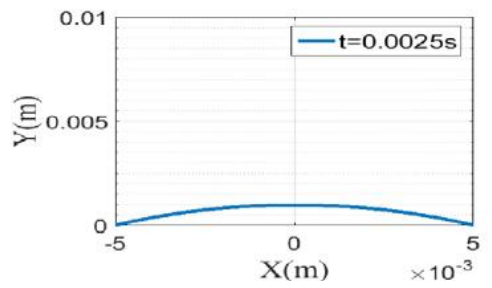
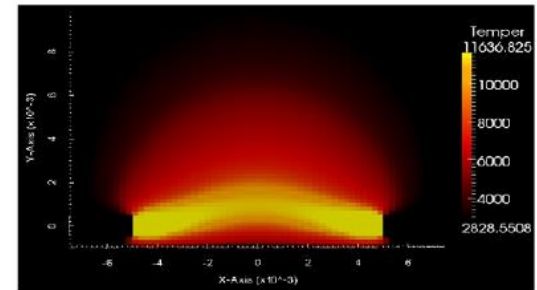
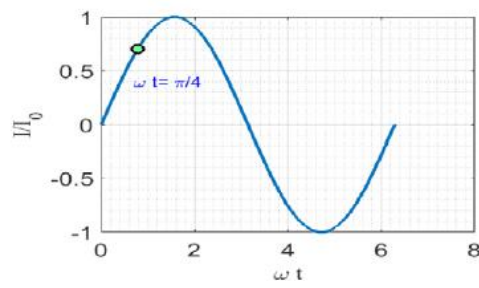
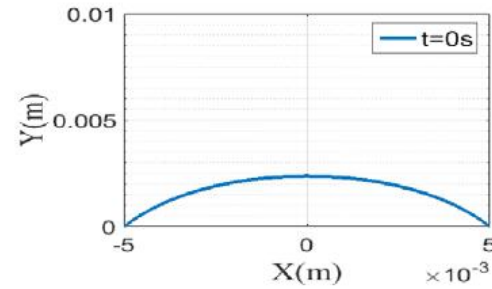
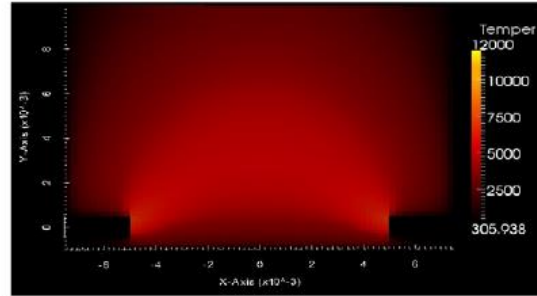
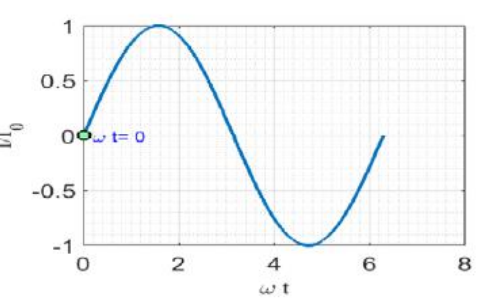
- Finding V_{arc} and V_{gas} in Frenet system with and without external and self-induced magnetic field from arc momentum equation
- Determining the cartesian or polar motion equation of the arc (2D planar case)



MHD simulation: Saturne Code, air, 10^5 Pa,
50 A for AC (50 Hz) and DC cases.

$$V_{in} = 1 \text{ m.s}^{-1}$$

Résultats



ωt	0		$\pi/4$		$\pi/2$	
Results	MHD	Theory	MHD	Theory	MHD	Theory
$S_{max} (W \cdot m^{-1})$	-	740	-	10940	-	15980
$T_{max} (K)$	5450	5280	7460	7120	11710	11680
$Y_{max} (mm)$	2.3	2.4	1.5	1.4	0.95	0.95
$a (mm)$	-	-	2	2.2	2.3	2.2
$E (V \cdot m^{-1})$	70	0	2950	2790	2450	2580

Time-dependent 3D simulation of nanopowder growth and transport in a turbulent field induced by a thermal plasma jet

M. Shigeta

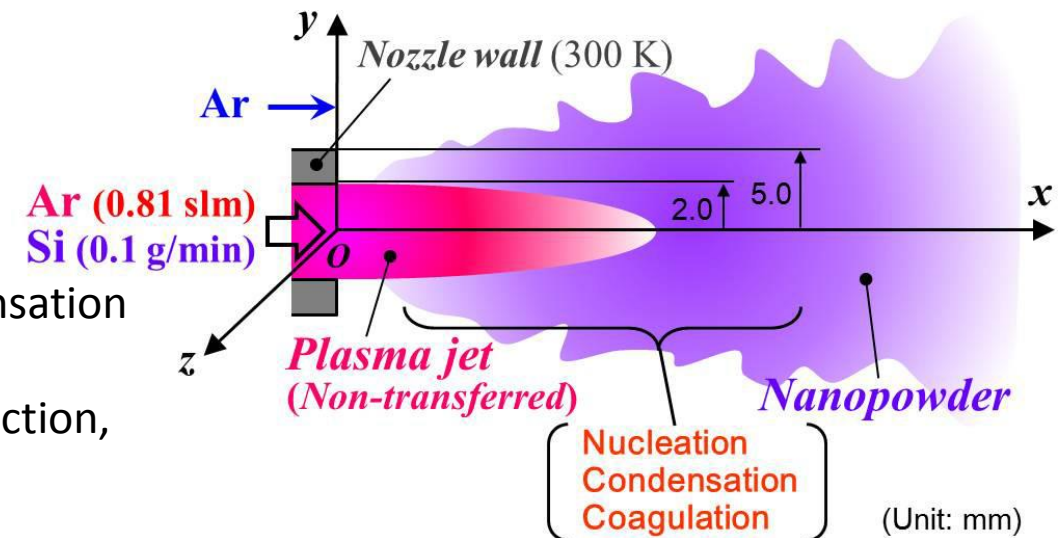
Joining and Welding Research Institute, Osaka University, Ibaraki, Osaka, Japan

Contexte et objectifs

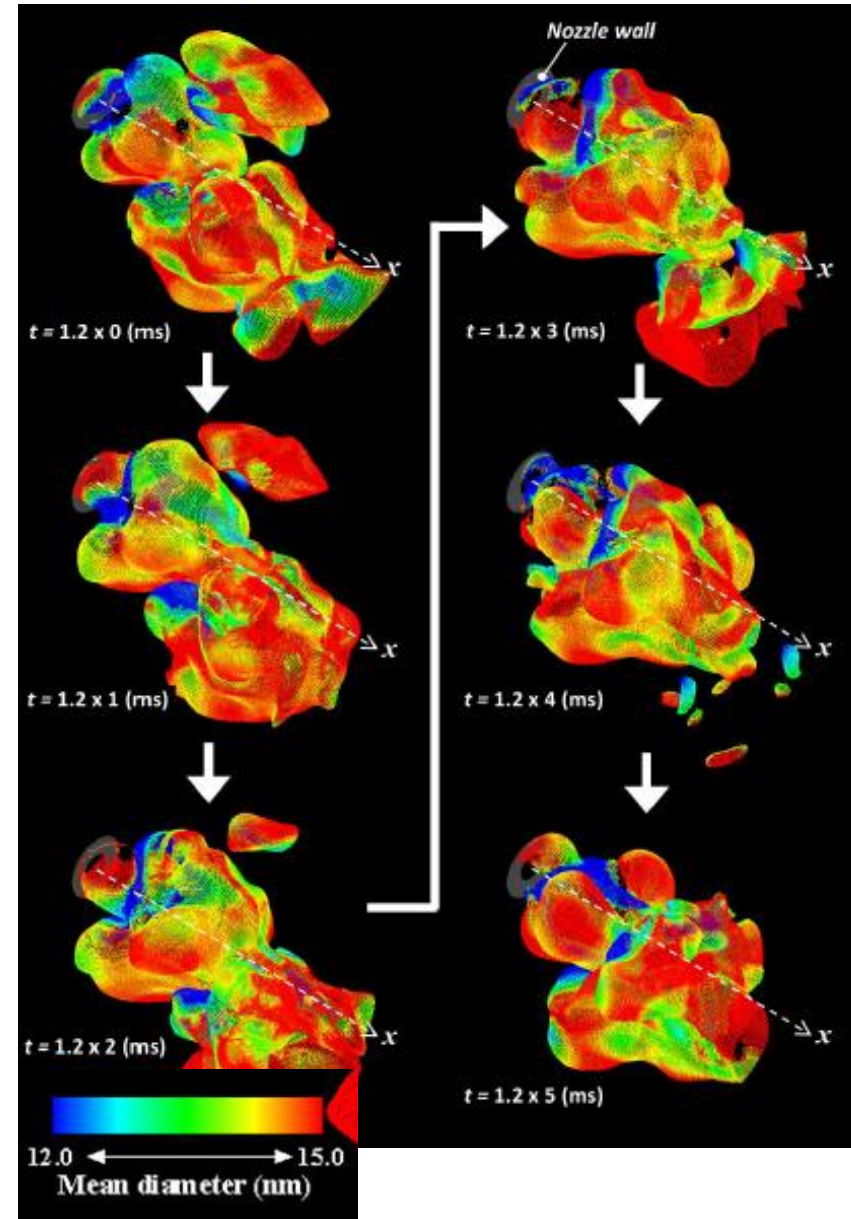
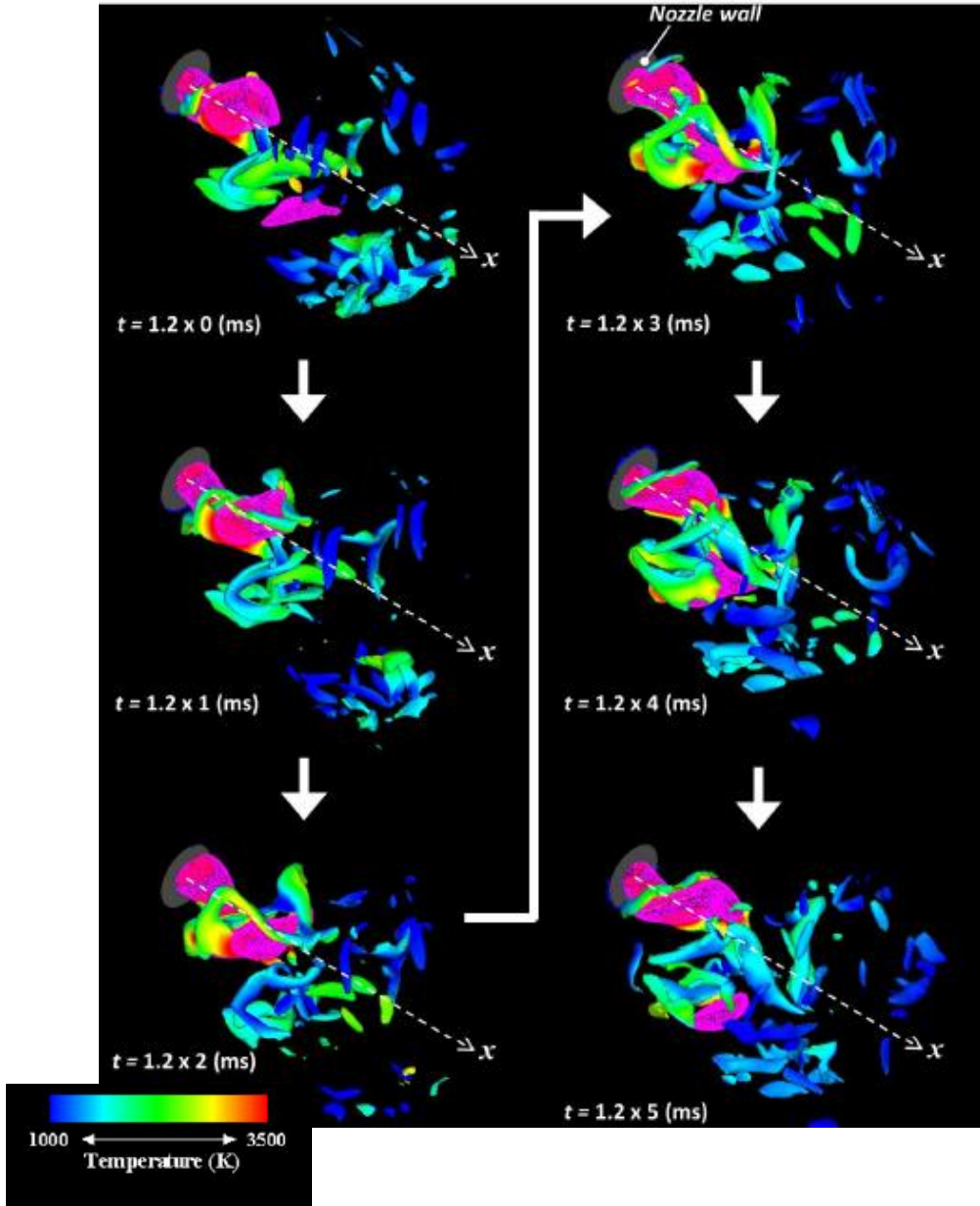
- Thermal plasma processes : high-speed fabrication of nanopowders due to high-temperature field with steep gradients at their fringes
- Growth of nano-scale particles from material vapour
- Considering turbulence : vortices formation and interaction because of fluid dynamic instability
- Modeling the transport of growing nanopowder by vortices

Méthodes

- Transient, 3D simulation of growing nanopowder in a turbulent field
- Plasma: LTE, optically thin, radiative loss, heat generation due to condensation, and viscous dissipation
- Material vapour (Si): homogeneous nucleation, heterogeneous condensation and coagulation between nanoparticles
- Governing equations describing the nanopowder's transport by convection, diffusion and thermophoresis



Résultats



Nanopowder exhibit complex distributions far from the core of the plasma jet because of the transport in the turbulent field around the plasma

Thermodynamic Nonequilibrium Simulation of an Arc in Crossflow

V. G. Bhigamudre and J.P. Trelles

Department of Mechanical Engineering, University of Massachusetts Lowell, 197 Riverside St., Lowell, MA 01854, USA

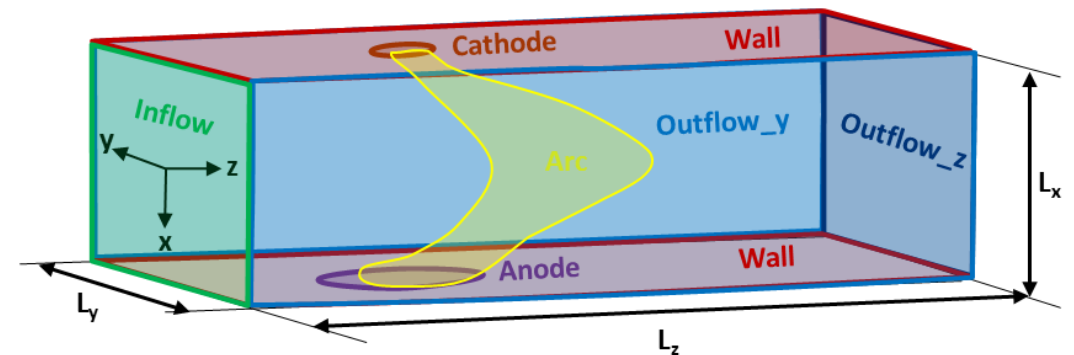
Programme P2-18-7 page 25
Recueil résumé page 720
Poster

Contexte et objectifs

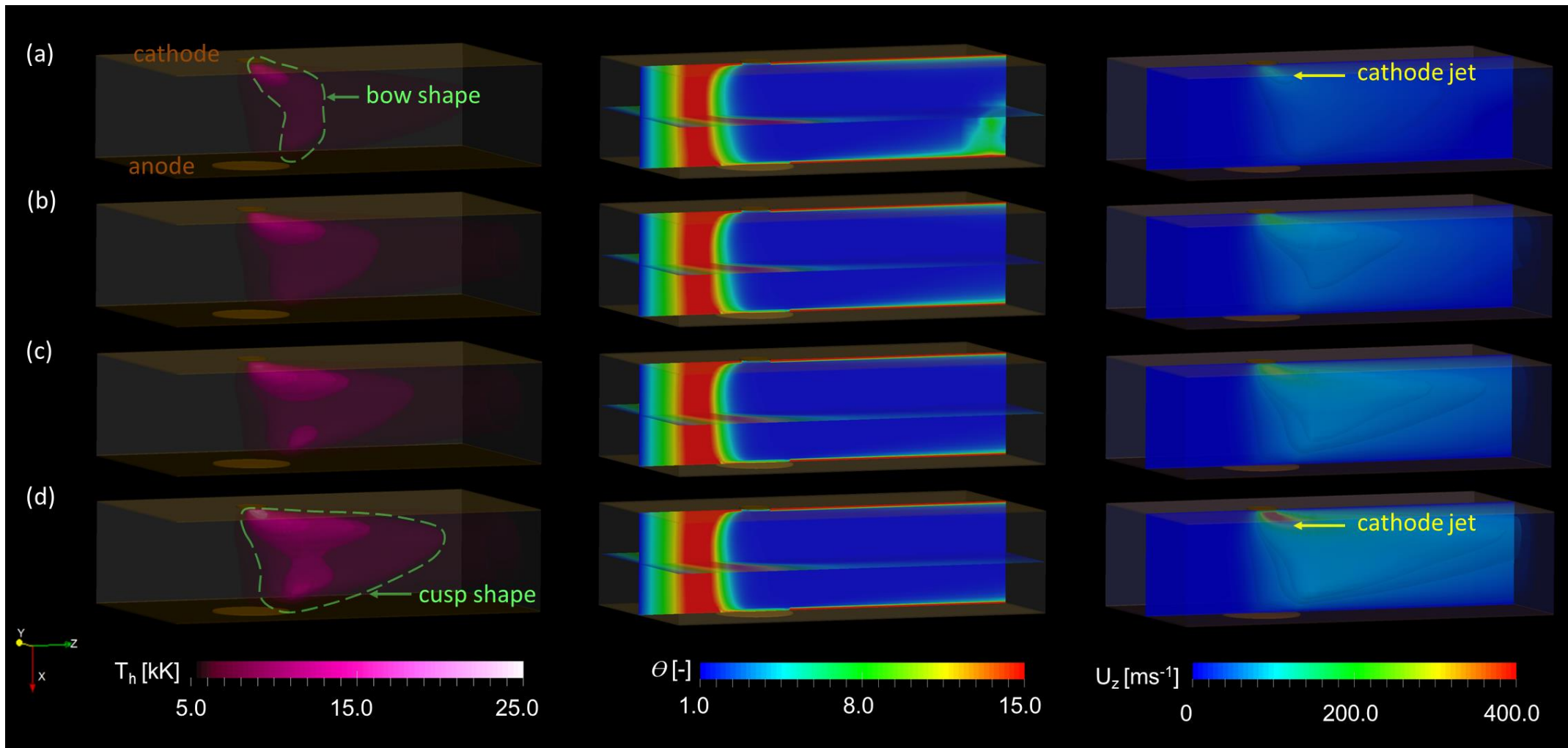
- Plasma applications such as wire-arc spraying and circuit breakers
- Interaction of an electric arc with a stream of cold gas flow perpendicular
- 3D, transient, thermodynamic nonequilibrium plasma flow model

Méthodes:

- an argon arc in crossflow using chemical equilibrium and thermodynamic non-equilibrium ($\theta=Te/Th$)
- fluid and electromagnetic equations in a fully-coupled manner using a Variational Multiscale Finite Element Method (VMS-FEM).
- Cathode current density applied at the cathode boundary follows a Gaussian distribution
- Cathode temperature T_c closer to the melting point of Tungsten
- Anode : exchange coefficient h_w
- Imposed currents 17, 25, 30 and and 34 A



- Asymmetry of flow due to cathode jet, diffuse attachment at the anode
- nonequilibrium upstream and close to the walls
- Cathode jet



Isosurfaces of heavy species temperature T_h (left), nonequilibrium parameter $\theta = T_e/T_h$ (center), and axial velocity u_z (right) for imposed currents (a) 17 [A], (b) 25 [A], (c) 30 [A], and (d) 34 [A] depicting the variation in arc shape from bow- to cusp-shape, the predominance of nonequilibrium upstream of the arc, and the cathode jet.

Numerical study of the non-local chemical equilibrium characteristics in a free-burning argon arc

Heng Guo¹, Jian Chen¹, Wen Zhou², Zeng-Yao Li², He-Ping Li¹

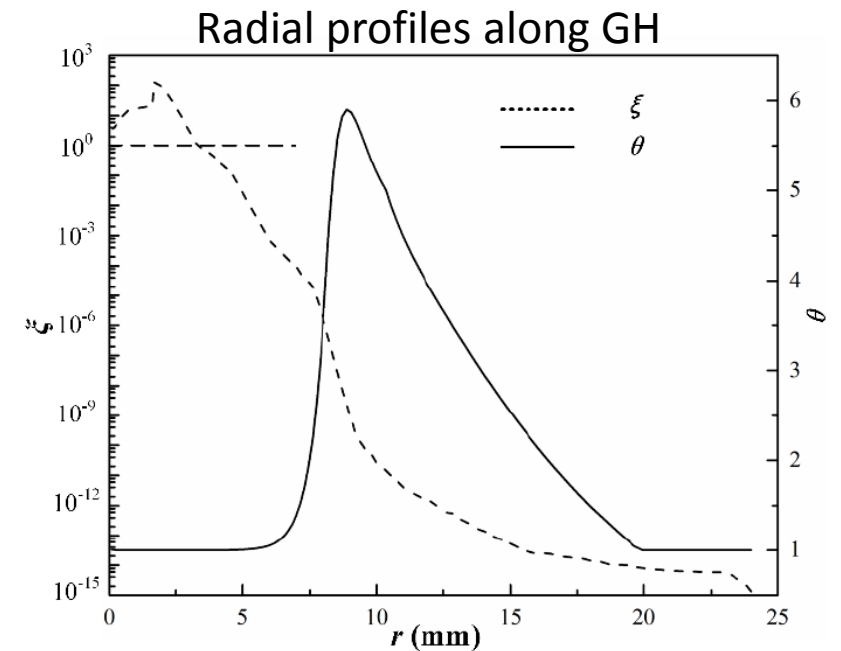
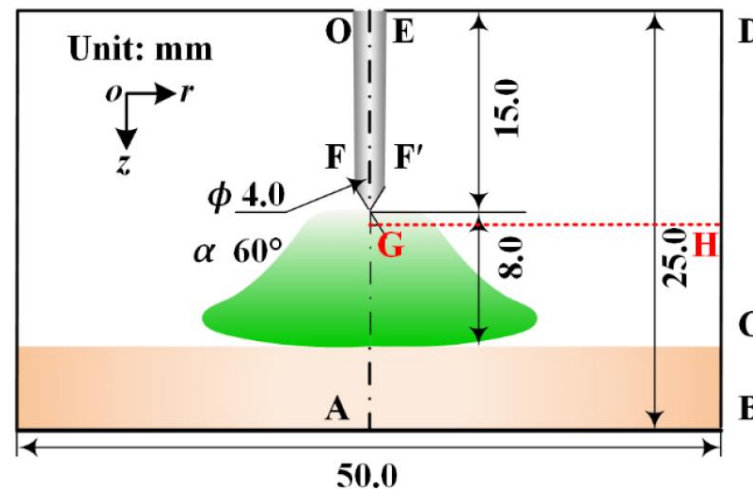
¹Department of Engineering Physics, Tsinghua University, Beijing 100084, P. R. China

²Key Laboratory of Thermal Fluid Science and Engineering, Ministry of Education, Xi'an Jiaotong University, Xi'an 710049, P. R. China

Abstract: A two-temperature non-local chemical equilibrium model is employed to study the chemical processes in a free-burning argon arc. The radial profiles of the temperature ratios (T_e/T_h) from the arc axis to the cold gas region are obtained. The modeling results show that the energy transfer and particle balance processes are coupled strongly; and the chemical processes not only affect the species spatial distributions, but also have great influences on the electron (T_e) and heavy-particle temperature (T_h) distributions.

- Free-burning argon arc
- 1-D collisionless electrode sheath model
- 2T model - $\theta = T_e/T_h$
- Chemical non-equilibrium

$$\xi = r_{\text{ioni}}/r_{\text{recomb}}$$



Modelling of three gas mixtures in gas metal arc welding

Hunkwan Park¹, Marcus Trautmann^{1,2} and Anthony B. Murphy¹

¹ CSIRO Manufacturing, PO Box 218, Lindfield NSW 2070, Australia

² Institute of Manufacturing Technology, Dresden University of Technology, George-Bahr-Str. 3c, D-01069 Dresden, Germany

Abstract: The initial simulation using combined diffusion coefficient method is presented to consider three gas mixtures in gas metal arc welding. It focuses on mixing of iron vapour and shielding gas of a mixture of two gases, and two separate equations of conservation of mass fraction for species are required. Results obtained by including and neglecting iron vapour or different shielding gas mixtures are compared. The model could be used for applications of thermal plasmas including three gas mixtures.

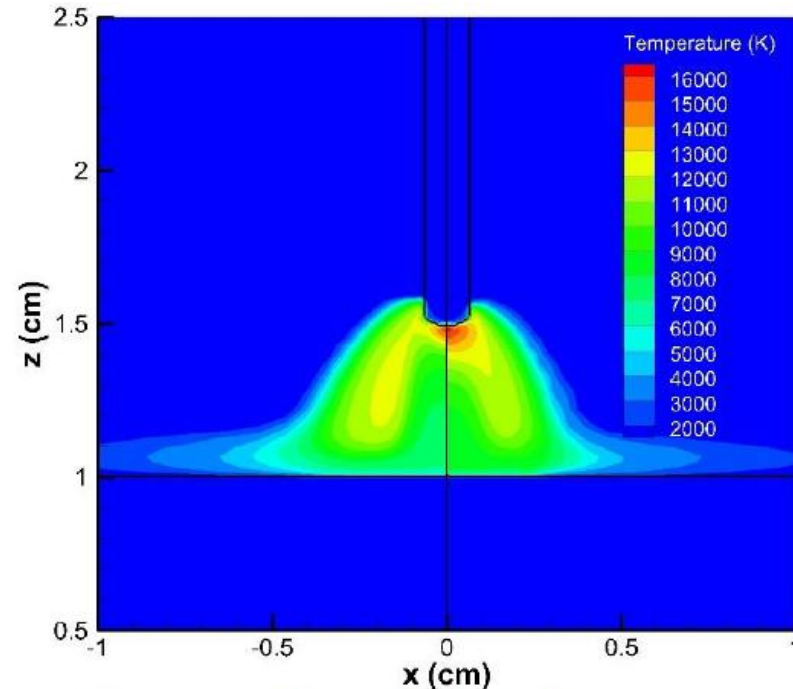
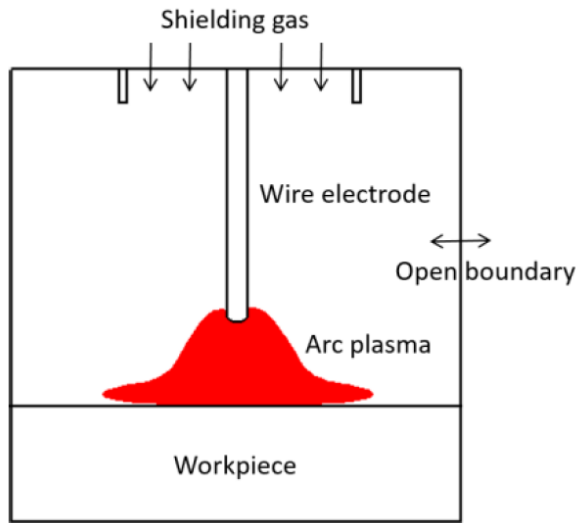


Fig. 4. Temperature distribution for shield gas containing 5 mol% oxygen (left) and 20 mol% oxygen (right)

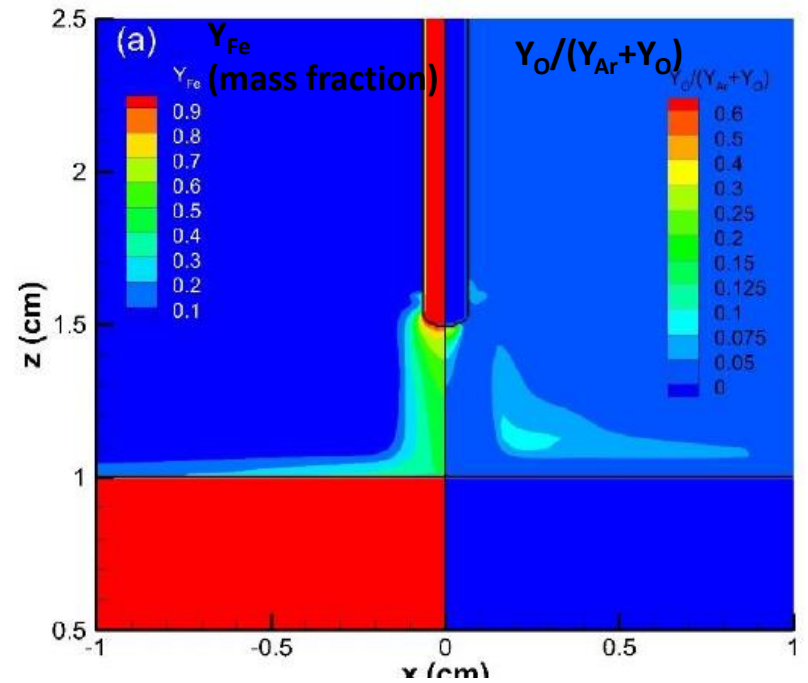


Fig. 3. Mass fraction of iron vapour (left) and oxygen in the shielding gas (right) for shielding gas containing (a) 5 mol% oxygen.

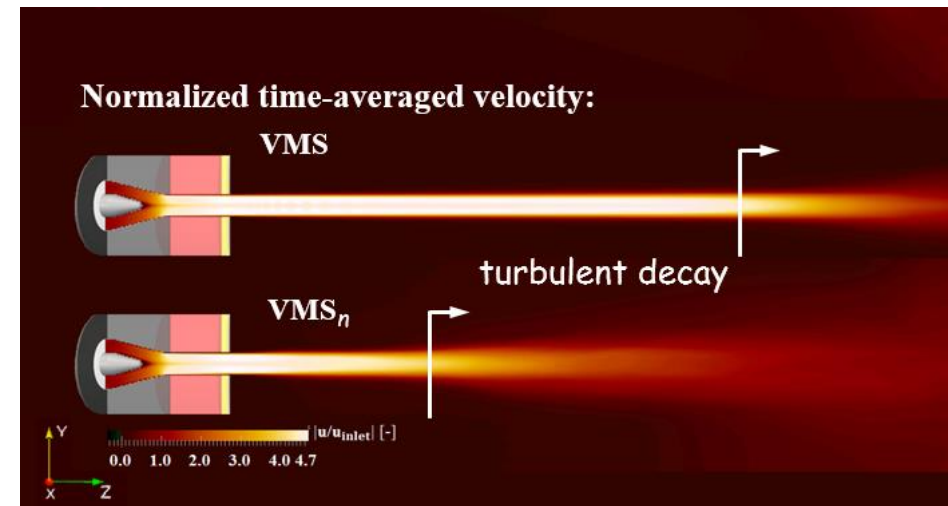
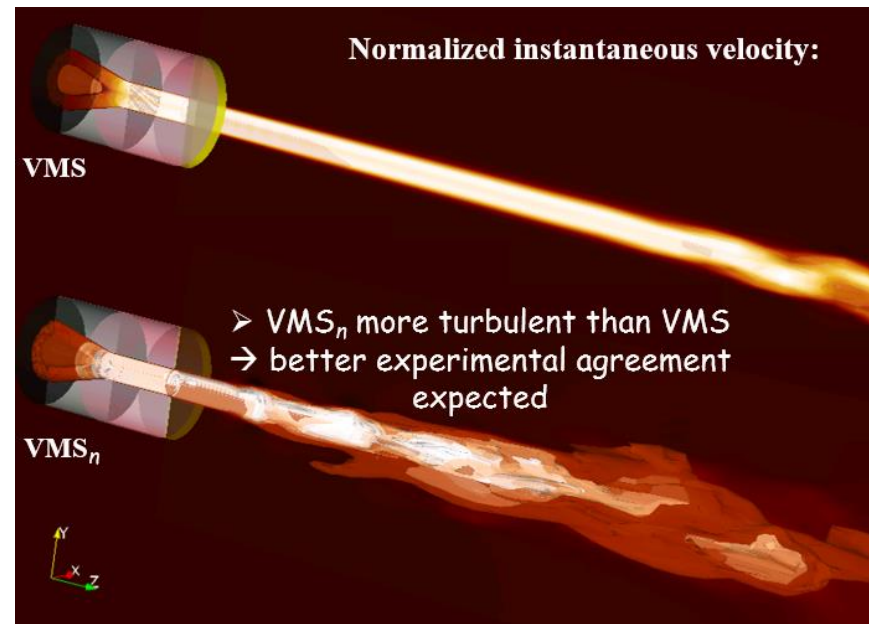
Simulation of the Turbulent Flow from a Non-Transferred Arc Plasma Torch

S.M. Modirkhazeni and J.P. Trelles

University of Massachusetts Lowell, Department of Mechanical Engineering, Lowell, MA, United States of America

Abstract: Non-transferred arc plasma torches are at the core of diverse applications such as plasma spray and waste treatment. The flow in these torches transitions from laminar inside the torch to turbulent in the emerging jet. There is no established approach for the modeling and simulation of turbulent plasma flows. The Variational Multiscale- n method is presented for the comprehensive modeling of general multiscale transport problems, such as turbulent plasma flows, and applied to the simulation of the flow in an arc plasma torch.

- Incompressible turbulent flow in a non-transferred arc jet
- 2T, argon



On the effect of inhomogeneous mixing of plasma species in argon–steam arc discharge

J. Jeništa¹, H. Takana², S. Uehara², H. Nishiyama², M. Bartlová³, V. Aubrecht³, A. B. Murphy⁴

¹*Institute of Plasma Physics AS CR, v.v.i., Praha 8, Czech Republic*

²*Institute of Fluid Science, Tohoku University, Sendai, Miyagi, Japan*

³*Brno University of Technology, Brno, Czech Republic*

⁴*CSIRO Materials Science and Engineering, Lindfield, NSW, Australia*

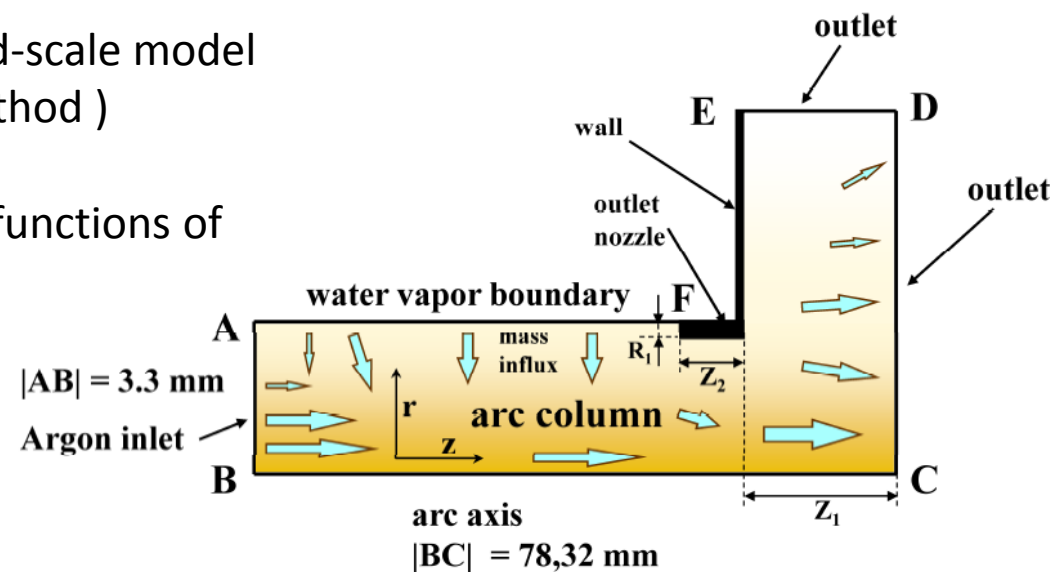
Contexte et objectifs

Investigation of the effect of mixing of argon, oxygen and hydrogen plasma species on the thermal and fluid-dynamic properties of the hybridstabilized argon-water electric arc

Méthodes

- Argon-water plasma at LTE, axisymmetrical 2D, turbulent flow (LES), compressible, Large eddy simulation (LES) with the Smagorinsky subgrid-scale model
Self-induced magnetic field, radiation losses (partial characteristics method)

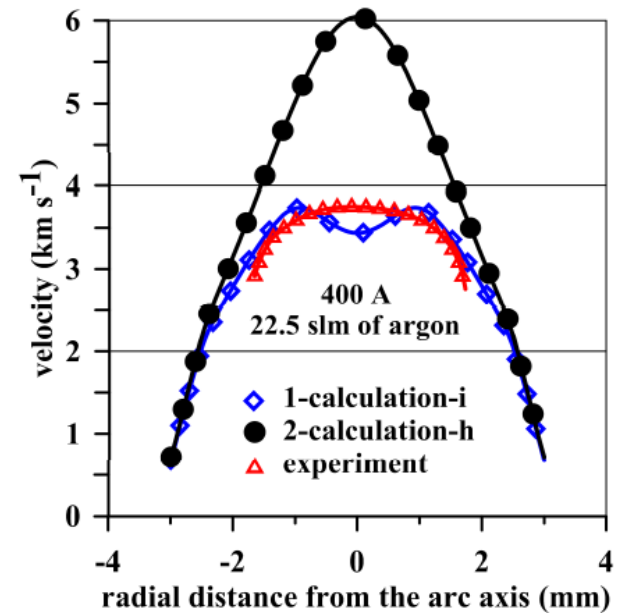
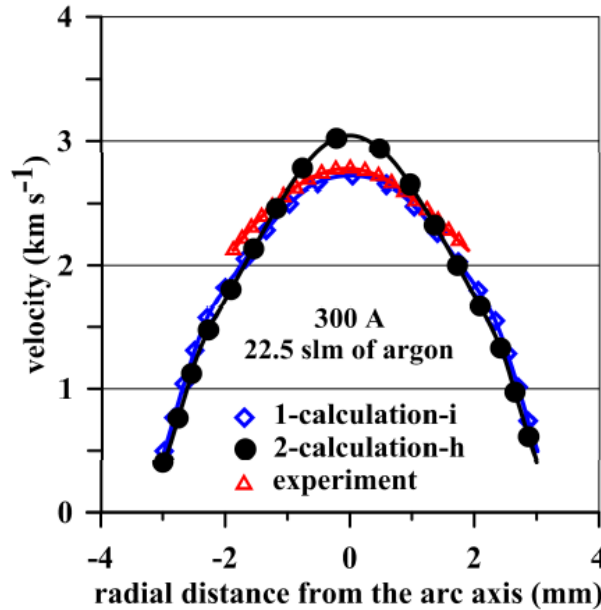
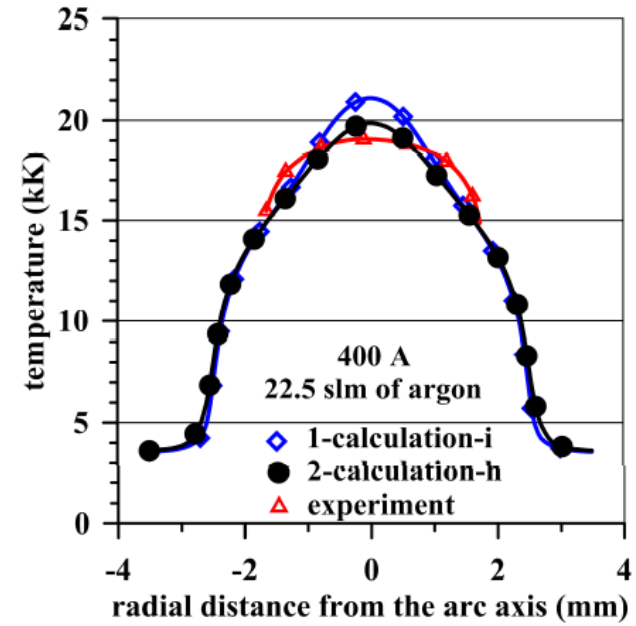
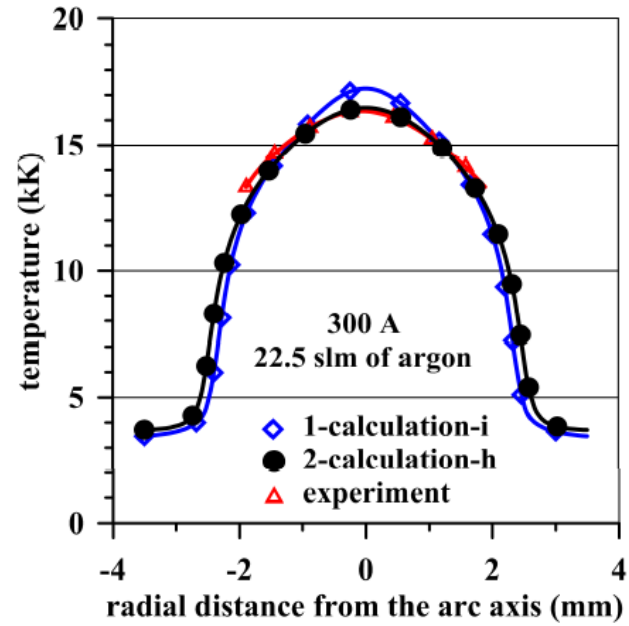
- Equation for argon species flux with combined diffusion coefficients (functions of temperature, pressure and argon mass fraction)



Résultats

h: homogeneous mixing model
Neglects the mixing process
argon mass fraction constant within the
calculation domain

i: inhomogeneous mixing model
considers the mixing process



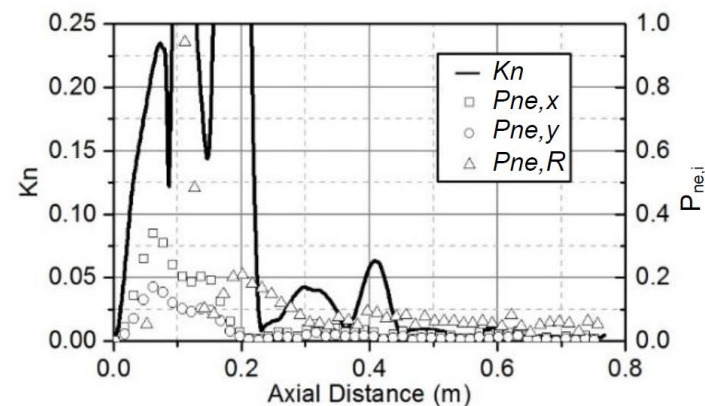
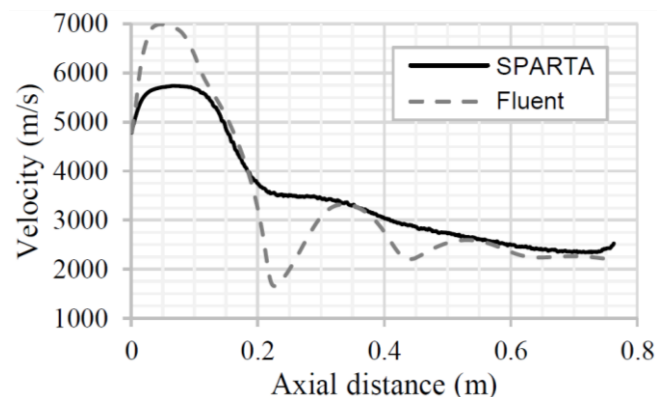
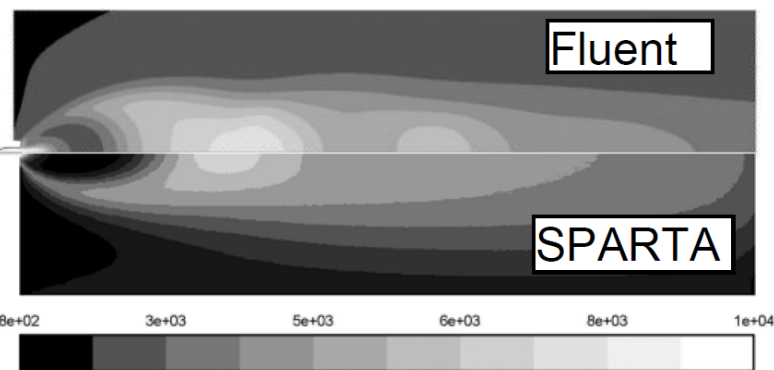
Validity of the continuum approach in the modelling of very low pressure plasma spraying

D. Ivchenko¹, T. Zhang¹, G. Mariaux¹, A. Vardelle¹, S. Goutier¹, T. E. Itina²

¹Université de Limoges, Limoges, France

²Université Jean Monnet, Saint-Étienne, France

Abstract: Plasma Spray Physical Vapor Deposition (PS-PVD) is a rapidly developing technology to producing thick nanostructured coatings with various microstructures. Further enhancement of the technology requires experimental and numerical studies. The commonly used continuum Computational Fluid Dynamics (CFD) approach, may be doubtful under PS-PVD conditions as the high pressure plasma jet issues in a low pressure (about 100 Pa) chamber. This work aims to compare the predictions of CFD and kinetic simulation for a set of typical PS-PVD operating conditions and investigate the breakdown of the CFD approach.



Plasma temperature
 Comparison CFD simulation (Fluent) with
 Direct Simulation Monte-Carlo (Sparta)

$$P_{Tne,i} = |(T_{Tr} - T_i)/T_{Tr}|$$

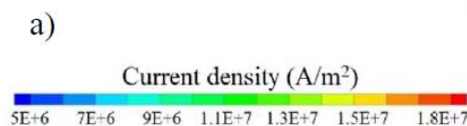
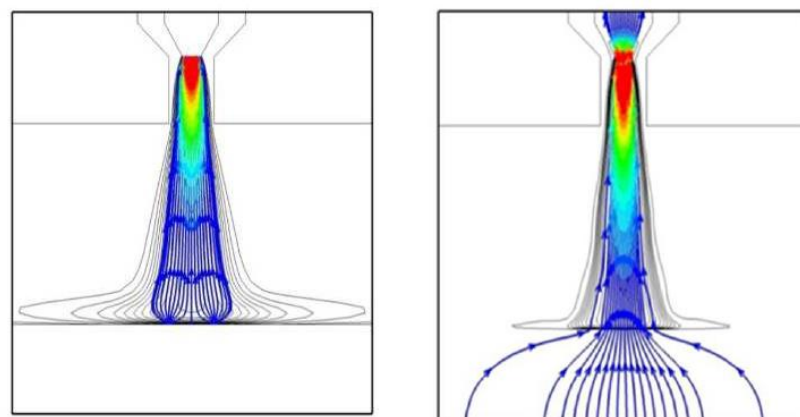
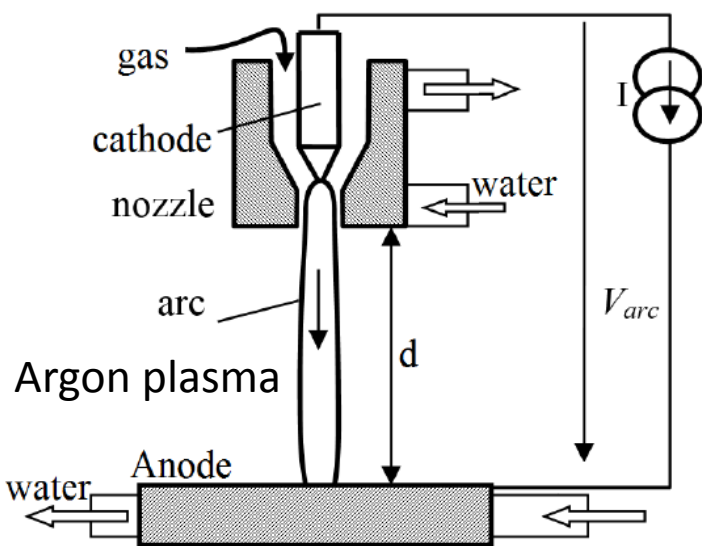
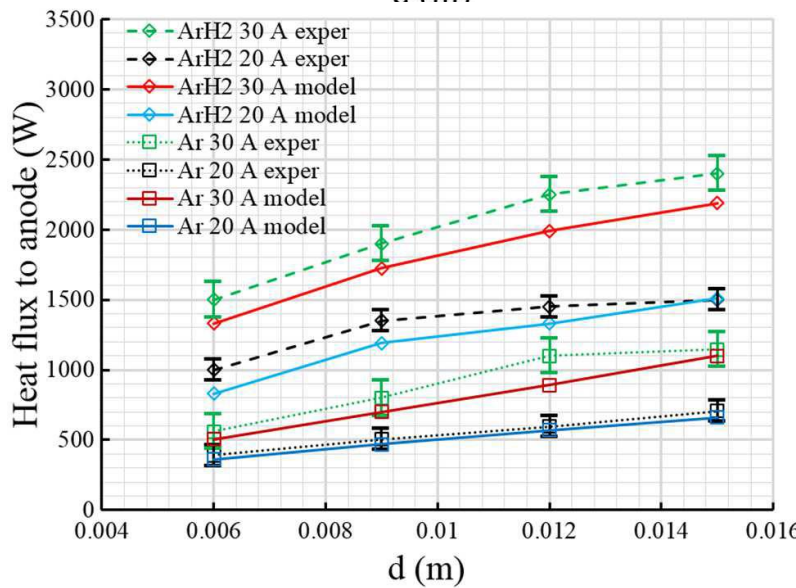
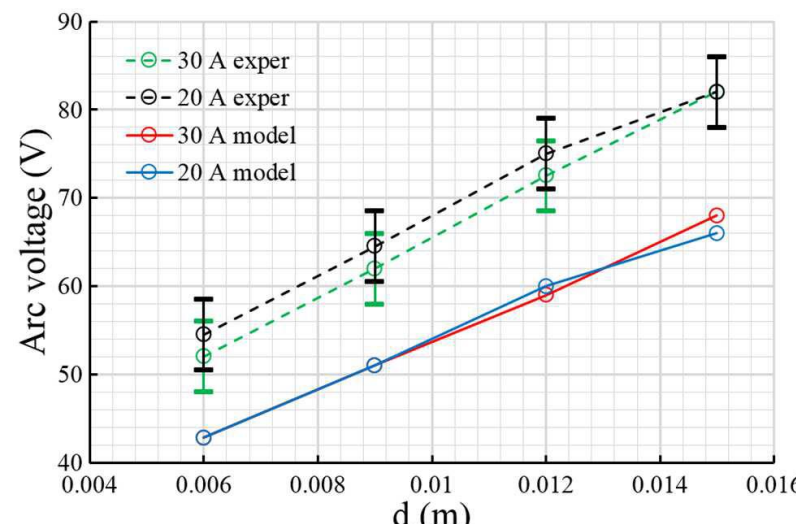
Model and validation of DC transferred arc with a constricting nozzle

C. Chazelas¹, R. Zhukovskii¹, M. Alaya² and A. Vardelle¹

¹Laboratoire Sciences des Procédés Céramiques et de Traitements de Surface, Université de Limoges, Limoges, France

²Algo'Tech Informatique, Bidart, France

Abstract: this study deals with the modelling of a transferred arc stabilized by a gas flow parallel to the cathode and a constricting nozzle. It is a step towards the predictive model of a plasma spray torch with a cascaded anode and thus an arc length fixed in a small range of variation. The model solved the heat and electromagnetic equations in the electrodes and gas and, the Navier-Stokes equations in the gas phase. The predictions of arc voltage and heat flux to anode were validated against experimental data. The model predicted correctly the trends with the variation of the operating parameters and the correct heat flux to anode. However, the predicted voltage was about 15 V lower than the experimental one whatever the operating conditions.



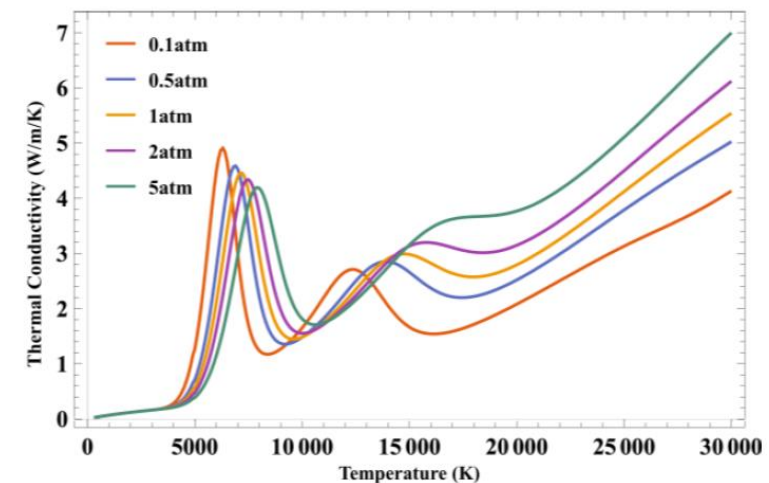
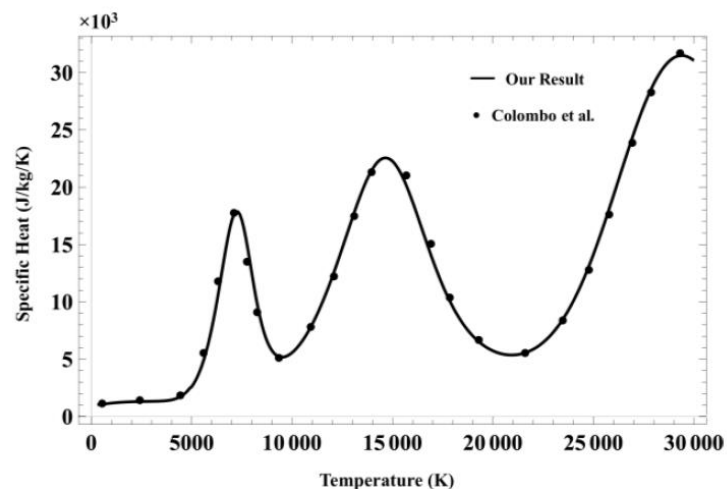
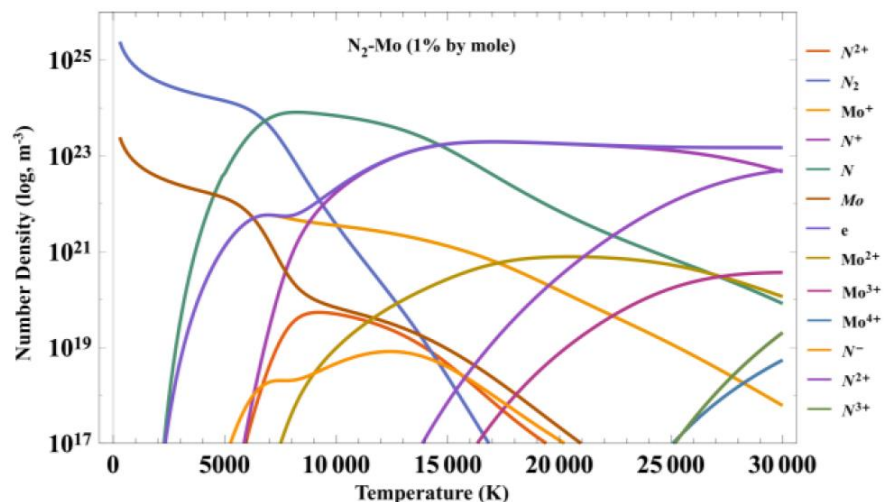
Thermodynamic and transport properties of nitrogen plasmas mixed with molybdenum vapor

Xiao-Ning Zhang¹, Anthony B. Murphy²

¹Research Centre of Space Basic Science, Harbin Institute of Technology, Harbin, Heilongjiang, China

²CSIRO Manufacturing, PO Box 218, Lindfield NSW, Australia

Abstract: Motivated by the influence of metal-electrode erosion on the performance of high-energy spark gap switches, the thermodynamic and transport coefficients of nitrogen plasmas mixed with molybdenum vapor are studied in this paper. The calculations, which assume local thermodynamic equilibrium, were performed for pressures from 0.1 to 5 atm and for the temperature range 300-30 000 K. Some of the results are compared with those of previously published studies, and the influence of molybdenum vapor is discussed.



Procédés et mesures

Time-resolved optical and spectroscopic study of the restrike mode in arc plasma torch

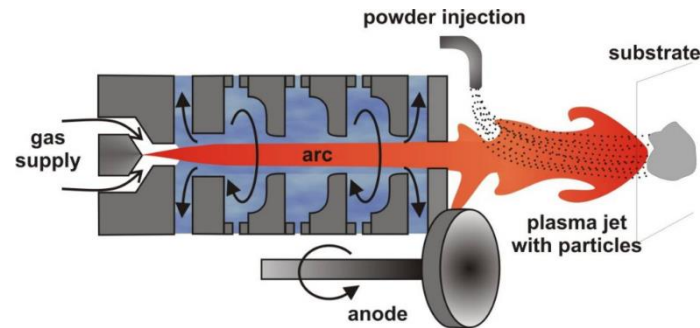
Alan Mašláni, Peter Ondáč, Viktor Sember, Milan Hrabovský

Institute of Plasma Physics AS CR, Prague, Czech Republic

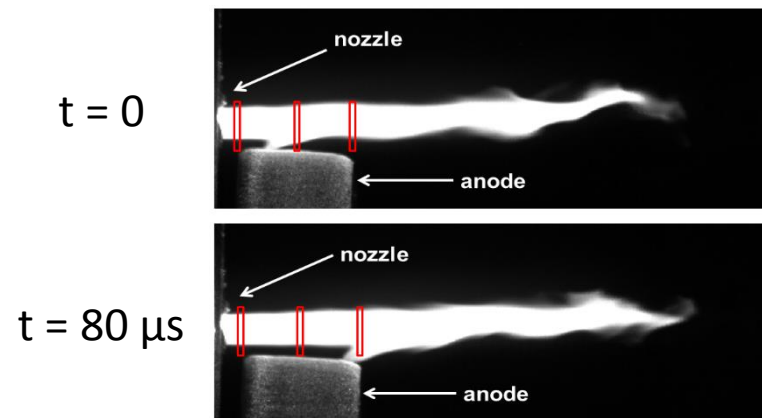
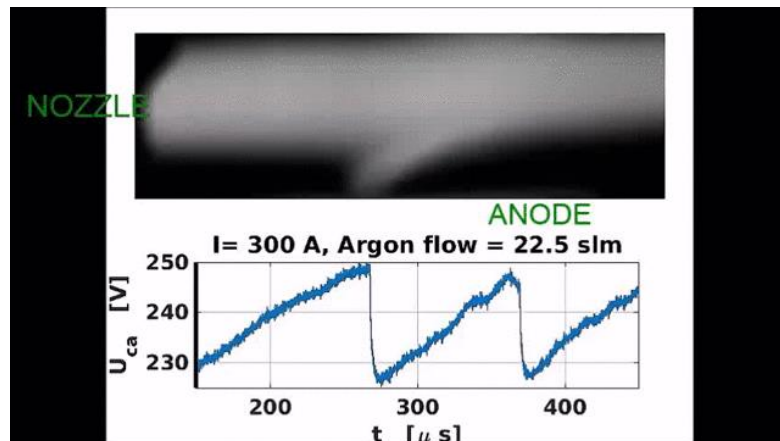
E-mail: maslani@ipp.cas.cz

Contexte et objectifs

- Plasma spraying, waste treatment and gasification of organic components – syngas (CO + H₂)
- Study of restrike mode by time-resolved optical emission spectroscopy and fast imaging
- Temperature measurements during restrike period



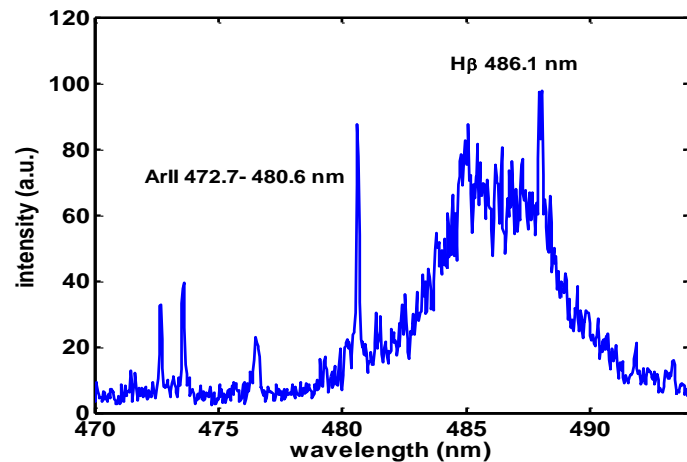
Méthodes



Different axial positions of spectrometer slit

Exposure time of fast imaging : 1 μs
Exposure of OES : 10- 20 μs
Spectra integrated line-of-sight and radially

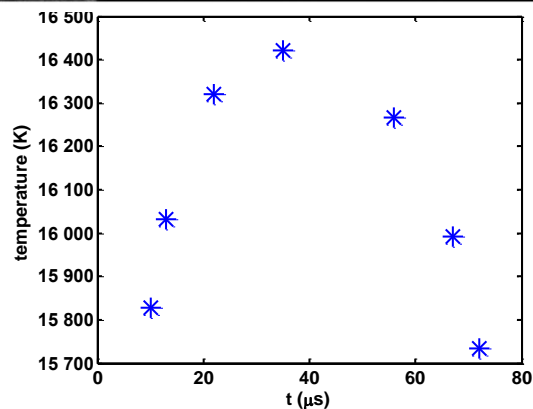
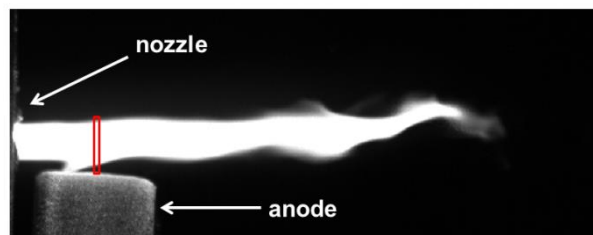
- Spectral window containing H β and four ArII lines
- LTE composition of H₂O-Ar plasma
- Ratio H β /ArII is very sensitive to temperature



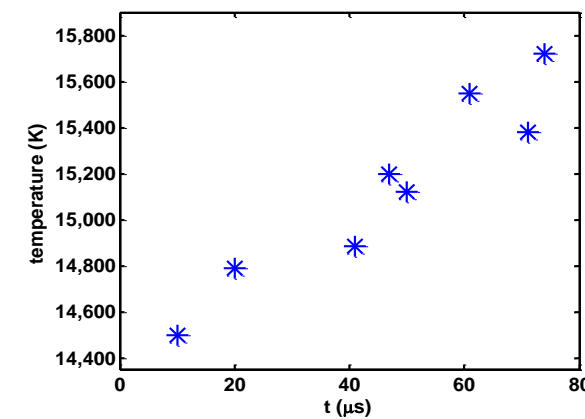
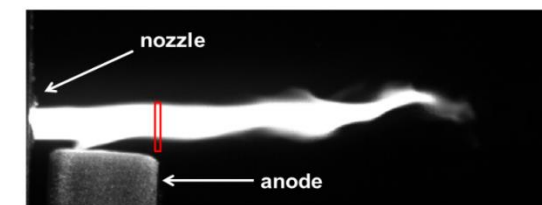
Experimental conditions

- Arc current (DC) 500 A
- Arc voltage ~ 280 V
- Arc power ~ 140 kW
- Argon flow rate 12 slm
- Arc column surrounded by water vortex - water evaporation rate ~ 0.3 g/s
- Nozzle diameter 6 mm
- Anode – rotating copper disc (thickness 16 mm, diameter 180 mm) 3 mm from the nozzle horizontally and 2 mm vertically

Résultats



Arc attachment goes through the entrance slit – departure from LTE near anode



Temperature increases with arc attachment approaching to the entrance slit

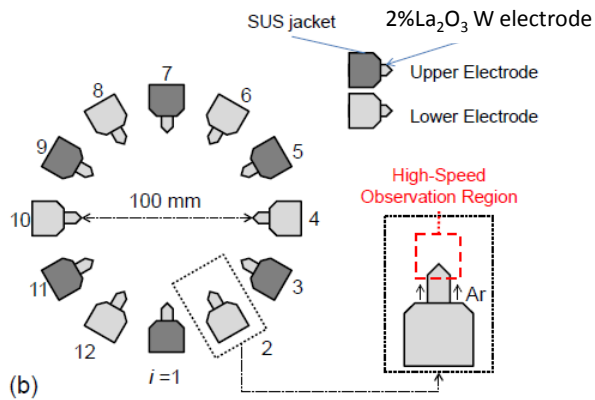
High-speed visualization of erosion phenomena of tungsten-based electrode in multiphase AC arc

T. Hashizume, M. Tanaka, T. Imatsuji, Y. Nawata and T. Watanabe
Department of Chemical Engineering, Kyushu University, Fukuoka, Japan

Contexte et objectifs

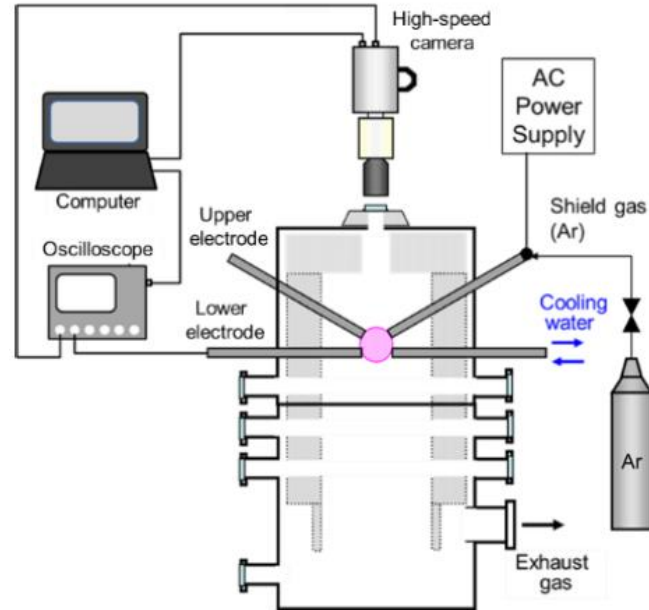
- Study of Multi-phase AC arc (MPA) for powder processing (nanopowder production, in-flight glass-melting technology)
- Improve electrode lifetime and purity of the products

Méthodes:

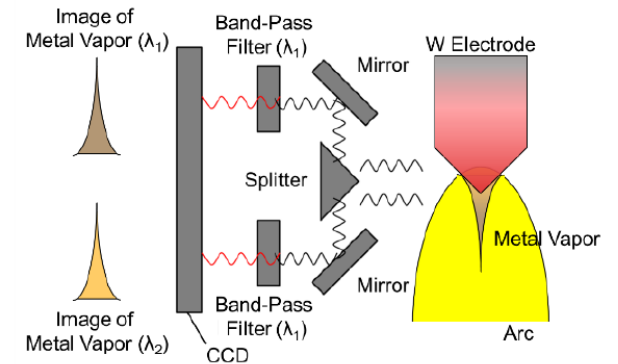


$$V_i^N = V_m^N \sin\left(\frac{\omega t - 2\pi(i-1)}{12}\right)$$

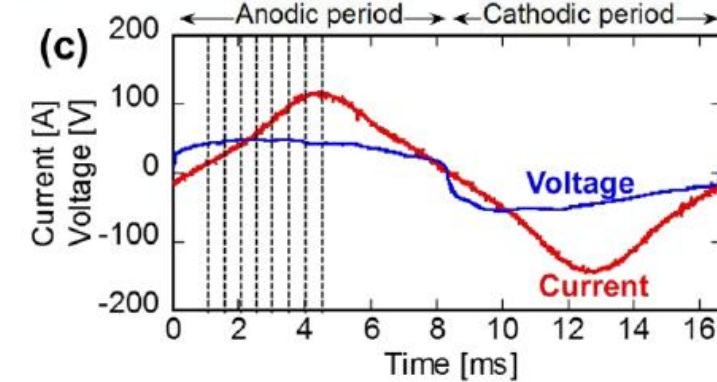
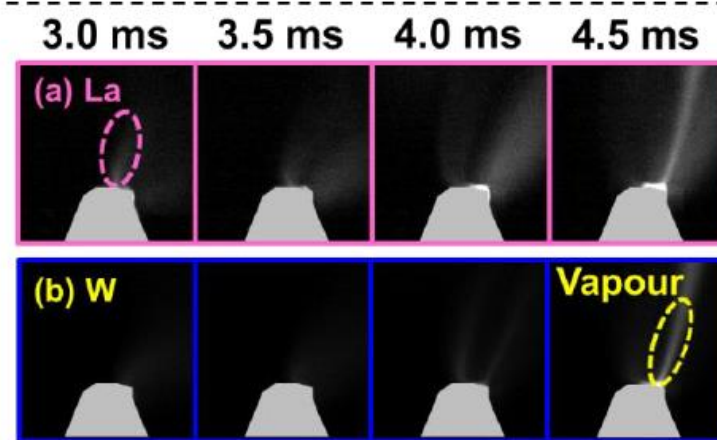
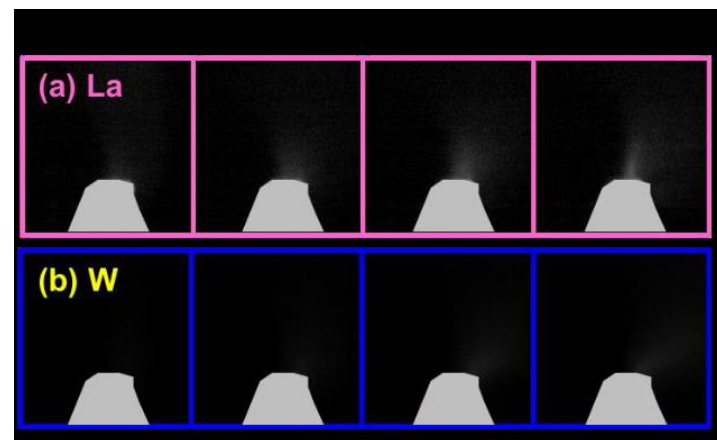
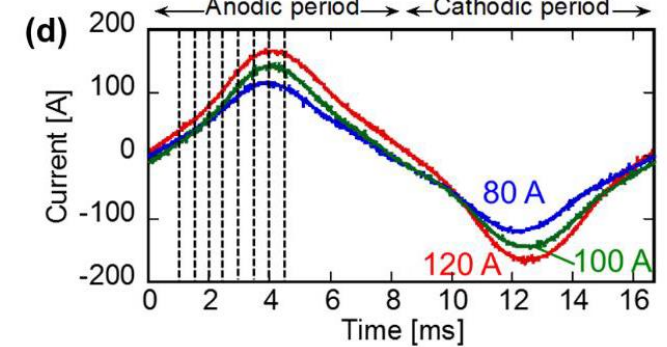
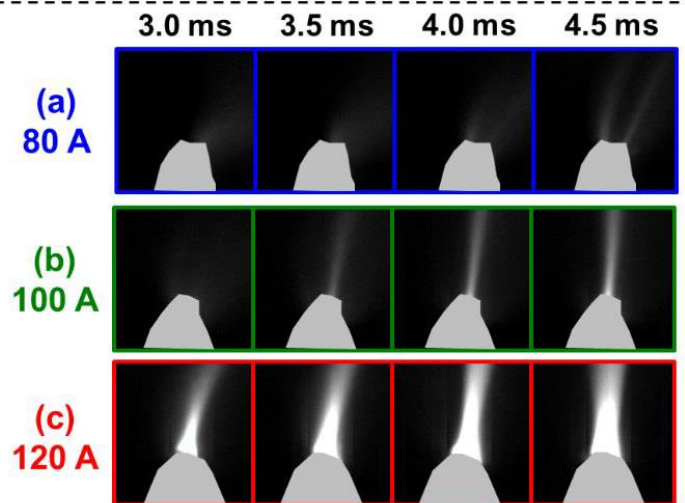
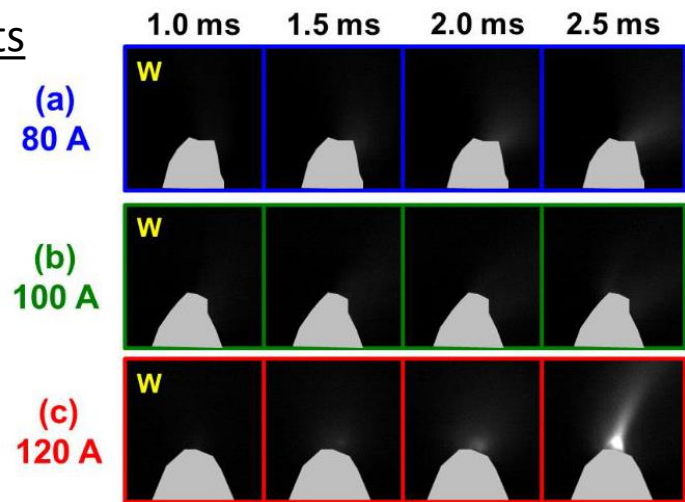
(220 V, AC 60Hz)



- High speed visualization of W vapor (393 nm) and La vapor (577 nm) during AC period
- Current 80-120 A



Résultats



- Evaporation of W electrode mainly observed at the anodic period
- W ions near the electrode tip return back to the electrode side due to electric field
- Higher evaporation as current increases and evaporation starts earlier during AC period
- La evaporation starts before W (lower boiling point for La oxide than W)
- La evaporation increases plasma electrical conductivity resulting in an increase of heat flux => W evaporation

Improvement of electrode erosion characteristics in diode-rectified multiphase AC arc

M. Tanaka¹, K. Saga¹, T. Hashizume¹, T. Matsuura² and T. Watanabe¹

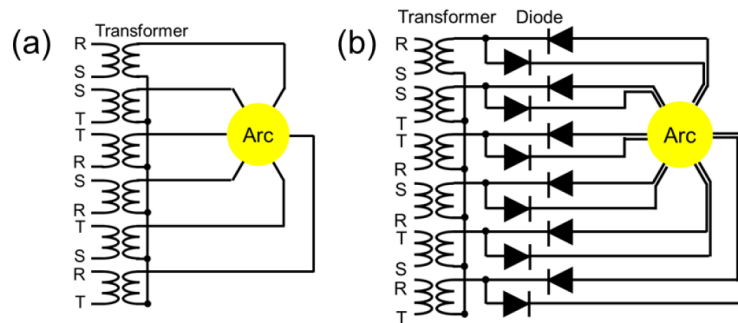
¹Department of Chemical Engineering, Kyushu University, Fukuoka, Japan

²Taso Arc Co., Fukui, Japan

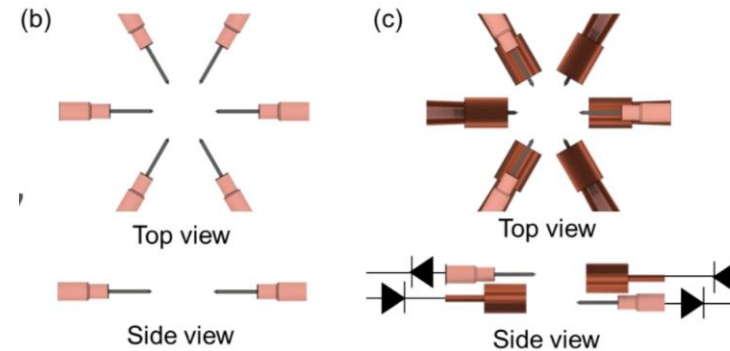
Contexte et objectifs

- Study of Multi-phase AC arc (MPA) for in-flight glass-melting technology
- Electrode erosion depends on material properties and arc current period (tungsten cathode, copper anode)
- Improve electrode lifetime and purity of the products by means of Diode-Rectified MPA

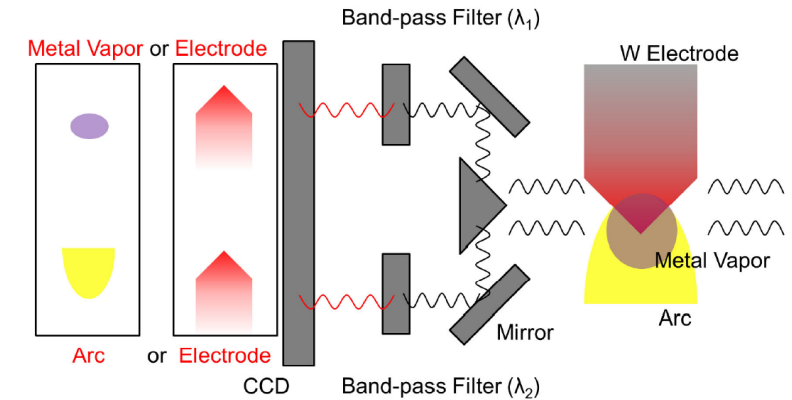
Méthodes:



Schematic electric circuits for conventional MPA (a) and innovative DRMPA (b).



schematic of electrode configuration for MPA (b) and DRMPA (c)



$$V_i^N = V_m^N \sin\left(\frac{\omega t - 2\pi(i-1)}{12}\right) \quad (220 \text{ V, AC } 60\text{Hz})$$

- Fast imaging (10⁴ f/s)
- Two color pyrometry by using high-speed camera with band-pass filters (785-880 nm)

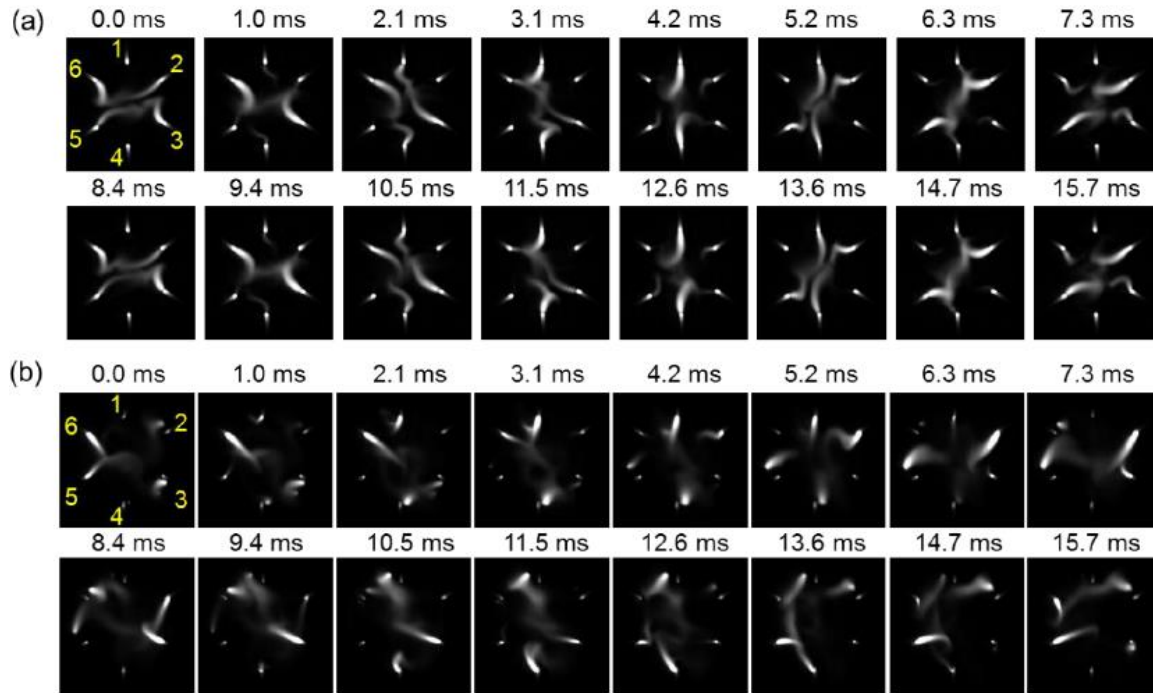


Fig. 3. High-speed snapshots of MPA (a) and DRMPA (b) during an AC cycle.

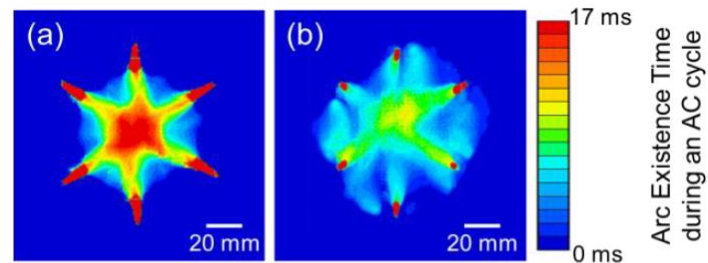


Fig. 4. Existence time of MPA (a) and DRMPA (b) during an AC cycle.

- MPA: arc constriction at electrode : anodic/cathodic jets
- DRMPA anode was not constricted: low evaporation of copper (high thermal conductivity of copper anode)
- Larger plasma volume with DRMPA
- Lower erosion with DRMAP
- DRMAP tungsten electrode temperature lower than melting point

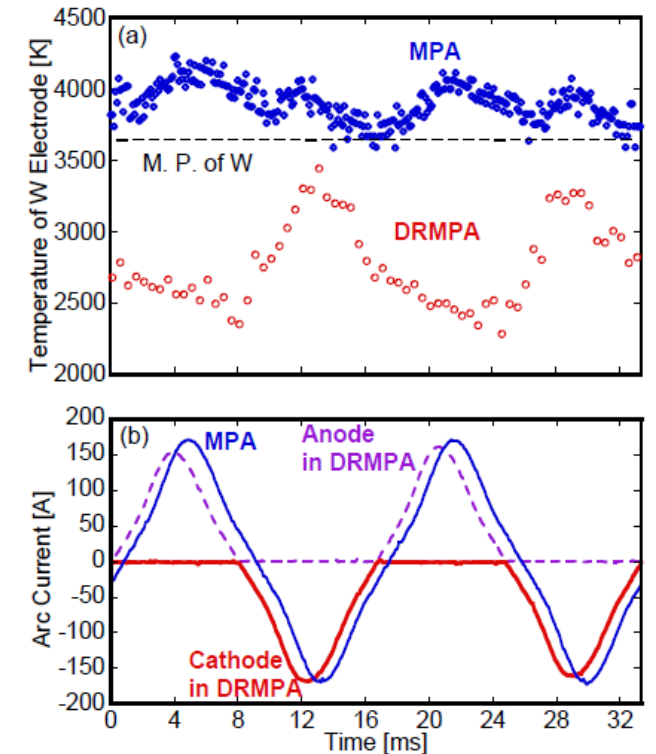
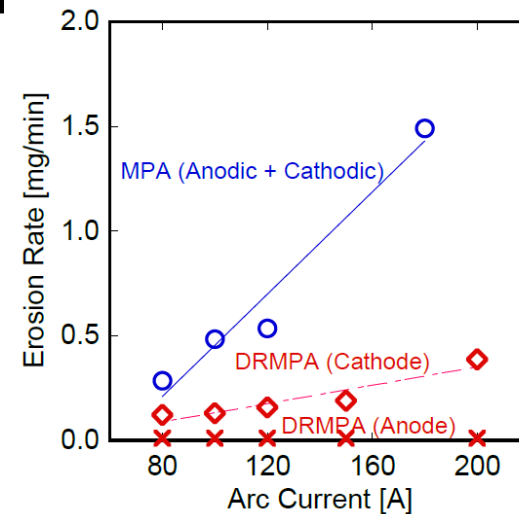


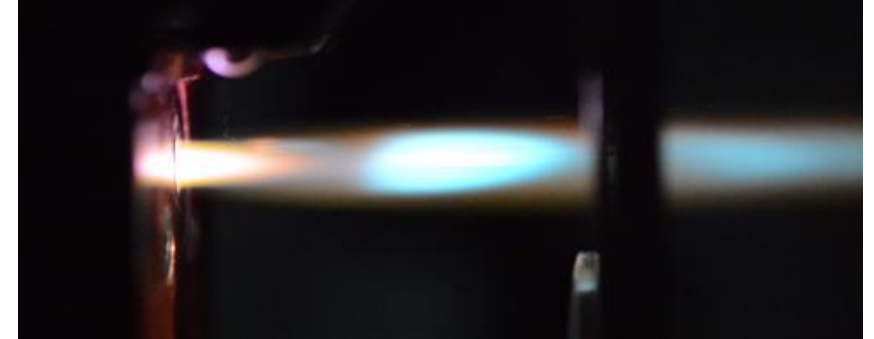
Fig. 7. Time variation of tungsten electrode temperature during an AC cycle (a) and corresponding waveforms of arc current (b).

DC arc plasma torch in pulsed mode: Properties and application to plasma spraying of liquid feedstock

Vincent Rat, Université de Limoges

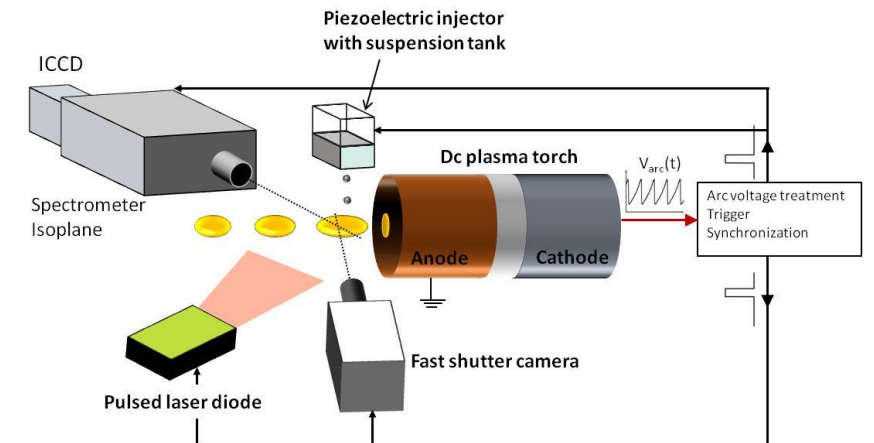
Contexte et objectifs

- Plasma spraying of liquid feedstock in pulsed mode
- Improve heat and momentum transfers to liquid and coating properties
- influence of arc current modulation
- Study of plasma properties and coating elaboration



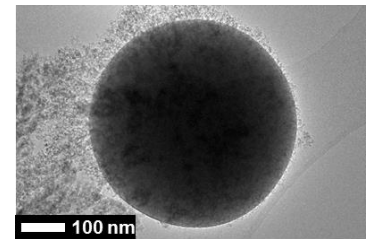
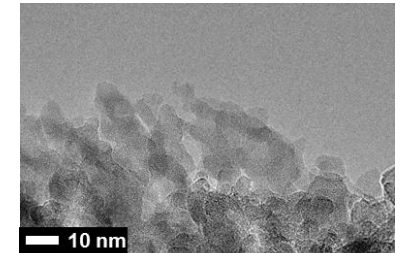
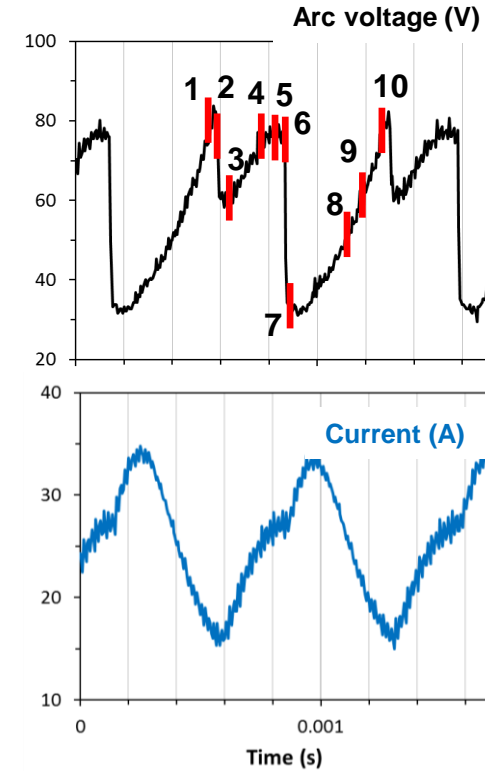
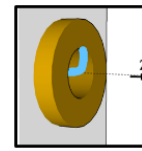
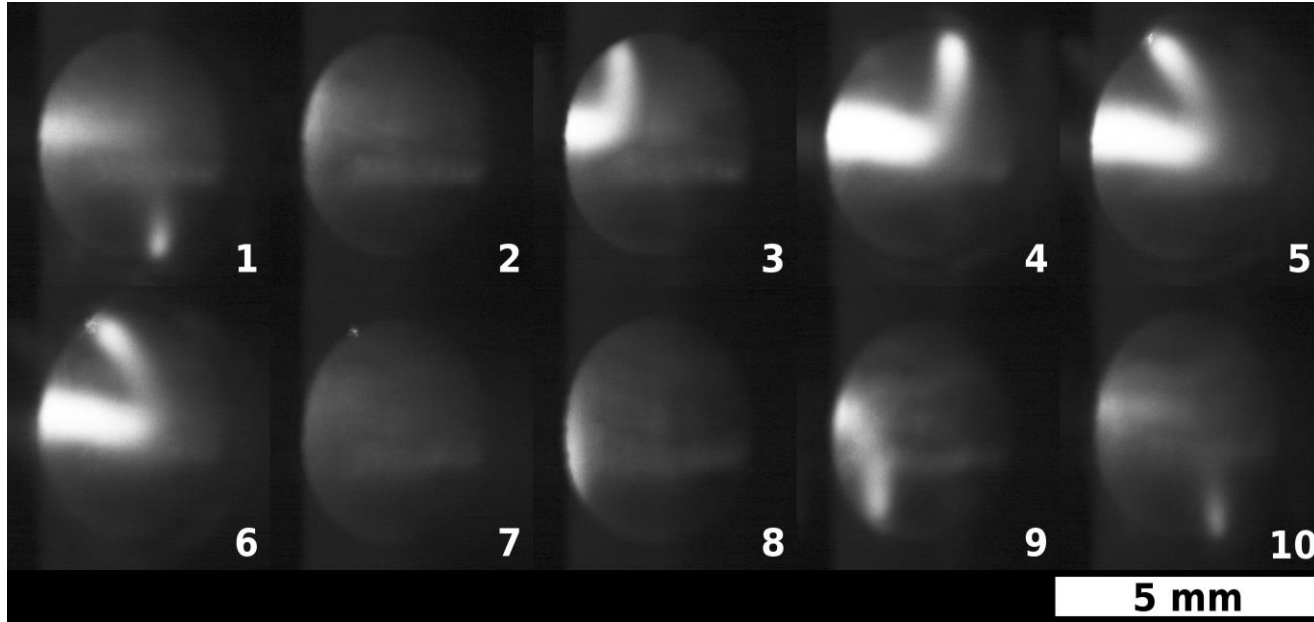
Méthodes:

- Application of arc current modulation $I(t) = I_0(1 + \alpha \sin(2\pi f_0 t))$
- Electrical and acoustical characterization
- Time-resolved end-on imaging of the arc inside the channel and time-resolved OES
- Synchronous injection of solution precursors (aluminum nitrate) : Imaging +OES
- Elaboration of aluminum oxide coatings (material characterizations)

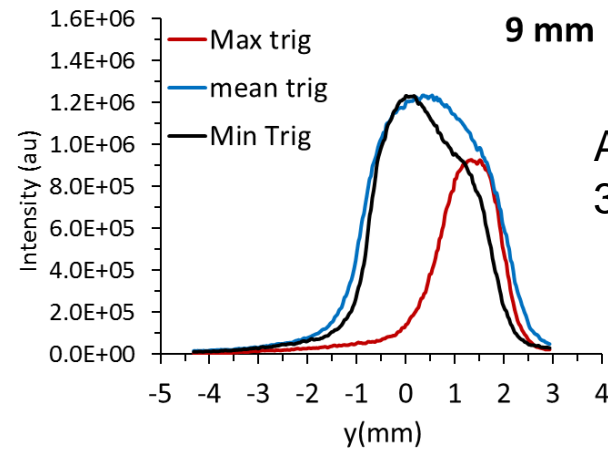
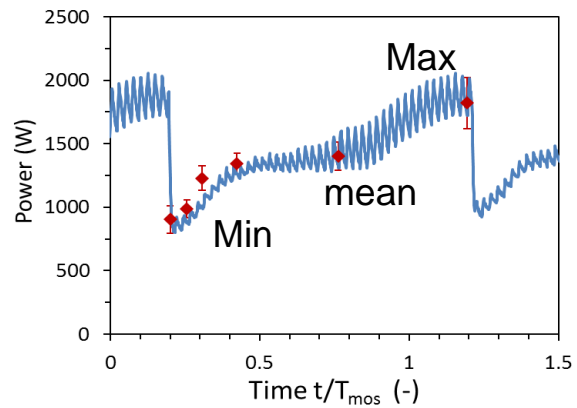


Résultats

Time-resolved end-on imaging

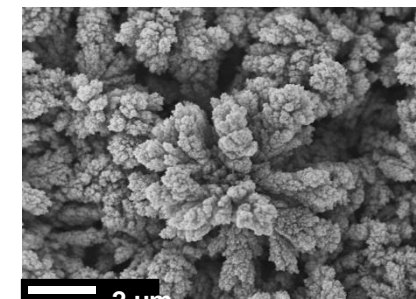


Influence of synchronous injection



Al (II)
 308 nm

Aluminum oxide coatings



Two-dimensional distribution of Ti vapor admixture ratio and Ti atomic density in the Ar ICTP torch during Ti feedstock injection

N. Kodama¹, Y. Ishisaka¹, K. Shimizu¹, Y. Tanaka¹, Y. Uesugi¹, T. Ishijima², S. Sueyasu³, S. Watanabe³, K. Nakamura³

¹Faculty of Electrical & Computer Eng., Kanazawa Univ., Kanazawa, Japan

²Research Center for Sustainable Energy & Technol., Univ., Kanazawa, Japan

³Research Center for Production & Technol., Nisshin Seifun Group Inc., Fujimino, Japan

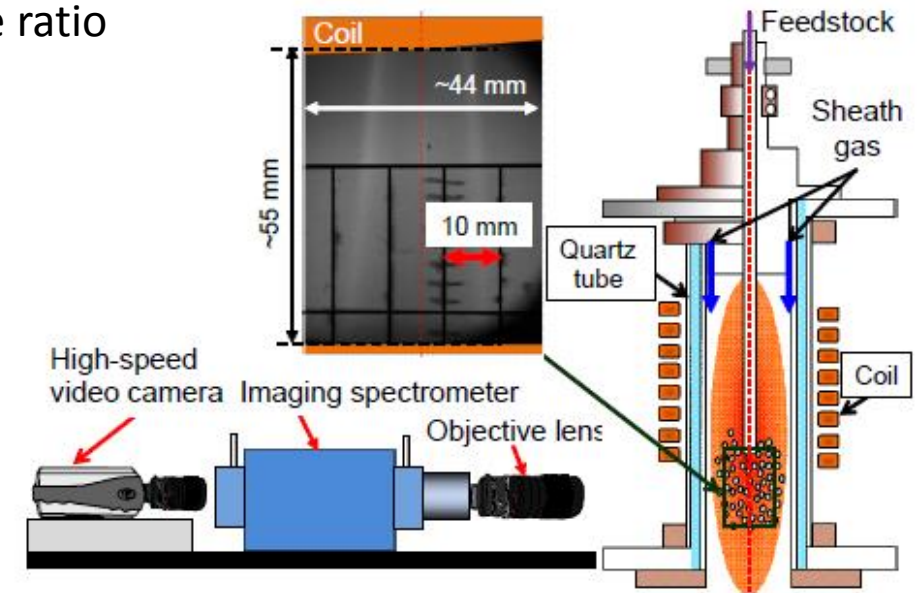
Contexte et objectifs

- Materials processing (nanomaterial synthesis or surface modification) by means of inductively coupled thermal plasma (ICTP)
- Experimental investigation on feedstock evaporation and spatial/temporal measurement of feedstock vapor during material processing using ICTPs (synthesis of TiO₂ nanoparticles)

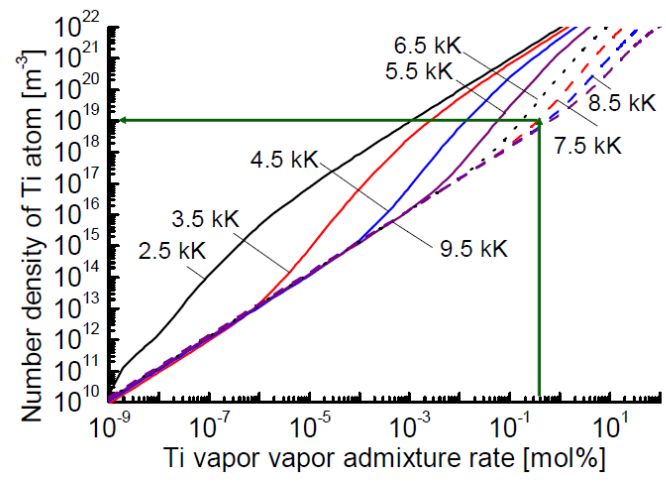
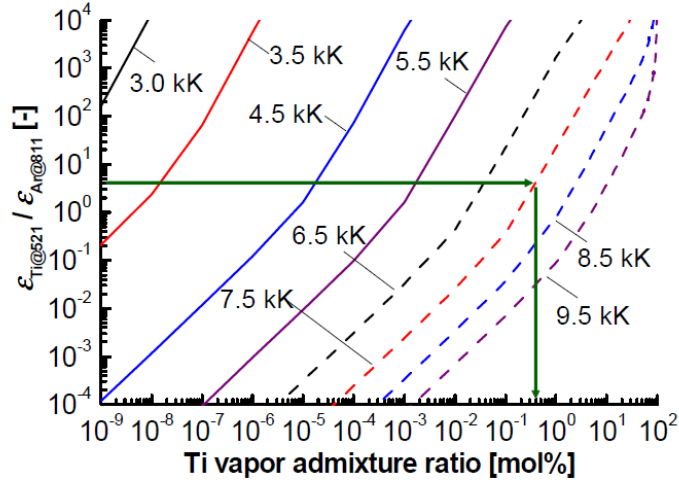
Méthodes:

- Spatio-temporal distribution of Ti excitation temperature, Ti vapor admixture ratio and number densities of Ti atoms and electrons during Ti feedstock injection into the Ar ICTP torch (LTE assumption)
- Continuous or intermittent injection of Ti feedstock

Observation area	44 × 55 mm ² region below the coil end
Diffraction grating	1200 grooves·mm ⁻¹
Wavelength resolution	0.8 nm
Spectral lines observed	Ti I (453.32 nm) and Ti I (521.04 nm) Ar I (811.53 nm)
Frame rate for high speed video camera	1000 fps



- Measurement of Ti excitation temperature estimated by two-line method $I(\text{Ti@453nm})/I(\text{Ti@521nm})$
- Calculation of Ar-Ti plasma composition (%molTi) and $\epsilon(\text{Ti@521nm})/\epsilon(\text{Ar@811nm})$
- Comparison with measurements of $I(\text{Ti@521nm})/I(\text{Ar@811nm})$



Résultats

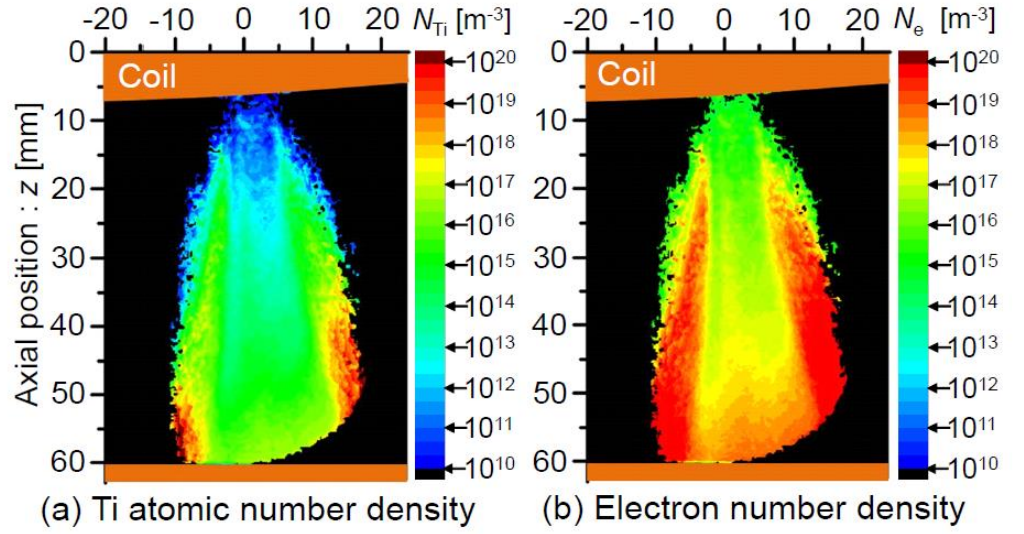
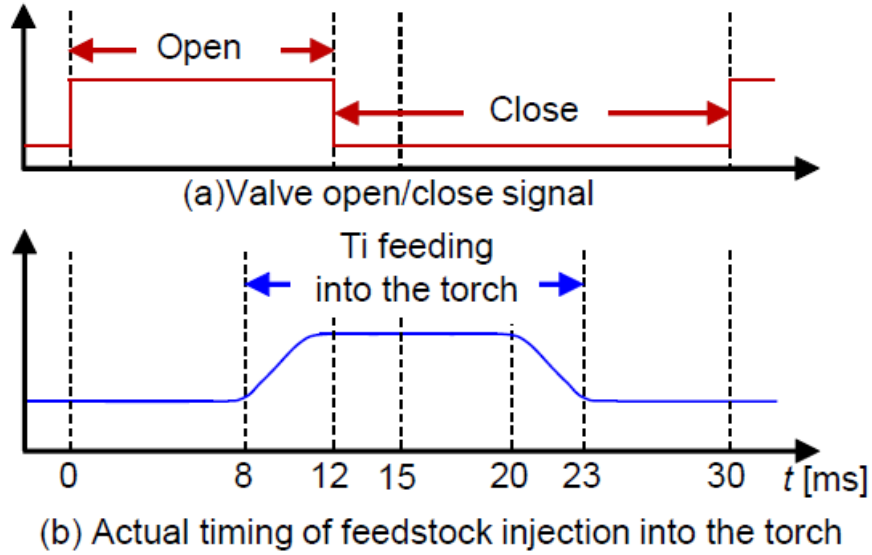


Fig. 10. N_{Ti} and N_e for IF condition at $t=18$ ms.

Plasma Torch Optimisation by Additive Manufacturing of Components

IJ van der Walt¹, PL Crouse², WB du Preez³

¹Plasma Technology Section, R&D, The South African Nuclear Energy Corporation SOC, Ltd., South Africa

² Department of Chemical Engineering, University of Pretoria, Private Bag X20, Hatfield 0028, South Africa.

³ Department of Mechanical and Mechatronics Engineering, Central University of Technology, Bloemfontein, South Africa

Contexte et objectifs

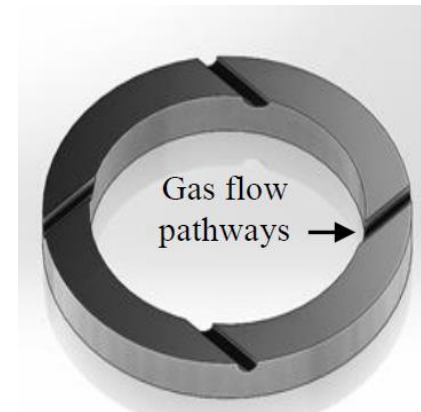
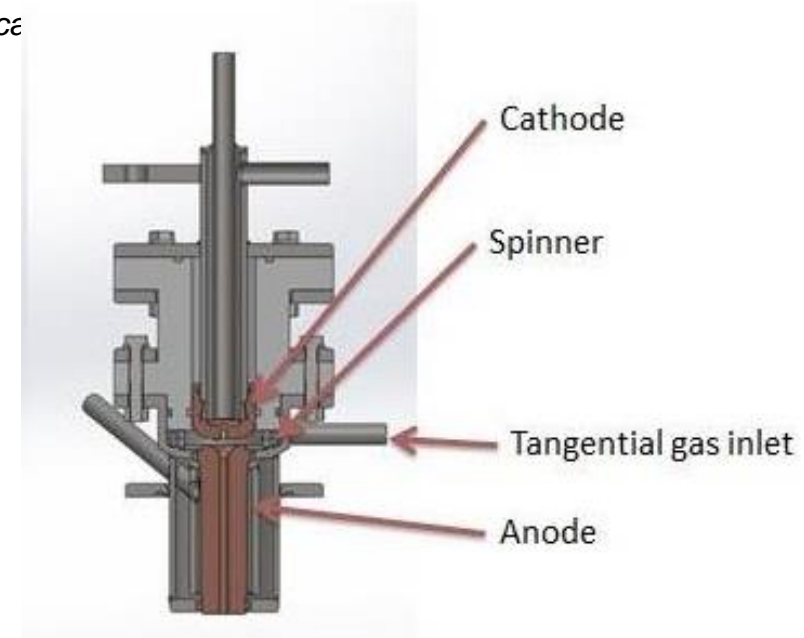
- Improve arc stability in dc non-transferred arc plasma torch
- Reduce heat losses to the electrode walls
- Conventional use of swirl injection of plasma forming gases
- Optimization of the gas swirl injection

Méthodes

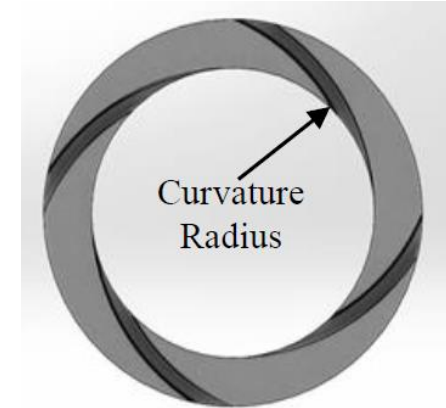
- Comparison between conventional injection ring (spinner) and an optimized one obtained by additive manufacturing

- Titanium alloy Ti6Al4V
- Direct Metal Laser Sintering (EOS M280)

Spinner	Number of holes		Size of holes [mm]	
	4	6	2	1
Spinner 1	x		x	
Spinner 2		x		x
Standard spinner	x		x	



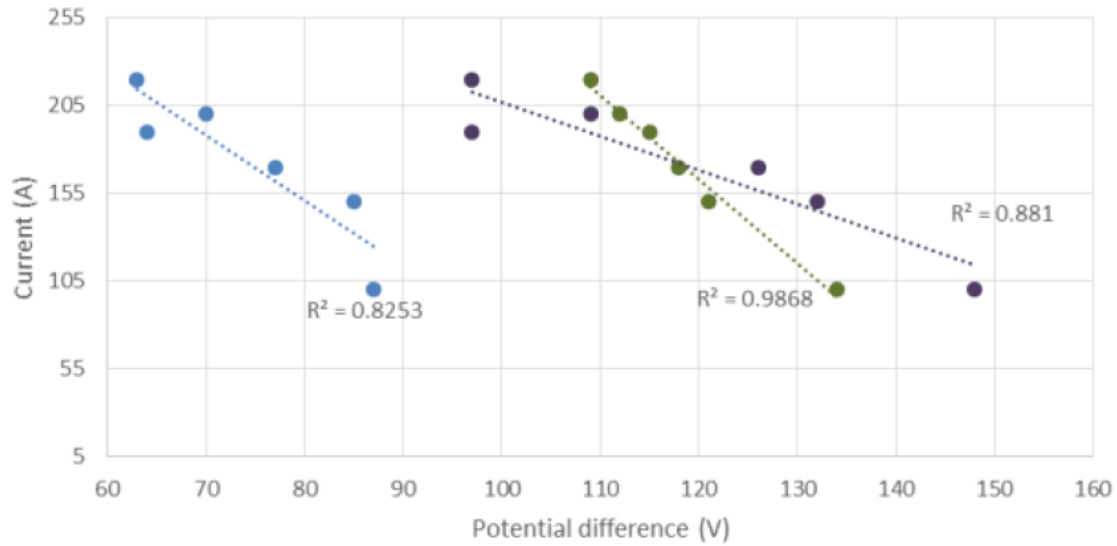
Conventional spinner



Optimized spinner

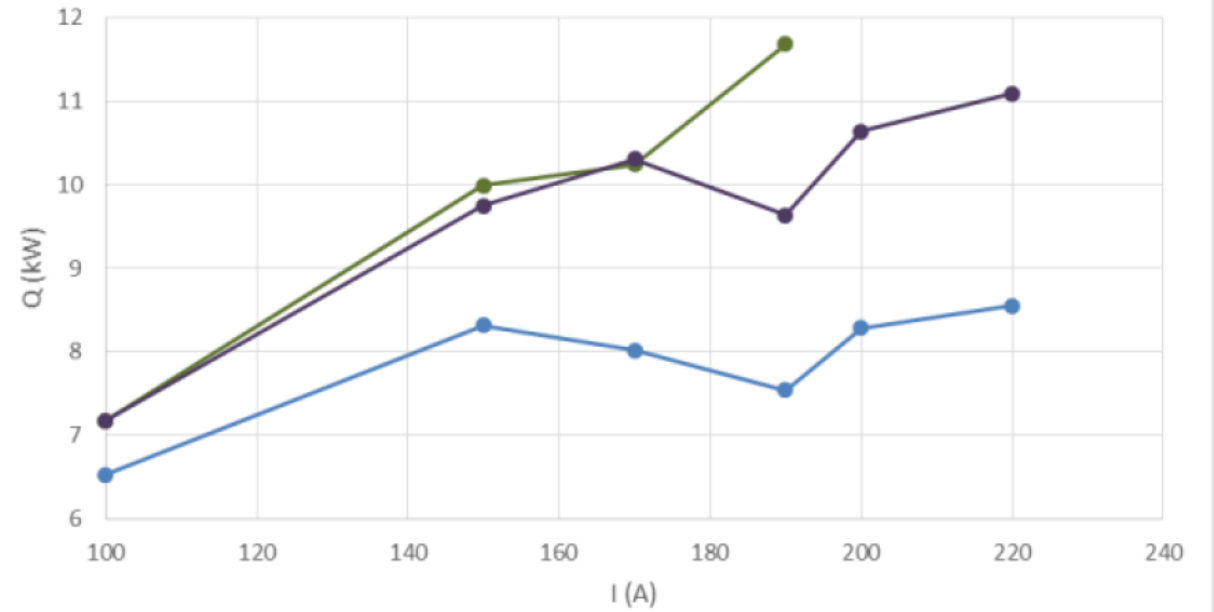
Pure N₂ plasma

Potential difference - Current plot at 2,59 g/s gas flow



● Standard Spinner ● Spinner 1 ● Spinner 2
⋯ Linear (Standard Spinner) ⋯ Linear (Spinner 1) ⋯ Linear (Spinner 2)

Heat loss-Current plot at 2,59 g/s gas flow



—●— Standard Spinner —●— Spinner 1 —●— Spinner 2

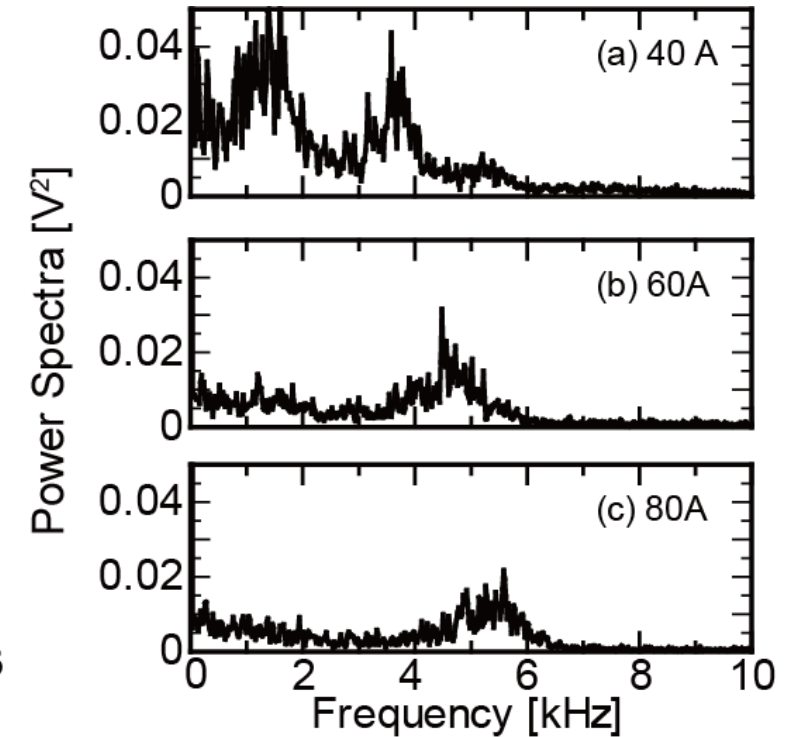
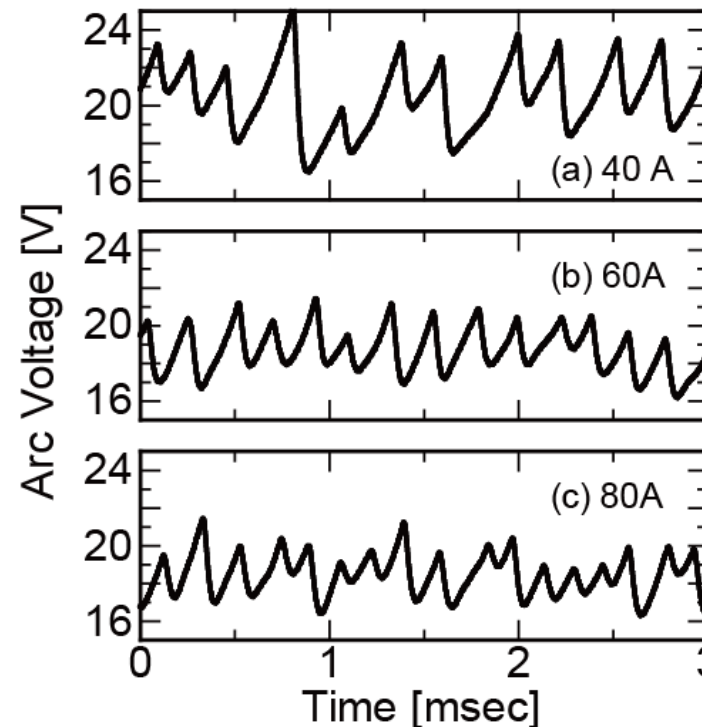
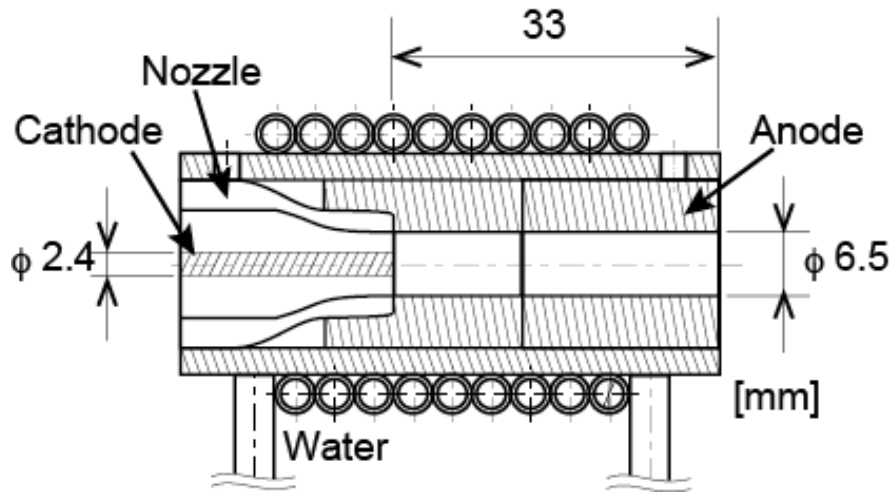
Voltage Fluctuation of A Few kW Class Non-Transferred DC Plasma Torch

T. Fujino¹ and K. Maeshima²

¹Faculty of Engineering, Information and Systems, University of Tsukuba, Tsukuba 305-8573, Japan

²Graduate School of Systems and Information Engineering, University of Tsukuba, Tsukuba 305-8573, Japan

Arc voltage's characteristics of a few kW class, non-transferred direct current plasma torch with argon gas were examined for arc currents of 30 to 100 A and gas volume flow rates of 30 to 50 slm. Measurement results of arc voltages showed that an average arc voltage decreases with increasing arc currents and it increases with increasing gas volume flow rates. In addition, a distinctive high frequency component of arc voltage is shifted to a much higher frequency side by increasing arc currents and gas volume flow rates.



Characteristics of aerodynamically dispersed arc in a converging-diverging nozzle

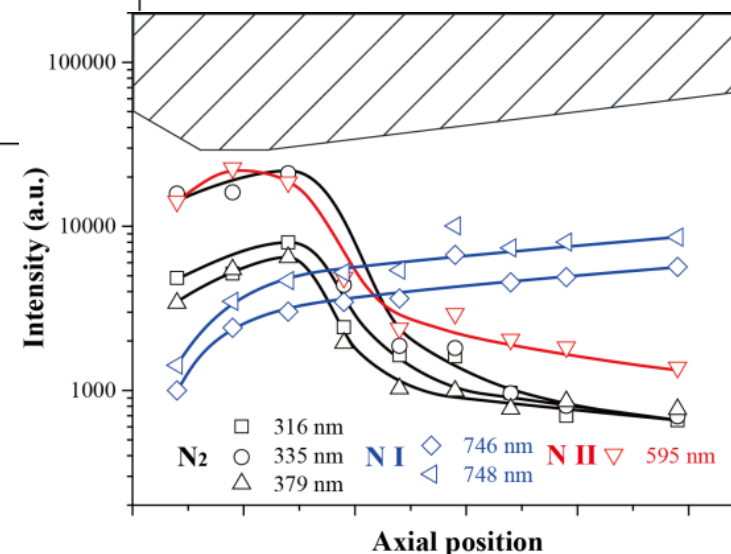
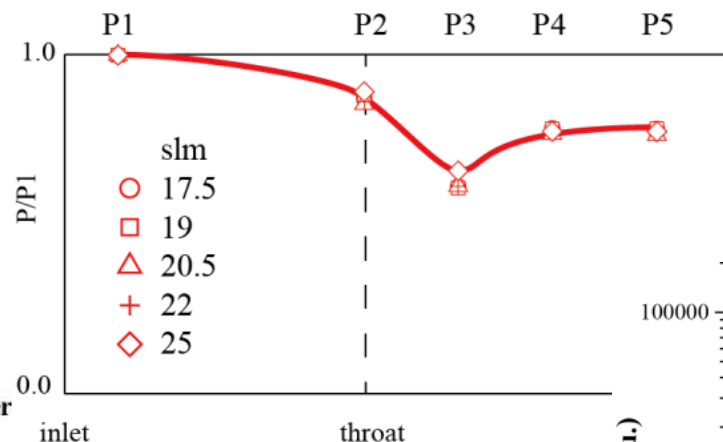
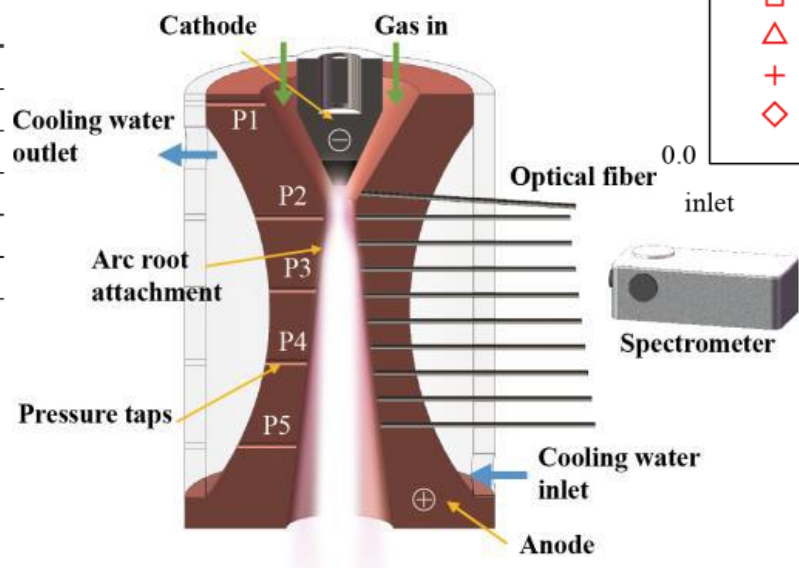
Heji Huang^{1, 2}, Wenxia Pan^{1, 2}, Xian Zhou¹, Lewen Chen¹, Chengkang Wu^{1, 2}

¹ The State Key Laboratory of High Temperature Gas Dynamics, Institute of Mechanics, Chinese Academy of Sciences, Beijing China

² School of Engineering Science, University of Chinese Academy of Sciences, Beijing 100049, China

Abstract: A converging-diverging nozzle facilitates aerodynamic expansion of the anode arc attachment for a direct current non-transferred plasma. Preliminary experimental and simulation study on the temperature, velocity, pressure and optical emission distributions of the aerodynamically dispersed arc in the nozzle was conducted. The results show that the flow is in subsonic region with considerable compressibility.

Diameter of the throat (mm)	3
Expansion half angle (°)	5 - 10
Plasma gas	N ₂ / N ₂ +Ar
Gas flow rate (slm)	4.5 - 30
Arc current (A)	80 - 130
Ambient pressure (atm)	1



Investigation of thermal plasma of electric arc discharge between composite C-Cu electrodes

S. Fesenko¹, A. Veklich¹, V. Boretskij¹, Y. Cressault² and Ph. Teulet²

¹Taras Shevchenko National University of Kyiv, Faculty of Radio Physics, Electronics and Computer Systems, 4g Glushkova Ave., Kyiv, Ukraine

²Université de Toulouse; UPS, INPT; LAPLACE; 118 route de Narbonne, F-31062 Toulouse cedex 9, France

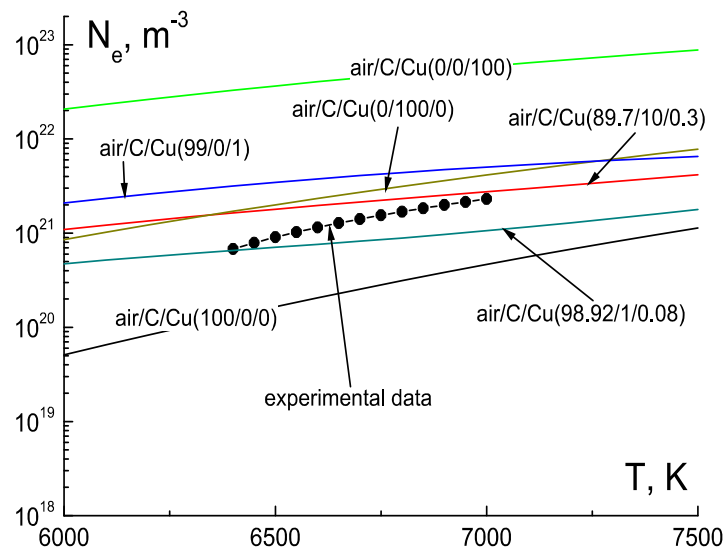
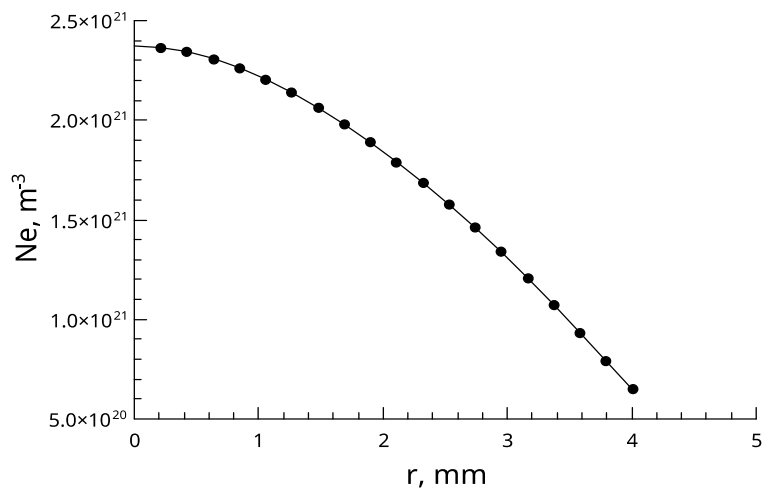
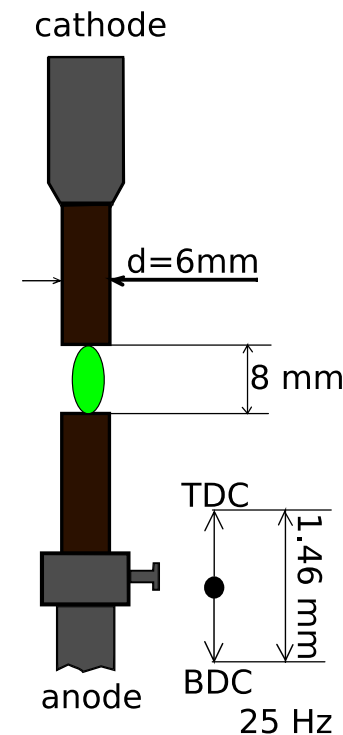
Contexte et objectifs

- Study of erosion contact surface of pantograph
- Graphite-copper electrodes

Méthodes et résultats:

- Determination of radial distribution of temperature in arc column plasma by means of Boltzmann plot
- Measurements electric field based on modulation of discharge gap

Interelectrode distance varied periodically with a frequency of 25 Hz using a specially designed device (electromechanical modulator)



LTE plasma composition
 Air-C-Cu

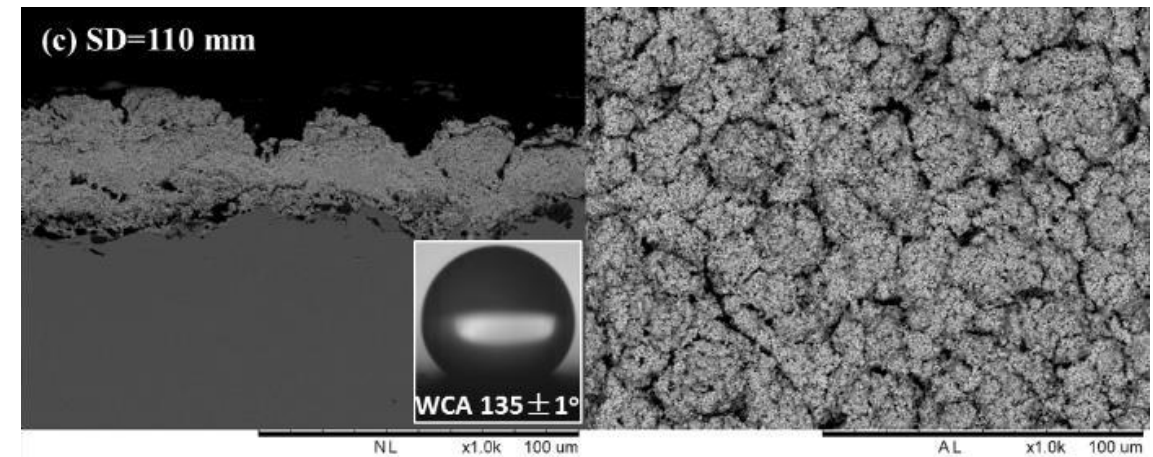
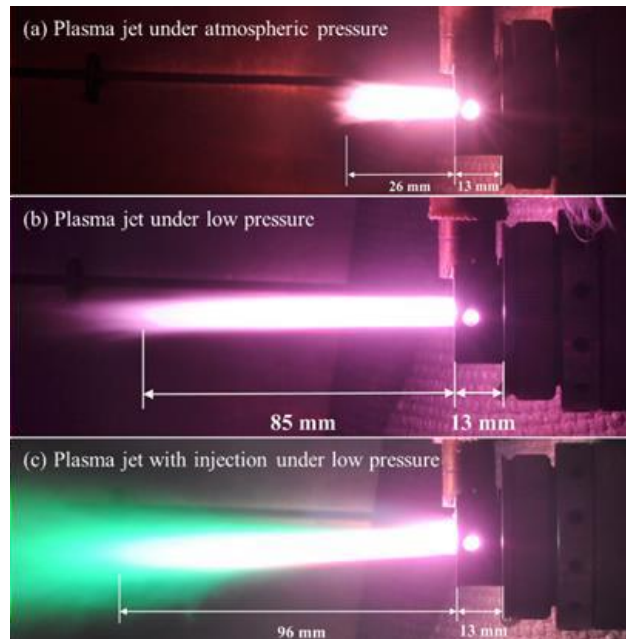
Solution precursor vacuum plasma spray of superhydrophobic ceramic coatings

Pengyun Xu, Javad Mostaghimi, Thomas W. Coyle and Larry Pershin

Centre for Advanced Coating Technologies, Department of Mechanical and Industrial Engineering, University of Toronto, Toronto, Ontario, Canada

Abstract: We studied a novel solution precursor vacuum plasma spray (SPVPS) process, which combines vacuum plasma spray and solution precursor to deposit superhydrophobic coatings. Ytterbium nitrate pentahydrate dissolved in water and/or ethanol mixture was used as solution precursors. Ytterbium oxide coatings were formed by injecting radially the solution into the low-pressure plasma jet generated by a commercial F4-VB torch (Oerlikon Metco) operated in a low-pressure (about 150 mbar) chamber with air as ambient gas. The coatings hydrophobicity was characterized by measuring the water contact and sliding angles. The microstructure and morphology of the cross section and top surface of the coatings were also investigated.

Current, Voltage	700 A, 60-61 V
Plasma gas	50Ar10H ₂ LPM
Solution injection	Radial injection via a 150 µm ID orifice
Solution feed rate	19-28 g/min
Standoff distance	90, 100, 110 and 120 mm
Operation pressure	150-160 mbar
Torch motion	The relative transverse speed was 1 m/s. The vertical step size was 5 mm. The total pass number was 15.



Effect of current changes on interacting arc structures in a twin-cathode DC electric arc furnace

D. Burkat¹, S.Coulombe¹

¹Plasma Processing Laboratory, Department of Chemical Engineering, McGill University, Montréal, Québec, Canada

Abstract: The structures of interacting arcs forming in a twin-cathode DC electric arc furnace are being investigated using high-speed imaging combined with current and voltage measurements. An image analysis program was developed to classify each frame into one of the two structures: separated or merged arcs on the common anode. The effect on the arcs' structure of suddenly doubling the current through one arc from its nominal value of 50 A was investigated for increasingly large cathode-anode distances. For low cathode-anode distance (lower than 2.50 cm as studied in this work), the sudden current increase led to an increased time the arcs spent in a merged structure, in accordance with the increased Lorentz force-induced interactions.

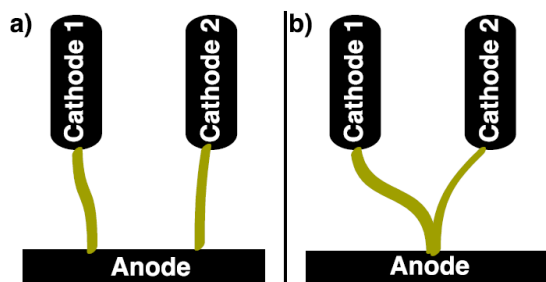
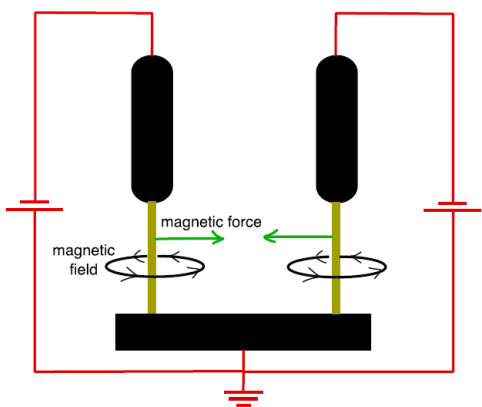
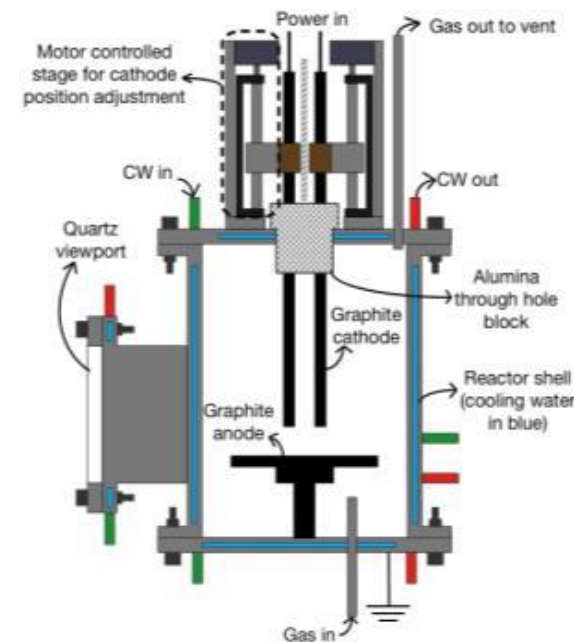
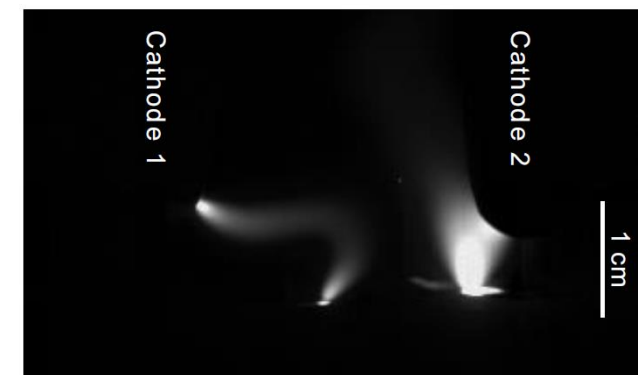
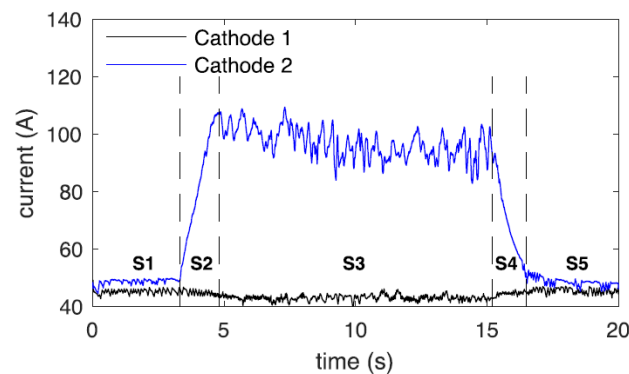


Figure 2. The two arcing structures observed in the twin-cathode EAF are: a) separate arcs, b) merged arcs.



Large amount synthesis of Si nanopowder/nanowires using pulse-modulated induction thermal Plasmas

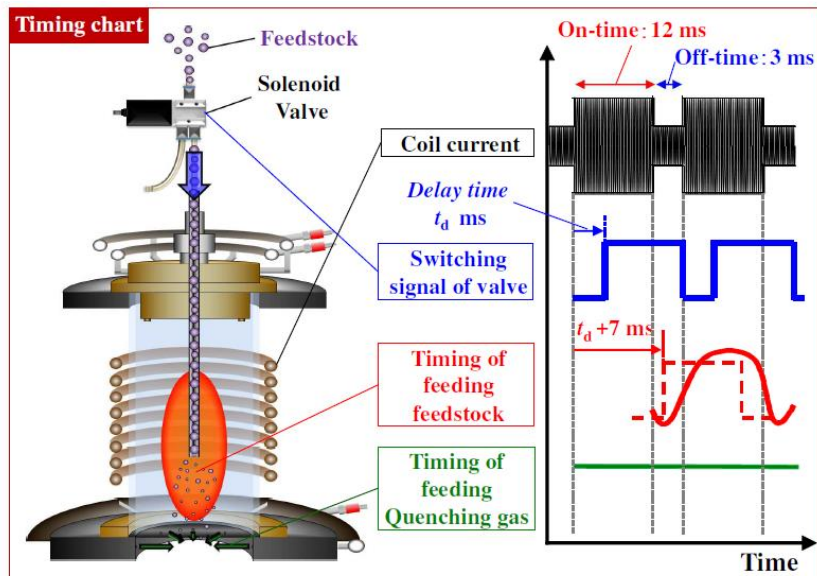
Yosuke Ishisaka¹, Naoto Kodama¹, Yasunori Tanaka^{1,2}, Yoshihiko Uesugi¹, Tatuso Ishijima², Shiori Sueyasu³, Shu Watanabe³, Keitaro Nakamura³

¹Faculty of Electrical & Computer Eng., Kanazawa Univ., Kanazawa, Japan

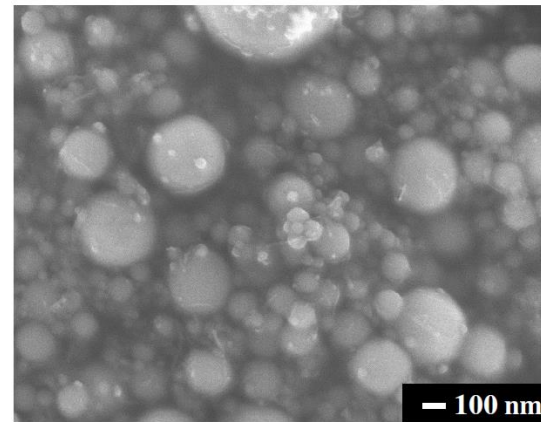
²Research Center for Sustainable Energy & Technol., Univ., Kanazawa, Japan

³Research Center for Production & Technol., Nisshin Seifun Group Inc., Fujimino, Japan

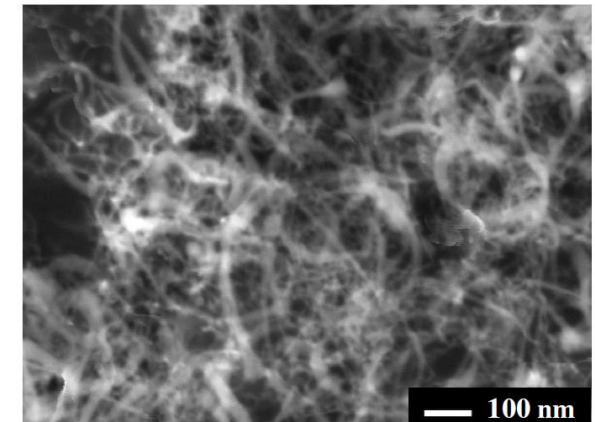
Abstract: Large amounts of Si nanoparticles (NPs) / nanowires (NWs) were synthesized using 20 kW Ar-H₂ pulse-modulated induction thermal plasmas (PMITP). Silicon NPs were synthesized by intermittently injecting Si feedstock at <4 g/min into the PMITP with quenching gas (QG), whereas Si NWs were found to be synthesized with Si feedstock at a heavy load feed rate ~7 g/min without QG. Synthesized products were analyzed using FE-SEM, BET, BF-TEM/EDX and XRD. The production rate of Si NWs was estimated as >1 g/h.



Injected feedstock
Si powder
19.2 μm



Si nanoparticles
120 g/h



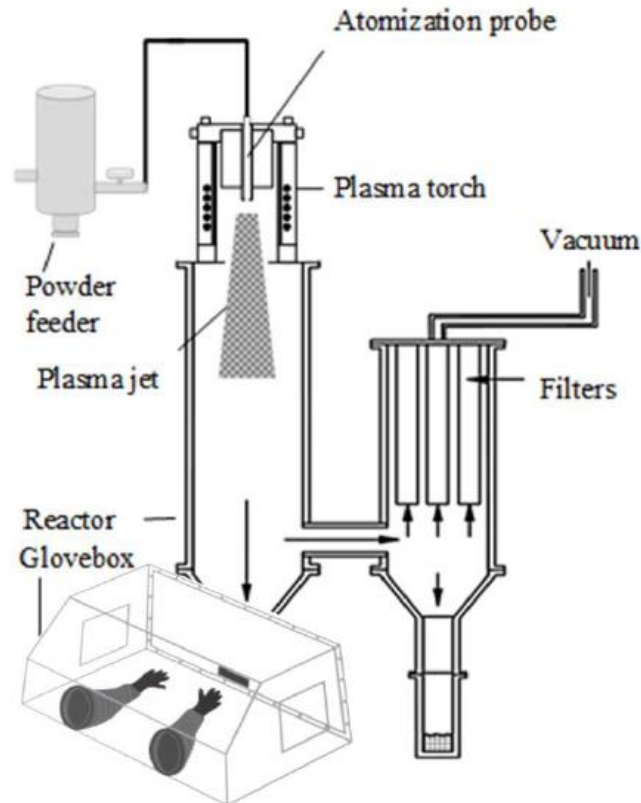
Si nanowires
1g/h

A plasma process in the preparation of Li_2S for lithium-ion battery applications

J. Nava-Avenidaño and J. Veilleux

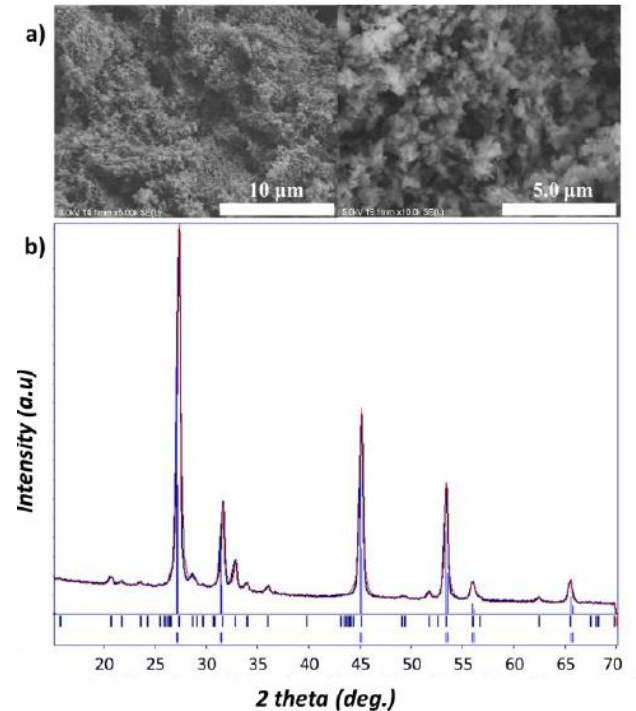
Department of Chemical Engineering and Biotechnological Engineering,
University of Sherbrooke, Sherbrooke (QC), Canada

Abstract: Plasma technologies are nowadays considered for the development of better performing and more affordable energy storage devices such as the lithium-ion batteries (LIB). Their versatility allows the synthesis of nanostructured electrodes with different morphologies and coatings of carbon or metal oxides, thin films, *etc.* Herein, we highlight the key advantages of their use in LIB technology and we introduce the synthesis of the promising cathode material Li_2S by means of inductively coupled thermal plasma.



Powdered precursors: $\text{LiOH}\cdot\text{H}_2\text{O}$ and S

Parameter	Gas (Lmin^{-1})
Sheath	Ar (80)
	H_2 (1.7)
Central	Ar (23)
Powder	Ar (20)



a) SEM image of plasma-synthesized Li_2S

b) XRD pattern

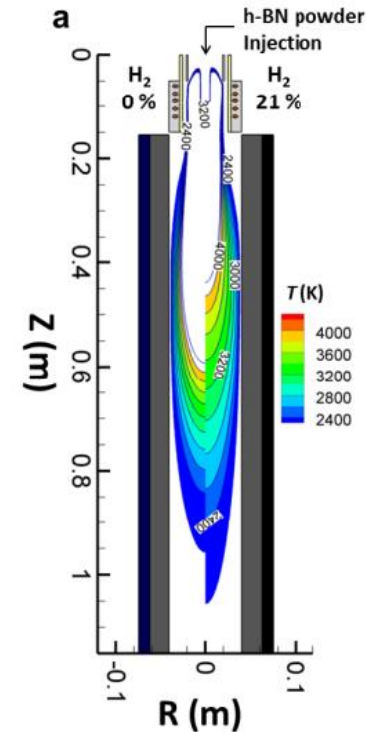
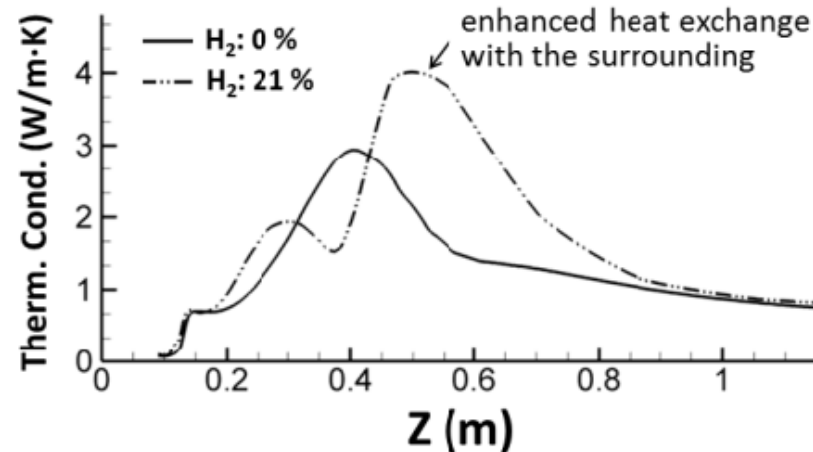
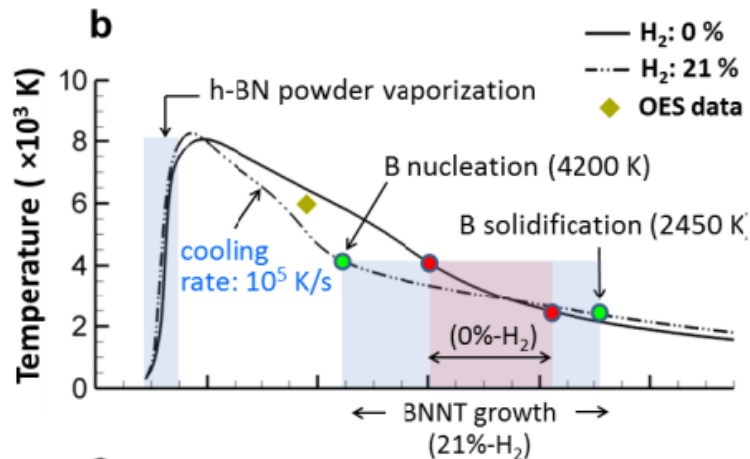
Role of hydrogen in high-yield growth of boron nitride nanotubes at atmospheric pressure by induction thermal plasma

Keun Su Kim¹, Martin Couillard², Homin Shin¹, Mark Plunkett¹, Dean Ruth¹, Christopher Kingston¹, and Benoit Simard¹

¹Security and Disruptive Technologies Portfolio, Emerging Technologies Division, National Research Council Canada, Ottawa, Ontario K1A 0R6, Canada

²Energy, Mining and Environment, Engineering Division, National Research Council Canada, Ottawa, Ontario K1A 0R6, Canada

Abstract: Recently, we demonstrated scalable manufacturing of boron nitride nanotubes (BNNTs) directly from h-BN powder by using induction thermal plasma with a high-yield rate approaching to 35 g/h (Kim *et al.*, ACS Nano 8. p.6211, 2014). The main finding was that the presence of hydrogen is crucial for the high-yield growth of BNNTs at atmospheric pressure. Here we investigate the detailed role of hydrogen using numerical modelling and *in-situ* optical emission spectroscopy (OES) and reveal that, in the presence of hydrogen, both the thermo-fluidic fields and chemical pathways are significantly altered in favour of rapid growth of BNNTs.



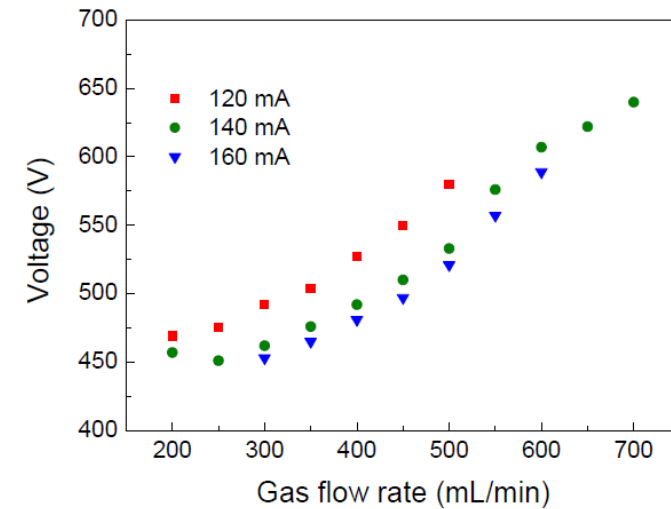
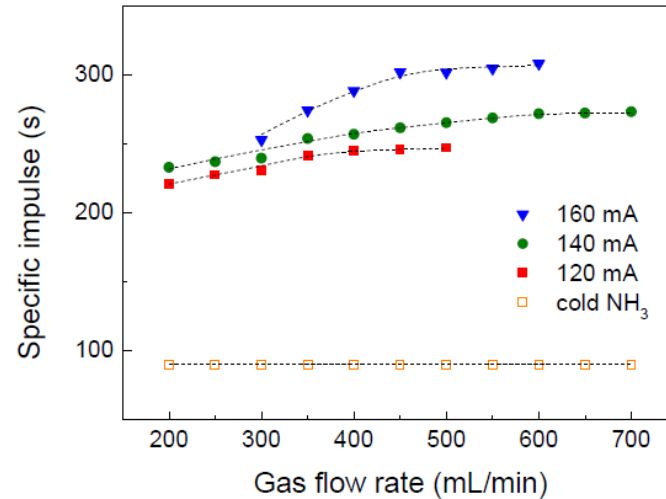
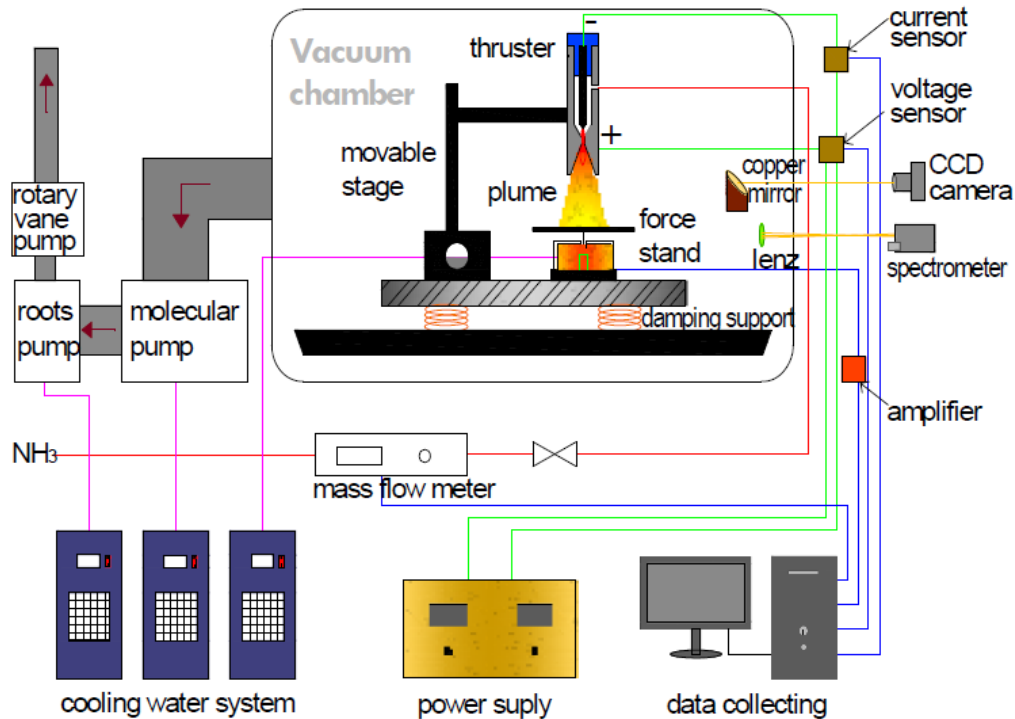
Performance of Low-Power Ammonia Arcjet Thruster

Xian Meng, Wenxia Pan, Chengkang Wu

State Key Laboratory of High Temperature Gas Dynamics,

Institute of Mechanics, Chinese Academy of Sciences, Beijing 100190, China

Abstract: A low-power arcjet thruster of 100W-class with natural-radiation-cooled nozzle can be stably operated using ammonia propellant. Thruster performance and discharge characteristics have been systematically studied. Experimental results show that the maximum specific impulse of the thruster is up to 300s, the arc voltage can exceed 600V, and the discharge shows falling volt-ampere characteristics.



Using Oscillated Arc Discharge at Solid/Liquid Interface for Linearly Growth of Ni-Cu Filled Carbon Nano/Micro-Tubes

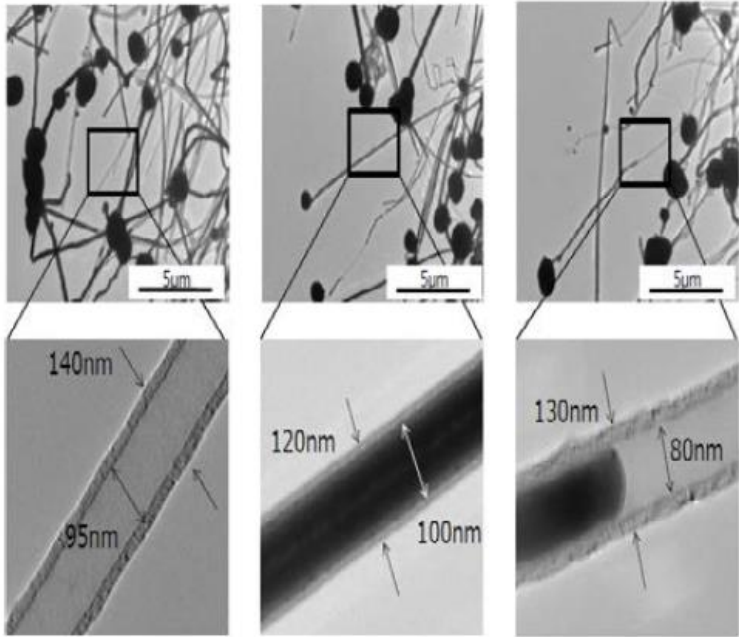
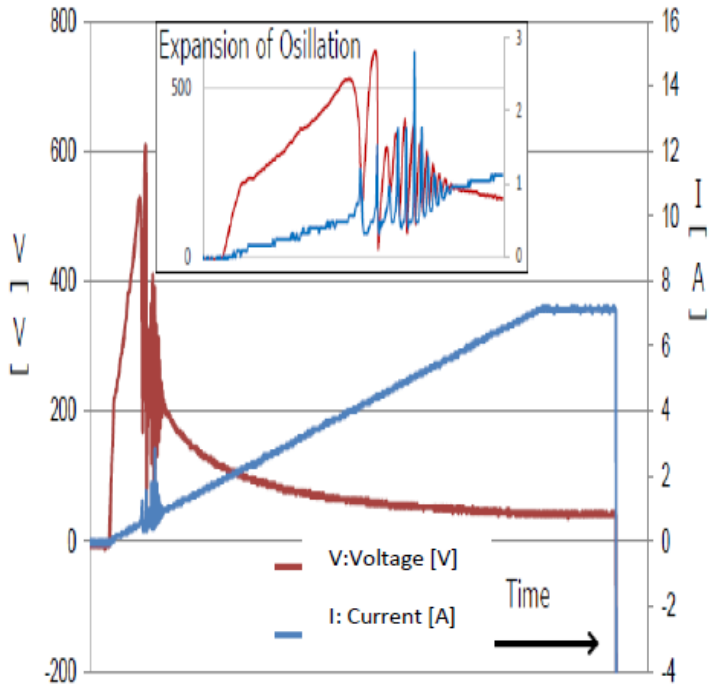
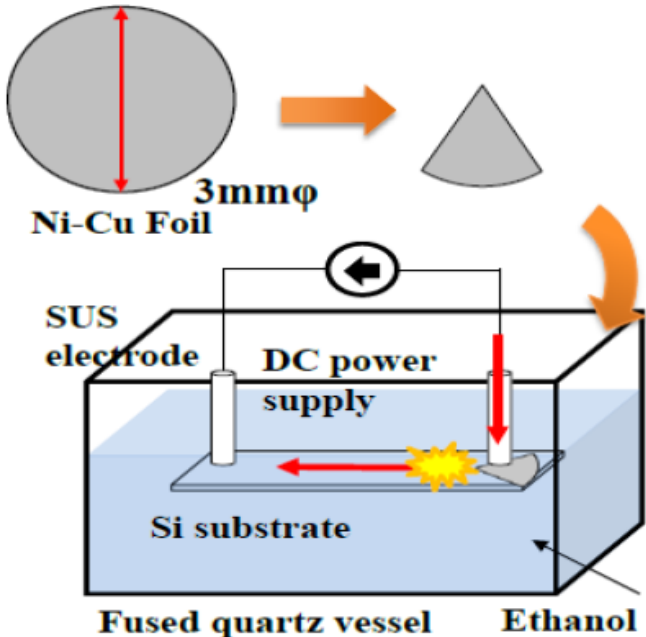
K.Suzuki¹, K. Mikami¹, T. Sagara², S.Kurumi¹, and K.Matsuda¹

¹Department of Electrical Engineering, College of Science and Technology, Nihon University, Tokyo, Japan

² Electrical and Electronics Engineering Course, Tokyo Metropolitan College of Industrial Technology, Tokyo, Japan

Programme P3-15-4 page 35
Recueil résumé page 422
Poster

Abstract: We report on a growth technique of carbon nano/micro-tubes whose core spaces were filled with Ni-Cu alloy nanowire using oscillated arc discharge pyrolysis at solid/liquid interface. SEM image around the carbon-deposited area where are top of sector-shape Ni-Cu foil shows the lot of linearly and long (20 μm - 50 μm) CNTs. TEM observation reveals fully Ni-Cu filled CNTs shows homogeneously, linearly, and clearly graphene layers.



Environnement

Combustion of organics liquids wastes with a submerged thermal plasma ELIPSE process

M. Marchand, D. Milelli, R. Magnin, A. Russello and F. Lemont

Laboratoire des Procédés Thermiques Innovants, DE2D/SEVT/LPTI, French Atomic Energy Commission, France

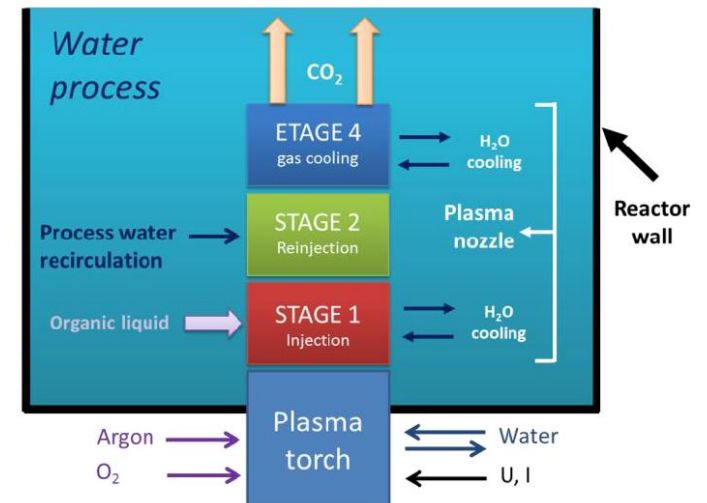
Contexte et objectifs

- Organic liquid incineration process (called ELIPSE process) with a non-transferred plasma torch working under water
- The objective is to treat a wide variety of organic liquids which are difficult to incinerate by conventional techniques
- Example : combustion of a mixture TBP (TriButyl phosphate)/dodecane without radioelements
TBP/dodecane : mixture used in the chemical Process PUREX (**P**lутonium **U**ranium **R**edox **E**Xtraction) used to purify nuclear fuel



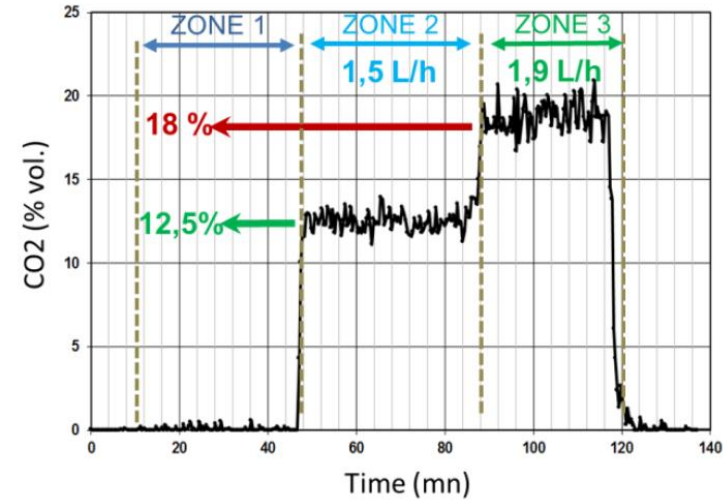
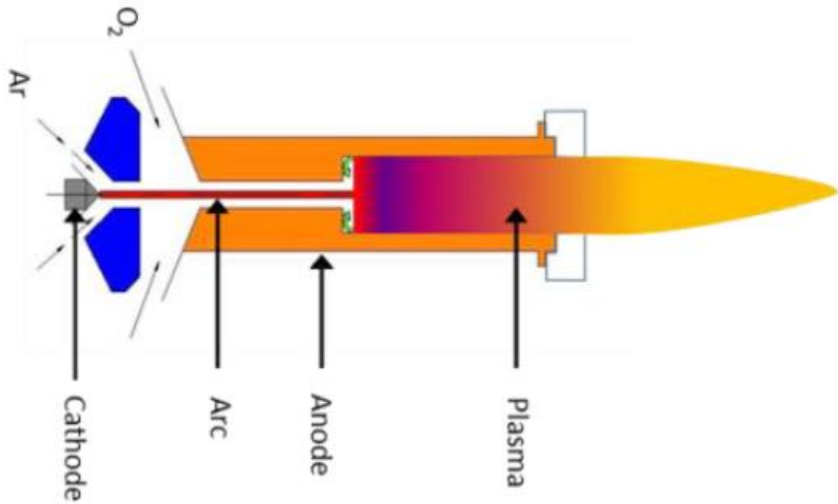
Méthodes:

- Evolution of power balance during treatment of TBP/dodecane mixture at variable feeding rates
- Evolution of the concentration of CO₂ versus time from different TBP/dodécane feeding rate (Infrared absorption to measure CO and CO₂ at the outlet of the condenser in a real time)

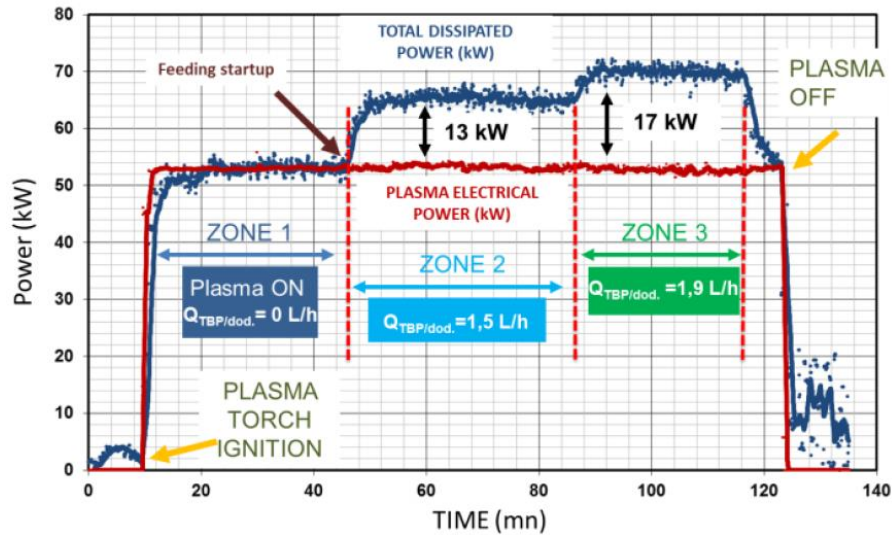


Résultats

45 kW, Ar (30 slm) O2 (200 slm)



Evolution of the concentration of CO2 versus time for different TBP/dodecane feeding rate



Power balance during treatment of TBP/dodecane mixture at variable feeding rates

Measurement of Total Organic Carbon (TOC) in the residual solution

$$n_{TBP/dodecane} = \frac{c_i - c_f}{c_i}$$

c_i : initial TOC
 c_f : final TOC

$$n_{TBP/dodecane} = 99.90 \pm 0.3\%$$

Degradation of phenol by a submerged DC non-transferred arc plasma jet

Jing-Lin Liu¹, Hyun-Woo Park¹, Min Suk Cha¹

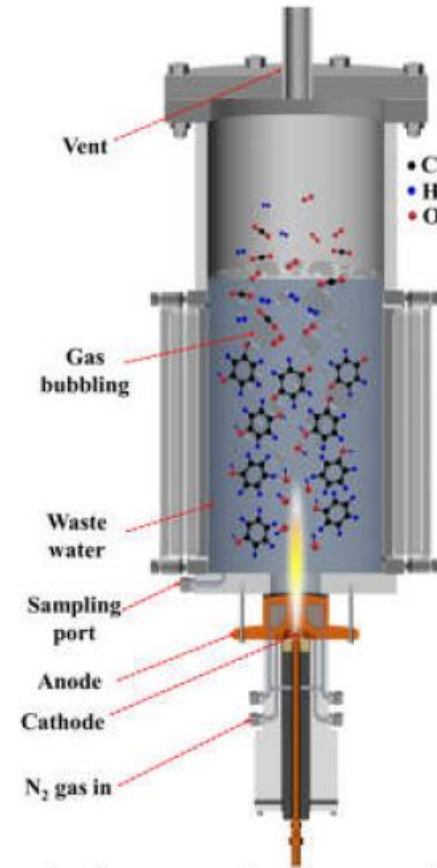
¹ King Abdullah University of Science and Technology (KAUST), Clean Combustion Research Center (CCRC) and Physical Science and Engineering Division (PSE), Thuwal 23955, Saudi Arabia

Contexte et objectifs

- Phenolic compounds: product of chemical industry
- Pollutant difficult to degrade due to the high salinity, high acidity, high chemical oxygen demand (COD) and low biodegradability of the wastewater containing phenolic compounds
- Use of submerged dc arc plasma torch

Méthodes:

- On-line measurement of phenol degradation as function of time-treatment and input energy per volume of treated wastewater (kJ/L)
- gas chromatography mass spectrometry with FID detector (Flame Ionization Detector)
- pH and electrical conductivity of treated water
- Chemical Oxygen Demand COD (mg/L): the amount of oxygen consumed in total chemical oxidation of the organic constituents present in the water. COD decreases with treatment.
- Use of COD photometer: photometric detection employing a linear relationship between absorbance and concentration



Schematic diagram of submerged arc plasma jet

$$SIE \text{ (kJ/L)} = \frac{P_{in} \cdot t}{V_L}$$

Degradation efficiency:

$$\eta_{Phenol} = \left(\frac{C_0 - C_t}{C_0} \right) \times 100$$

Energy efficiency:

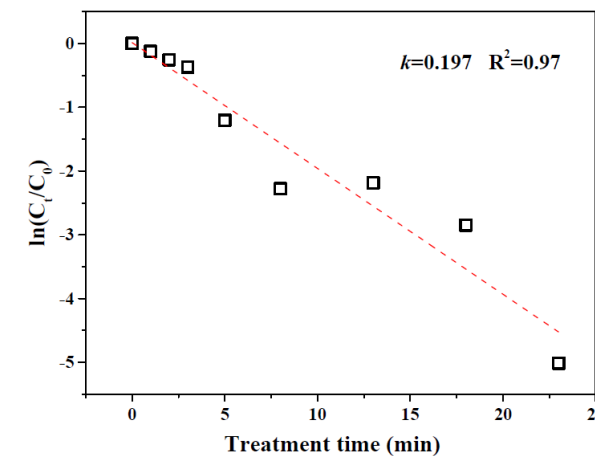
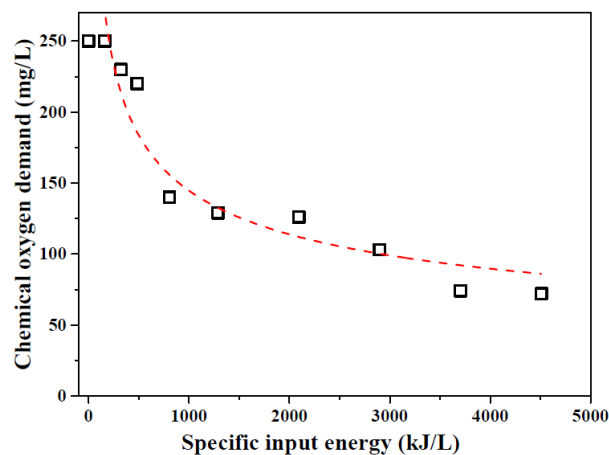
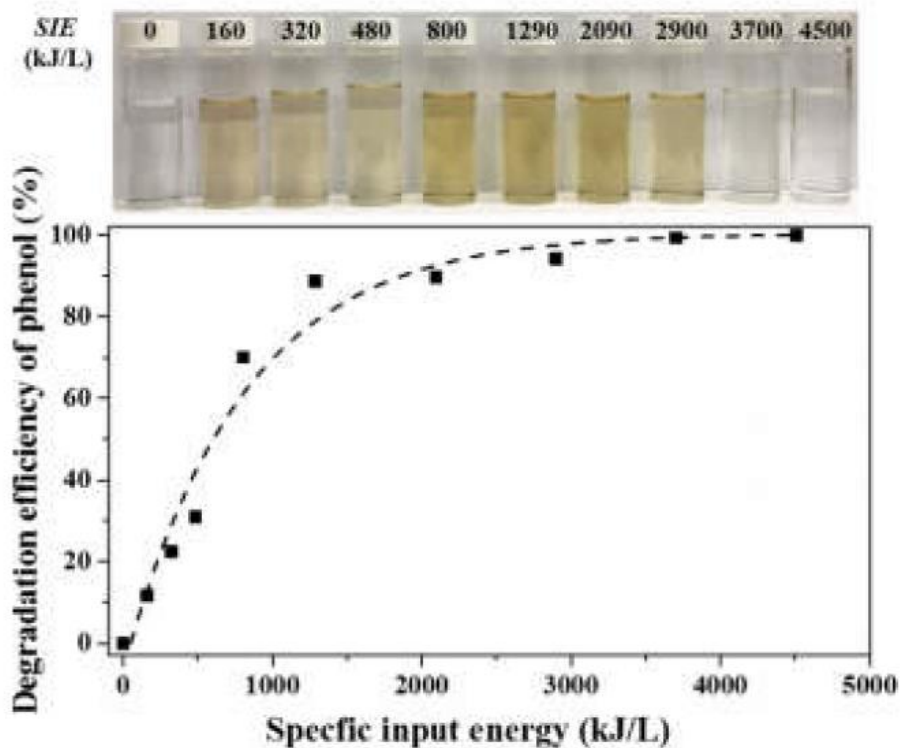
$$EE_{Phenol} \text{ (g/kWh)} = \frac{C_0 \cdot V_L \cdot \eta_{Phenol}}{P_{in} \cdot t}$$

COD removal:

$$\eta_{COD} = \left(\frac{COD_0 - COD_t}{COD_0} \right) \times 100$$

Energy efficiency of COD:

$$EE_{COD} \text{ (g/kWh)} = \frac{C_0 \cdot V_L \cdot \eta_{COD}}{P_{in} \cdot t}$$



- 90% of phenol degradation and 50% of COD removal were achieved at SIE of 2090 kJ/L.
- Rate constant (0.197) is much higher than that in corona (0.02) and that in DBD (0.018).

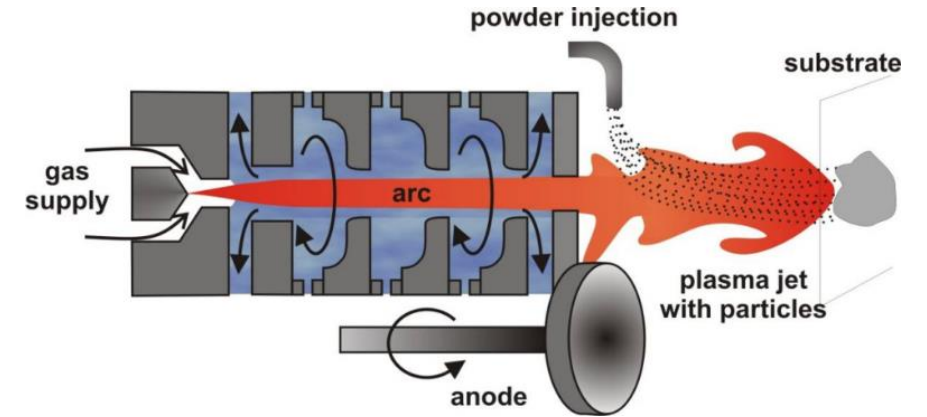
Conversion of a lignite into a synthetic gas using water-stabilized plasma torch

A.A. Serov, M. Hrabovsky, V. Kopecky, A. Maslani, M. Hlina

Thermal Plasma Department, Institute of Plasma Physics of the Czech Academy of Science, Prague, Czech Republic

Contexte et objectifs

- Plasma treatment of an organic waste using water stabilized plasma torch
- Production of syngas by decomposition of lignite
- Lignite: a fossilized wood, nonhydrolysable complex organic compound, contains high amount of water and unsuitable for energy obtaining by usual combustion.



Méthodes:

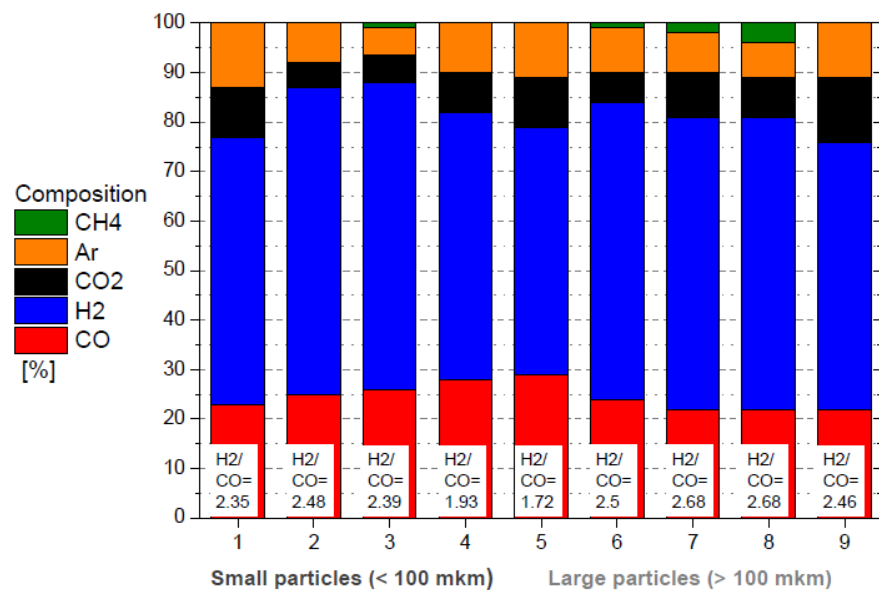
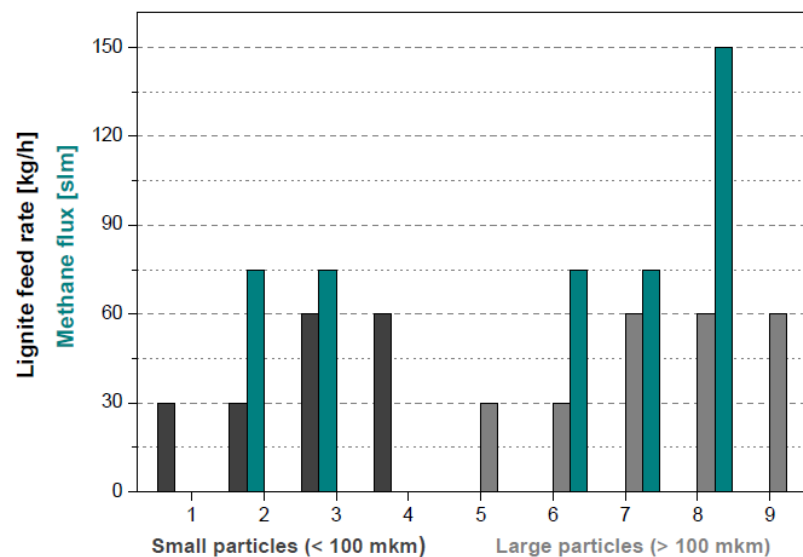
- High feeding rates of lignite particles (30-60 kg/h)
- Methane injection
- Measurement of gas composition by mass spectrometry analysis

Table 2. Feed material chemical composition.

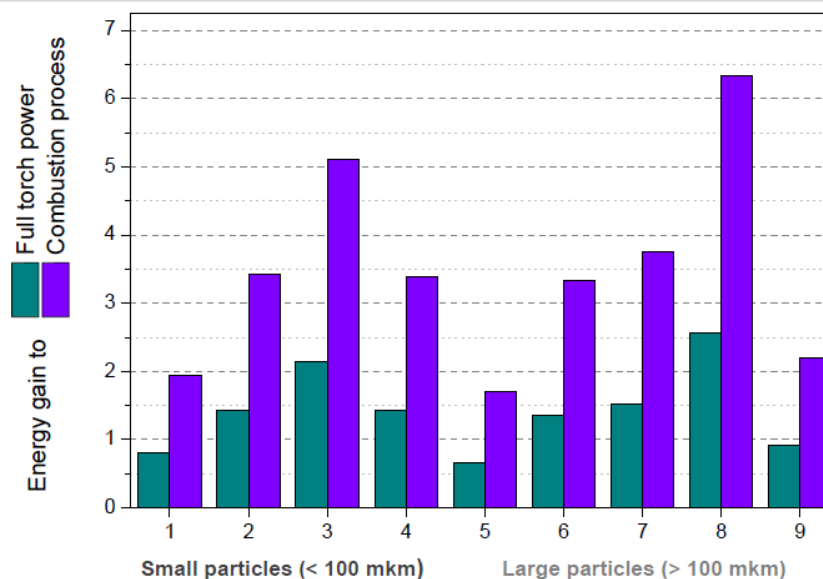
Experiment	H ₂ (%)	C (%)	O (%)
1	40.5	24.5	35
2	42.8	25.3	31.9
3	42.7	25.7	31.6
4	40.3	25	34.7
5	40.3	25	34.7
6	42.6	25.8	31.6
7	42.5	26.2	31.3
8	44.5	26.8	28.7
9	40.1	25.5	34.4

Résultats

Arc current	400 A
Arc power	114 - 131 kW
Lignite feed rate	30 and 60 kg
Lignite particle size	<100 mkm and >100 mkm
Calibration gas	Ar (argon)
Additional gas	CH ₄ (methane)
Additional gas flow rate	75 and 150 slm



Concentration H₂+CO > 80 %



Ratio of calorific value of the syngas to full torch power and to the energy expended in the combustion process

Synthesis of Carbon Blacks from HDPE plastic by 3-phase AC thermal plasma

F. Fabry and L. Fulcheri

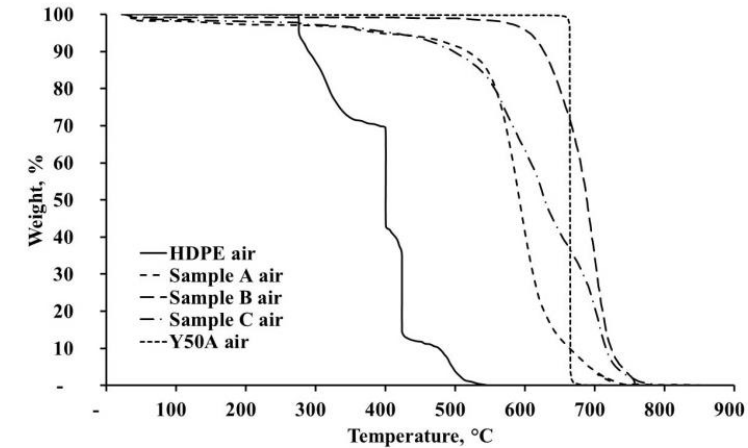
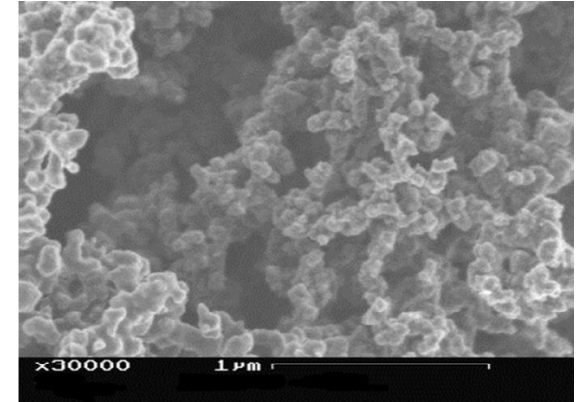
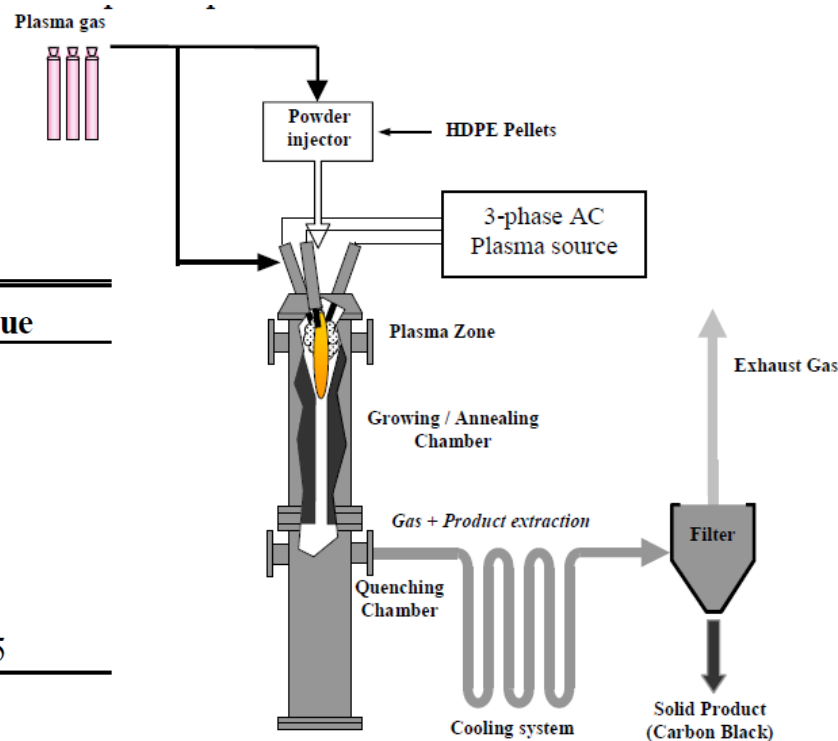
MINES ParisTech, PSL - Research University, PERSEE - Centre for processes, renewable energy and energy systems, CS 10207, rue Claude Daunesse, 06904 Sophia Antipolis, France

Abstract: This paper reviews the last results obtained on the 3-phase AC plasma technology developed at the Centre PERSEE, MINES ParisTech, PSL for the treatment of domiciliary and industrial wastes for nanomaterial synthesis with a special focus on preliminary results obtained for the production of carbon blacks from plastics (HDPE pellets). Carbon blacks obtained from HDPE have shown a highly nanostructured organization very similar to those of acetylene black.

3-phase AC plasma power supply
600 Hz, 0-400 A, 263 kVA maximum power

Property	Unit	Value
Average Power	kW	50
Average Current	A	220
Average Voltage	V	175
Plasma gas flowrate (N ₂)	Nm ³ .h ⁻¹	2
Carrier gas flowrate (N ₂)	Nm ³ .h ⁻¹	2
HDPE Flowrate	Kg.h ⁻¹	0.25

High density Polyethylene



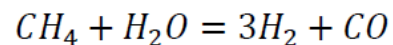
Thermal Plasma Methane Reforming for Hydrogen Production

M. Hrabovsky, M. Hlina, V. Kopecky, A. Maslani, A. Serov, O. Hurba

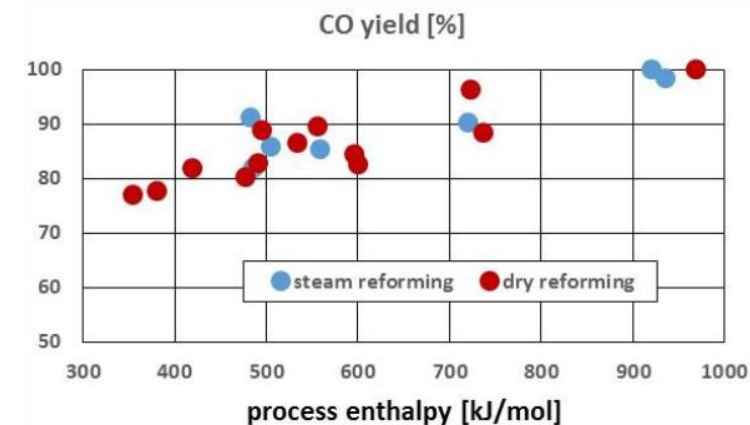
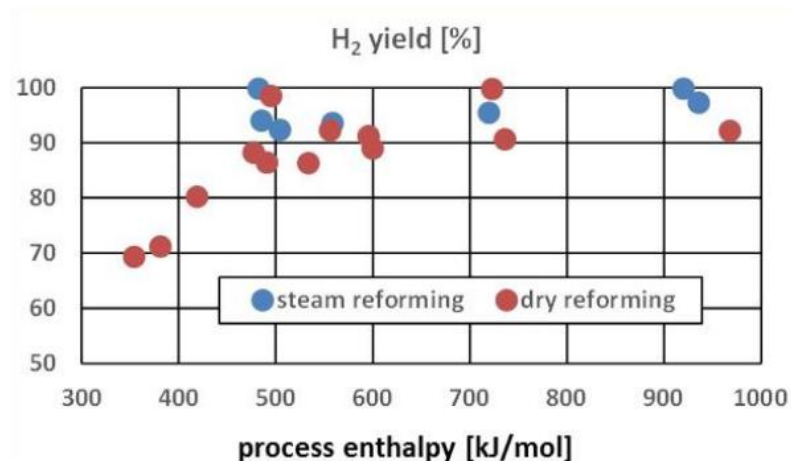
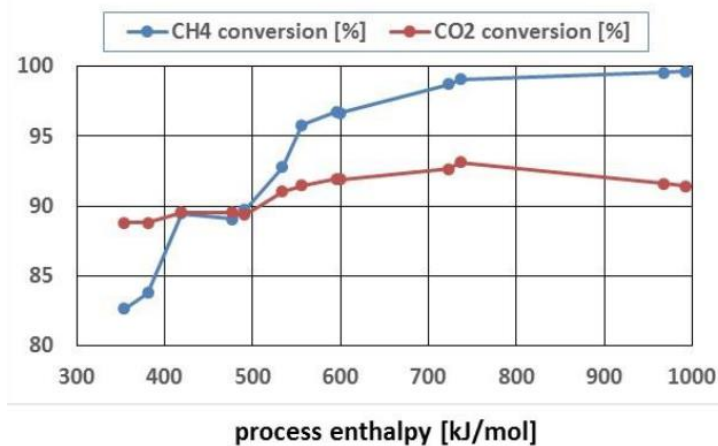
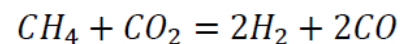
Institute of Plasma Physics ASCR, Za Slovankou 3, Praha 8, Czech Republic

Abstract: Reactions of methane with water and CO₂ in steam plasma flow were studied for the torch power 88 to 136 kW and methane flow rates 75 to 150 slm. The output H₂/CO ratio could be adjusted by a choice of feed rates of input reactants in the range 1.1 to 3.4. Depending on experimental conditions the conversions of methane was up to 99.5%, the selectivity of H₂ was up to 99.9%, and minimum energy needed for production of one mole of hydrogen was 158 kJ/mol. Effect of conditions on process characteristics was studied.

Steam reforming



Dry reforming



Phénomènes aux électrodes

Experimental Observation of Macro-particles Behaviours in High-current Vacuum Arc

Min Li¹, Renjie Lin², Xiao Zhang², Lijun Wang²

¹ Pinggao Group Co., Ltd., Pingdingshan, China

² State Key Laboratory of Electrical Insulation and Power Equipment, Xi'an Jiaotong University, Xi'an, China

Abstract: In this paper, macro-particles (MPs) behaviours are observed by high-speed camera. From a series of clear images, the behaviours of MPs from cathode and melting old anode (new cathode) are investigated respectively. Some MPs from cathode move toward anode and others toward radial vacuum environment. MPs located in the center positions of electrode have smaller velocities, on the contrary, MPs near to arc edge have larger radial and axial velocities, maximum radial and axial velocities reaches to about 13m/s and 7.5m/s respectively. MPs located in different electrode positions have different velocity characteristics. Separation phenomena of MPs also have been observed. The diameters of MPs from anode melting pool (AMP) are bigger than that from cathode. Due to the swirl effect of AMP and motion inertia, MPs from AMP will continue rotating and reach vacuum environment and seldom reach other electrode. When the current zero lasts for a long time, the MP velocity is smaller (about 0.7m/s) than that with short current zero time. The MPs should be in part responsible for the re-ignition of vacuum arc and failure of vacuum interruption

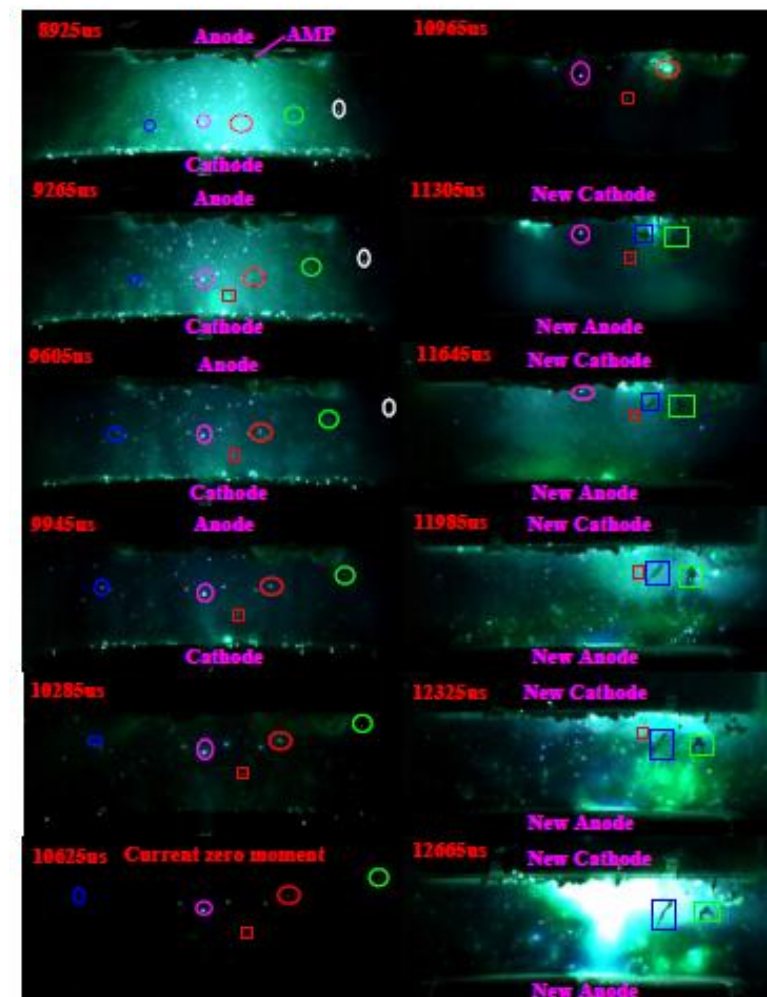
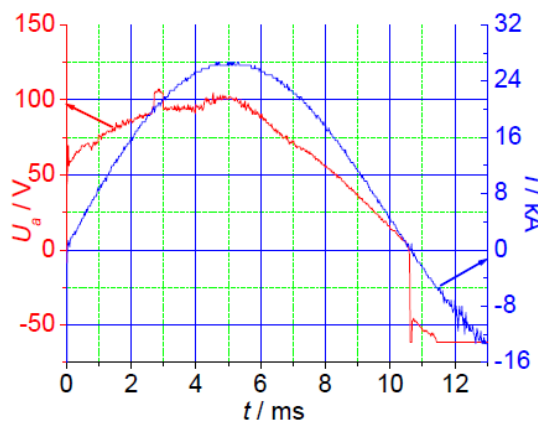
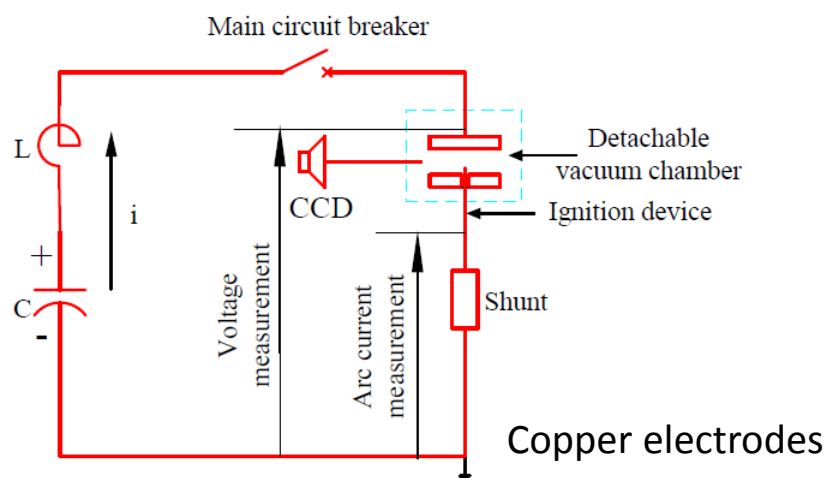


Fig.4 MPs behavior tracking before and after current zero moment ($D = 58\text{mm}$; $h = 16\text{mm}$; $I = 20\text{kA}$ (rms); Cu electrode)

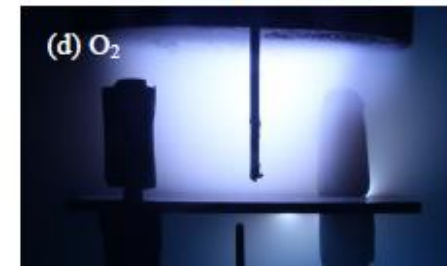
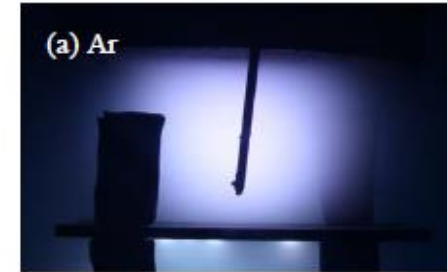
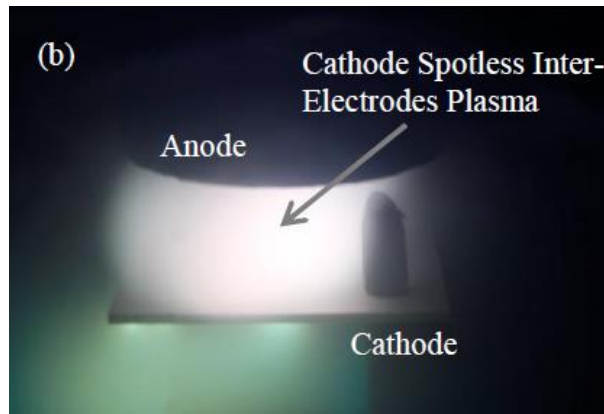
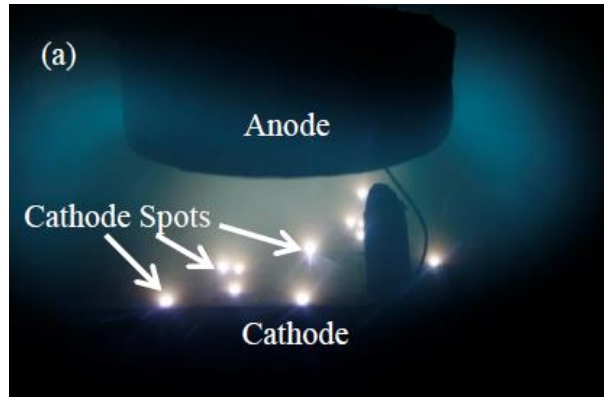
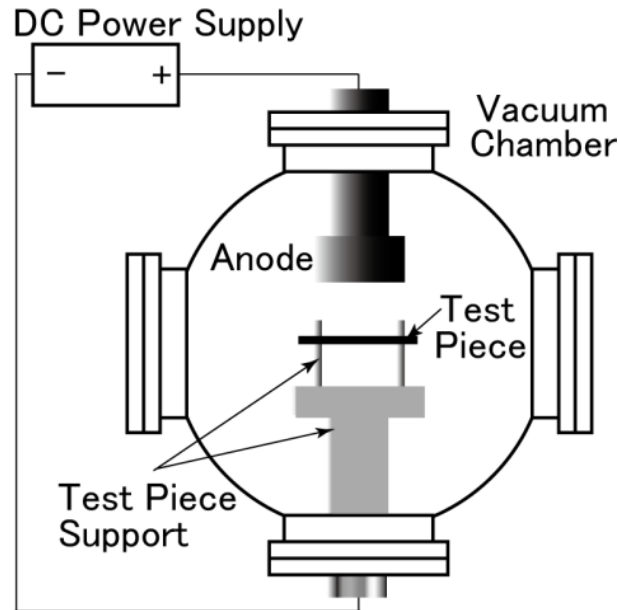
Features of Cathode Spotless Inter-Electrodes Plasma Appeared in Low Vacuum Arc during Removal of Oxide Layer from Steel Surface

M. Sugimoto and S. Iha

Department of Machine Intelligence and Systems Engineering, Faculty of Systems Science and Technology, Akita Prefectural University, Yurihonjo, Akita, Japan

Abstract: Cathode spotless inter-electrodes plasma, which appears in low vacuum arc removal treatment of oxide layer from steel surface plate, is experimentally investigated. That plasma can be sustained even when most part of cathode surface facing the anode is insulated. Colour of that plasma changes depending upon the gas introduced into the inter-electrodes region during discharge.

- Descaling experiments
- Steel plate 100 mm² covered with 5µm-thick oxide layer
- P=10 Pa
- Electrode gap 40-50 mm
- 50-120 A
- Zinc wire to initiate the discharge



Emission Spectroscopy of Atmospheric-Pressure Ball Plasmoids: Higher Energy Reveals Rich Chemistry

Programme P1-3-1 page 16
Recueil résumé page 121
Poster

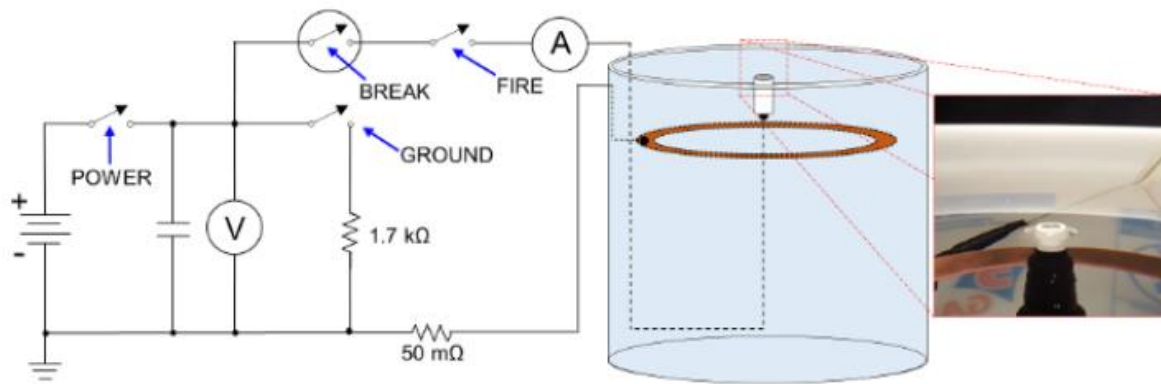
S.E. Dubowsky¹, A.N. Rose¹, N. Glumac², and B.J. McCall³

¹*Department of Chemistry, University of Illinois at Urbana-Champaign, Urbana, IL, USA*

²*Department of Mechanical Science and Engineering, University of Illinois at Urbana-Champaign, Urbana, IL, USA*

³*Departments of Chemistry and Astronomy, University of Illinois at Urbana-Champaign, Urbana, IL, USA*

Abstract: Ball plasmoid discharges have lifetimes of hundreds of milliseconds at ambient conditions, however, the mechanism(s) by which these plasmoids are stabilized remains unknown. We report an analysis of ball plasmoids using optical emission spectroscopy. The spectra presented here are obtained at higher energies and as a result are much more complex than what has previously been reported for this system. These data are guiding detailed investigations into the physicochemical processes by which ball plasmoids are stabilized.



(5-8 kV, tens of Amps)

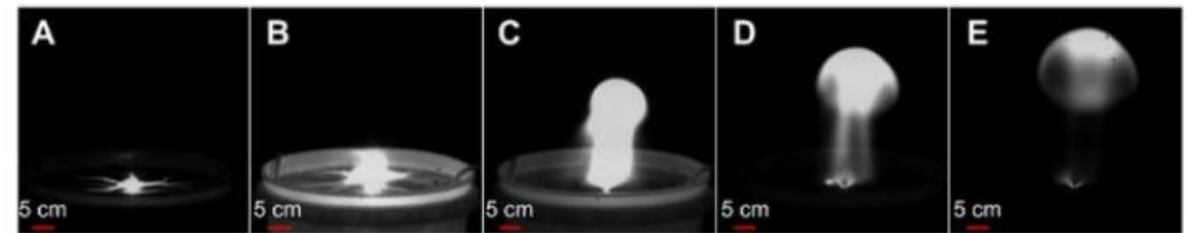


Fig. 1. High-speed images of single plasmoid discharge obtained with Phantom v5.2 camera at 1000 fps.

